

# High-density hard-core model on triangular and hexagonal lattices

A. Mazel<sup>1</sup>, I. Stuhl<sup>2</sup>, Y. Suhov<sup>2–4</sup>

## Abstract

We perform a rigorous study of the Gibbs statistics of high-density hard-core random configurations on a unit triangular lattice  $\mathbb{A}_2$  and a unit honeycomb graph  $\mathbb{H}_2$ , for any value of the (Euclidean) repulsion diameter  $D > 0$ . Only attainable values of  $D$  are relevant, for which  $D^2 = a^2 + b^2 + ab$ ,  $a, b \in \mathbb{Z}$  (Löschian numbers). Depending on arithmetic properties of  $D^2$ , we identify, for large fugacities, the pure phases (extreme Gibbs measures) and specify their symmetries. The answers depend on the way(s) an equilateral triangle of side-length  $D$  can be inscribed in  $\mathbb{A}_2$  or  $\mathbb{H}_2$ . On  $\mathbb{A}_2$ , our approach works for all attainable  $D^2$ ; on  $\mathbb{H}_2$  we have to exclude  $D^2 = 4, 7, 31, 133$ , where a sliding phenomenon occurs, similar to that on a unit square lattice  $\mathbb{Z}^2$ . For all values  $D^2$  apart from the excluded ones we prove the existence of a first-order phase transition where the number of co-existing pure phases grows at least as  $O(D^2)$ .

The proof is based on the Pirogov–Sinai theory which requires non-trivial verifications of key assumptions: finiteness of the set of periodic ground states and the Peierls bound. To establish the Peierls bound, we develop a general method based on the concept of a re-distributed area for Delaunay triangles. Some of the presented proofs are computer-assisted.

As a by-product of the ground state identification, we solve the disk-packing problem on  $\mathbb{A}_2$  and  $\mathbb{H}_2$  for any value of the disk diameter  $D$ .

## 1 A summary of results

### 1.1 Introduction

We analyze properties of random configurations of hard disks of a given diameter  $D$ , with centers in a unit triangular lattice  $\mathbb{A}_2$  and a unit honeycomb lattice<sup>1)</sup>  $\mathbb{H}_2$ , both

---

2010 *Mathematics Subject Classification*: primary 60G60, 82B20, 82B26

*Key words and phrases*: triangular lattice, hexagonal lattice, hard-core configuration, disk-packing, extreme Gibbs measure, high-density/large fugacity, periodic ground state, Delaunay triangulation, minimal re-distributed area of a triangle, maximally-dense sub-lattice, maximally-dense non-sub-lattice configuration, contour representation of the partition function, Peierls bound, Pirogov-Sinai theory, dominance, local repelling forces, computer-assisted enumeration, sliding

<sup>1</sup> AMC Health, New York, NY, USA; <sup>2</sup> Math Dept, Penn State University, PA, USA; <sup>3</sup> DPMMS, University of Cambridge and St John's College, Cambridge, UK, <sup>4</sup> IITP RAS, Moscow, RF

<sup>1)</sup>Strictly speaking,  $\mathbb{H}_2$  is not a lattice in the algebraic sense. However, we follow a physical tradition and refer to  $\mathbb{H}_2$  as a lattice.

embedded in  $\mathbb{R}^2$ . It is also convenient to consider  $\mathbb{H}_2$  as a subset in  $\mathbb{A}_2$ . Cf. Figure 1. Together with a unit square lattice  $\mathbb{Z}^2$ , these are popular examples of ‘regular’ planar graphs for a number of probabilistic models, including percolation and phase transitions. A separate place belongs to a model of hard disks in  $\mathbb{R}^2$ . Historically, the hard-core model emerged about a 150 years ago in an attempt to describe a system of atoms, molecules or granules, as represented by rigid spheres of a given diameter; a famous example of its application was the Boltzmann equation. Since then, the model proliferated in a number of pure and applied mathematical disciplines and generated a substantial literature. A comprehensive discussion of various aspects of the hard-core model and its applications (including elements of criticism) can be found, e.g., in [5], [20], [21], [1], [16].

The study of lattice hard-core (H-C) models started with the result by Dobrushin [8] about non-uniqueness of pure phases on  $\mathbb{Z}^d$ ,  $d \geq 2$ , with a nearest-neighbor exclusion in a high-density/large fugacity regime. The paper [12] established non-uniqueness of a pure phase for a particular sequence of exclusion distances on  $\mathbb{A}_2$ , without specifying the pure phases. We also note the (rather remarkable) result of paper [2] where a critical value of fugacity  $u_{\text{cr}} = \frac{1}{2}(11 + 5\sqrt{5})$  has been calculated, for the H-C diameter  $D = \sqrt{3}$  on  $\mathbb{A}_2$ . This, apparently, indicates an upper limiting value for fugacity  $u$  for the low-density regime where a pure phase is unique and given via a polymer expansion around an empty configuration. The paper [15] establishes existence of order-disorder phase transitions for a class of ‘non-sliding’ H-C lattice particle systems on a lattice in two or more dimensions.

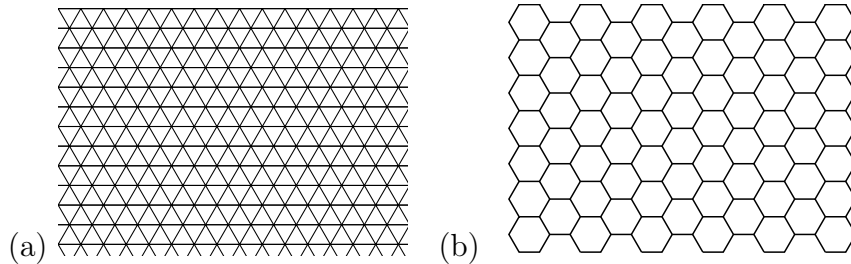


Figure 1: Fragments of lattices  $\mathbb{A}_2$  and  $\mathbb{H}_2$

The present paper continues and extends the works [8] and [12] in a general setting. A detailed study of the H-C model on  $\mathbb{Z}^2$  has been performed in [17]. We analyze the *ground states* and *Gibbs* or *DLR* measures for the (H-C) model on  $\mathbb{A}_2/\mathbb{H}_2$ , in a regime of high-density/large-fugacity. The assumption that the fugacity  $u$  is large is adopted throughout the paper without stressing it every time again. The analysis of Gibbs measures is reduced to *extreme Gibbs measure* (EGM, or *D*-EGM when dependence on  $D$  is emphasized). An EGM is interpreted as a *pure phase* in the phase diagram of the model. Formal definitions of the notions used in Introduction are provided in Sections 2. The H-C exclusion is imposed in the Euclidean  $\mathbb{R}^2$ -metric and is defined by the H-C *exclusion diameter*  $D$ : the shortest allowed distance between two occupied sites. Without loss of generality we assume throughout the paper that the value  $D$  (or  $D^2$ ) is *attainable*, i.e., there are pairs of sites in  $\mathbb{A}_2$  and  $\mathbb{H}_2$  with the distance exactly  $D$  between them. The set of attainable values is the same for  $\mathbb{A}_2$  and  $\mathbb{H}_2$  and is characterized through a *Löschian decomposition* of the number  $D^2$ . Referring to  $D^2$  rather than to  $D$  is more convenient since  $D^2$  is a positive integer.

The problem of identification of the EGM structure is reduced – via the *Pirogov–Sinai* (PS) *theory* [22], [26] – to an analysis of *periodic ground states* (PGSs or  $D$ -PGSs), including a verification of the *Peierls bound*. Informally, speaking, the outcome of the PS theory is that every EGM is generated by a PGS. The inverse is not always true: there may be PGSs that do not generate EGMs. The PGSs that generate EGMs are referred to as *dominant* (stable in the terminology of [26]).

Our results can be briefly summarized as follows.

- (i) On both  $\mathbb{A}_2$  and  $\mathbb{H}_2$  we describe the ground states (periodic and non-periodic) for all values of  $D$  and fugacity  $u > 1$ . See Remark 4.1. This solves the disk-packing problem on  $\mathbb{A}_2$  and  $\mathbb{H}_2$  for any disk diameter  $D$ ; cf.[6]. The PGSs are naturally partitioned into equivalence classes defined by lattice symmetries (shifts and reflections). Apart from 13 values of  $D$  on  $\mathbb{H}_2$ , all  $D$ -PGSs are constructed from sub-lattices.
- (ii) For the PGSs we establish a Peierls bound where the Peierls constant grows with  $u$  and decreases with  $D$ . See Lemmas 5.1 and 5.4.
- (iii) The structure of  $D$ -EGMs (the phase diagram) inherits that of  $D$ -PGSs. First, for at least one PGS-equivalence class, each PGS from the class generates a distinct EGM. That is, we have a first-order phase transition. This fact is proven for every  $D$ , except for 4 values of  $D$  on  $\mathbb{H}_2$ . See Theorem III in Section 3.2.
- (iv) In the case where the PGS-equivalence class is unique, we obtain a complete phase diagram. The sets of values  $D$  with a unique PGS-equivalence class on  $\mathbb{A}_2$  and  $\mathbb{H}_2$  are infinite and explicitly described. The number of  $D$ -EGMs in this case grows as  $O(D^2)$  and is further specified. See Theorems 1, 2, 7, 8, 11, 12 in Section 3.
- (v) The sets of values  $D$  for which the PGS-equivalence class is non-unique is also infinite and explicitly described, on both  $\mathbb{A}_2$  and  $\mathbb{H}_2$ . The number of  $D$ -EGMs in this case grows at least as  $O(D^2)$ . The question which classes are dominant, i.e., generate EGMs requires an additional analysis. We conduct such analysis on a number of values  $D$  on  $\mathbb{A}_2$  and  $\mathbb{H}_2$  exploring various emerging possibilities. See Theorems 4, 5, 6, 10 in Section 3.
- (vi) We establish that a phenomenon of *sliding* occurs only on  $\mathbb{H}_2$ , for  $D^2 = 4, 7, 31, 133$ . See Lemmas 4.7 - 4.10. For these values, the structure of the phase diagram remains open. Cf. Section 8. The phenomenon of sliding was first discovered by Dobrushin (1968) on  $\mathbb{Z}^2$ . Cf. [17].

## 1.2 The PGSs and EGMs

The structure of PGSs on both  $\mathbb{A}_2$  and  $\mathbb{H}_2$  (and also on  $\mathbb{Z}^2$ : cf. [17]) depends on arithmetic properties of the number  $D^2$ . Moreover, the image of a  $D$ -PGS under a *symmetry* (of  $\mathbb{A}_2$  or  $\mathbb{H}_2$ ), i.e., a lattice shift or reflection, is also a  $D$ -PGS, and one can speak about the corresponding *equivalence classes* of PGSs with respect to  $\mathbb{A}_2/\mathbb{H}_2$ -symmetries. This is important since dominance is a class property: if an equivalence class contains a dominant PGS then all PGSs from the class are dominant.

Referring to the formation of PGS-equivalence classes, the entire set of attainable values of  $D$  (or  $D^2$ ) is divided into disjoint subsets. For lattice  $\mathbb{A}_2$  we consider two subsets of values  $D^2$  (both infinite), called Classes TA and TB. On  $\mathbb{H}_2$  we deal with six subsets of values  $D^2$  called Classes HA, HB, HC (infinite) and HD, HE, HS (finite). Here T stands for triangular and H for honeycomb. These subsets are further divided, regarding specific aspects of the structure of PGSs and EGMs. Cf. Sections 1.3, 1.4.

Physically speaking, the above subsets are characterized by a possibility (or possibilities or a lack of them) to inscribe an equilateral triangle of side-length  $D$  in  $\mathbb{A}_2$  or  $\mathbb{H}_2$ . In the case of  $\mathbb{A}_2$  this is always possible, but the inscription may be non-unique. For  $\mathbb{H}_2$  it is not always possible, which leads to a more complicated partition of the values  $D^2$ .

On  $\mathbb{A}_2$ , the  $D$ -PGSs are constructed from  $D$ -sub-lattices, i.e., sub-lattices for which a fundamental parallelogram is a  $D$ -rhombus formed by 2 equilateral triangles of side-length  $D$  ( $D$ -triangles, for short). If  $D^2$  is from Class TA, the  $D$ -sub-lattice is unique, and the PGSs form a single equivalence class. Consequently, for Class TA we establish a complete phase diagram in the large-fugacity regime. In this regime each PGS applied as a boundary condition generates a distinct  $D$ -EGM, and all  $D$ -EGMs are obtained in this way; cf. Theorems 1, 2 in Section 3.3. In other words, for values  $D$  from Class TA all PGSs are dominant. Also, the EGMs inherit symmetries between their generating PGSs. Similar properties hold true for Class HA on  $\mathbb{H}_2$ ; cf. Theorems 7, 8 in Section 3.5. Classes TA and HA yield the simplest cases of the PGS/EGM analysis on  $\mathbb{A}_2/\mathbb{H}_2$ .

For  $D^2$  from Classes TB or HB, the  $D$ -PGSs are still constructed from  $D$ -sub-lattices, but there are multiple PGS-equivalence classes. There is always a dominant equivalence class (we conjecture that it is unique), but the problem of identifying which classes are dominant is more involved. Here we solve it for some specific values of  $D$ , indicating various emerging possibilities for a plausible general answer.

Arithmetically, Classes HA and HB are formed by the values  $D^2$  from Classes TA and TB divisible by 3.

Next, Classes HC, HD, HE, and HS on  $\mathbb{H}_2$  consist of values  $D^2$  non-divisible by 3. These classes stem from the above-mentioned features of  $\mathbb{H}_2$ , about a lack of possibility to inscribe a  $D$ -triangle for some values of  $D$ . Class HC (which covers a bulk of values of  $D$  on  $\mathbb{H}_2$ ) is determined by the condition that  $D^2$  is not divisible by 3 and is non-exceptional in a sense made precise below. For values  $D$  from Class HC we look for the attainable  $D^* > D$  which (i) has  $(D^*)^2$  divisible by 3 (i.e., falls in Class HA or HB) and (ii)  $D^*$  is nearest to  $D$  with this property. Then the PGSs and EGMs for  $D^2$  are the same as for  $(D^*)^2$ , i.e., are constructed from  $D^*$ -sub-lattices.

Classes HD, HE and HS are deemed exceptional and are dealt with on a case-by-case basis (with the help of a computer). Cf. Section 1.4. For these classes not all PGSs are constructed from  $D$ - or  $D^*$ -sub-lattices. (For  $D^2$  from Class HD none of the PGSs is a sub-lattice.) In particular, Class HS consists of values  $D^2 = 4, 7, 31, 133$  which exhibit a phenomenon of sliding on  $\mathbb{H}_2$ . A similar phenomenon occurs on lattice  $\mathbb{Z}^2$  as well; cf. [17]. For the values of  $D^2$  with sliding, the PS theory is not applicable since the number of PGSs is infinite and – more importantly – the Peierls bound does not hold. Our conjecture is that the EGM for these values of  $D$  is unique when fugacity  $u$  is large enough (and, indeed, for all values  $u > 0$ ). We briefly comment on sliding on  $\mathbb{H}_2$  in Section 8. Cf. Section 2.2 in [17] where the similar problem is treated on lattice  $\mathbb{Z}^2$ .

As was mentioned before, an attainable value  $D^2$  admits a L\"oschian decomposition.



It means that  $D^2$  is a positive integer of the form  $a^2 + b^2 + ab$  where  $a$  and  $b$  are integers. Lösschian numbers arise naturally in this context as they are the norms of Eisenstein integers that form  $\mathbb{A}_2$ . The Lösschian numbers are the sequence A003136 in OEIS, the on-line Encyclopedia of integer sequences and their initial list is:

1, 3, 4, 7, 9, 12, 13, 16, 19, 21, 25, 27, 28, 31, 36, 37, 39, 43, 48, 49, 52, 57, 61, 63, 64, 67, 73, 75, 76, 79, 81, 84, 91, 93, 97, 100, 103, 108, 109, 111, 112, 117, 121, 124, 127, 129, 133, 139, 144, 147, 148, 151, 156, 157, 163, 169, 171, 172, 175, 181, 183, 189, 192, 193, 196, 199, 201, 208, 211, 217, 219, 223, 225, 228, 229, 237, 241, 243, 244, 247, 252, 256, 259, 268, 271, 273, 277, 279, 283, 289, 291, 292, 300, 301, 304, 307, 309, 313, 316, 324, 325, 327, 331, 333, 336, 337, 343, 351, 361, 363, 364, 367, 372, 379, 387, 388, 397, 399, 400, 403, 409, 412, 417, 421, 427, 432, 433, 436, 439, 441, 444, 448, 453, 457, 463, 468, 469, 471, 475, 481, 484, 487, 489.

An equivalent characterization of a Lösschian number is that its rational prime factorization must contain primes of the form  $3v + 2$ ,  $v \in \mathbb{Z}_+$  in even powers (there is no restriction on factor 3 or primes of the form  $3v + 1$ ). We use some classical results regarding these integers which are presented in a convenient form in [18, 19]. A compendium of the related theory is given in the monograph [7].

The PGS identification and a specification of the Peierls-bound is done with the help of *Voronoi cells* (V-cells) or through the construction of Delaunay  $\mathbb{A}_2/\mathbb{H}_2$ -triangles which *minimize the re-distributed area* (MRA-triangles). As was said, the Peierls bound is given in Theorem II from Section 3.2. In this paper we employ the approach based on MRA-triangles (also used in [17]), but for completeness provide a brief account of the V-cell method as well. Cf. Sections 4, 5.

In Sections 1.3 and 1.4 we give a description of our results on PGSs for the H-C model on  $\mathbb{A}_2$  and  $\mathbb{H}_2$ .

### 1.3 PGSs and EGMs on $\mathbb{A}_2$

On  $\mathbb{A}_2$  the situation is made easier by the above-mentioned fact that the PGSs are constructed from  $D$ -sub-lattices. That is, a PGS-equivalence class is determined either by a  $D$ -sub-lattice – if it is reflection-invariant – or by a pair of  $D$ -sub-lattices taken to each other by a reflection. Consequently, a PGS-class contains  $D^2$  or  $2D^2$  PGSs obtained from each other by lattice shifts and reflections. The value  $D^2$  represents the number of sites in a  $D$ -rhombus which gives the number of different lattice shifts for PGSs.

The number of PGS-equivalence classes is related to the number and structure of non-negative solutions to the equation  $D^2 = a^2 + b^2 + ab$ . Accordingly, it is natural to extract the following classes of values of  $D^2$ .

- Class TA1:  $D^2$  is an integer whose prime decomposition contains (i) a factor 3 in any power, (ii) primes of the form  $3v + 2$ , in even powers, possibly zero, and (iii) no prime of the form  $3v + 1$ . This happens iff  $D^2 = a^2$  or  $3a^2$  where  $a \in \mathbb{N}$  has only primes  $3v + 2$  in its prime decomposition. The first 40 values of  $D^2$  falling in this category are  $D^2 = 1, 3, 4, 9, 12, 16, 25, 27, 36, 48, 64, 75, 81, 100, 108, 121, 144, 192, 225, 243, 256, 289, 300, 324, 363, 400, 432, 484, 529, 576, 625, 675, 729, 768, 841, 867, 900, 972, 1024, 1089$ .

- Class TA2:  $D^2$  is an integer whose prime decomposition contains (i) a factor 3 in any power, (ii) primes of the form  $3v + 2$ , in even powers, possibly zero, and (iii) a single prime of the form  $3v + 1$  (entering in power 1). This happens iff  $D^2$  admits a unique

decomposition as  $a^2 + b^2 + ab$  (modulo the permutation of  $a$  and  $b$ ) and we have  $a, b \in \mathbb{N}$ ,  $a \neq b$ . The first 40 values of  $D^2$  from Class TA2 are 7, 13, 19, 21, 28, 31, 37, 39, 43, 52, 57, 61, 63, 67, 73, 76, 79, 84, 93, 97, 103, 109, 111, 112, 117, 124, 127, 129, 139, 148, 151, 156, 157, 163, 171, 172, 175, 181, 183, 189.

- Class TA: the union of Classes TA1 and TA2.

- Class TB: All remaining attainable values of  $D$  (or  $D^2$ ). Class TB consists of positive integers  $D^2$  that contain (i) a factor 3 in any power, (ii) primes of the form  $3v + 2$ , in even powers, possibly zero, and (iii) at least two primes of the form  $3v + 1$  (possibly, identical). It occurs iff  $D^2$  admits a non-unique L\"oschian decomposition, i.e., there are more than 1 solutions  $(a, b)$  to the Diophantine equation  $D^2 = a^2 + b^2 + ab$ , with  $a, b$  non-negative integers, again, modulo the permutation of  $a, b$ . The first 40 values of  $D^2$  from Class TB are 49, 91, 133, 147, 169, 196, 217, 247, 259, 273, 301, 343, 361, 364, 399, 403, 427, 441, 469, 481, 507, 511, 532, 553, 559, 588, 589, 637, 651, 676, 679, 703, 721, 741, 763, 777, 784, 793, 817, 819.

For  $D^2$  from TA there is a single PGS-equivalence class, while for  $D^2$  from TB the number of PGS-equivalence classes is greater than one.

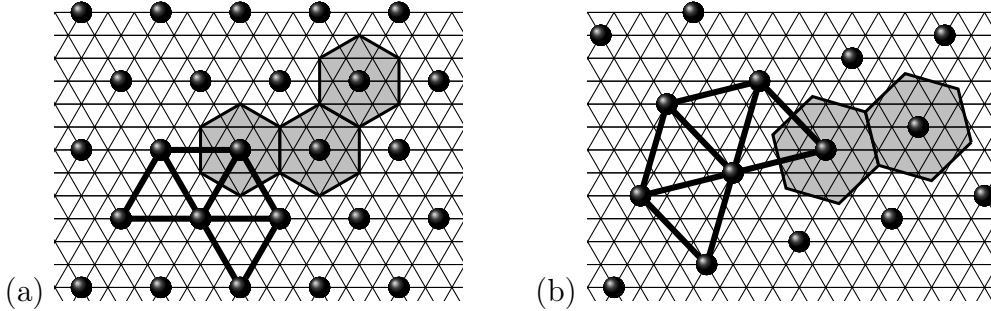


Figure 2: PGSs on  $\mathbb{A}_2$  for  $D^2 = 9$  (Class TA1), and  $D^2 = 13$  (Class TA2), with V-cells (gray hexagons) and choices of  $D$ -rhombuses.

The number of PGSs and EGMs for  $D^2 = 9$  is 9 (frame (a)), and for  $D^2 = 13$  is 26 (frame (b)). The PGSs for  $D^2 = 9$  are horizontal and for  $D^2 = 13$  are inclined.

It is convenient to refer to triangles with vertices in  $\mathbb{A}_2$  as  $\mathbb{A}_2$ -triangles. As we saw earlier, an important role is played by  $D$ -triangles. We will distinguish between 3 types of  $D$ -triangles: *horizontal*, with sides fitting  $\mathbb{A}_2$ , *vertical*, with sides perpendicular to constituent lines of  $\mathbb{A}_2$ , and *inclined*, covering the remaining cases. We will also use  $D$ -triangles in the plane  $\mathbb{R}^2$ , for general diameters  $D > 0$ . The above terminology is extended to the  $D$ -sub-lattices and  $D$ -PGSs: we speak of horizontal PGSs, vertical PGSs and inclined PGSs, respectively, on both  $\mathbb{A}_2/\mathbb{H}_2$ .

The PGSs for Class TA1 are all horizontal when  $D^2 = a^2$  and all vertical when  $D^2 = 3a^2$ ; for Class TA2 they are all inclined.

As was said before, in Theorems 1, 2 from Section 3.3 we prove that in the large-fugacity regime on  $\mathbb{A}_2$ , there are exactly  $D^2$  EGMs if  $D$  is from Class TA1 and exactly  $2D^2$  EGMs if  $D$  is from Class TA2. In both cases, there is a single PGS-equivalence class which is dominant.

For every  $D^2$  from Class TB we prove that at least one PGS-equivalence class generates  $D$ -EGMs. See Theorem 3 in Section 3.4. As we mentioned before, the structure of EGMs

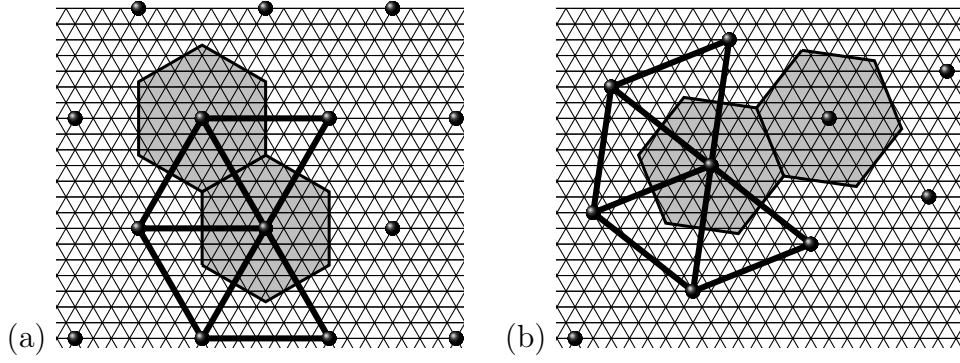


Figure 3: PGSs on  $\mathbb{A}_2$  for  $D^2 = 49$  (Class TB), with V-cells (gray hexagons) and choices of  $D$ -rhombuses.  
There are 49 horizontal PGSs (frame (a)), and 98 inclined PGSs (frame (b)). The horizontal PGSs are the only dominant, so there are only 49 EGMs.

is defined by the property of dominance of PGSs. For the specific values  $D^2 = 49, 147, 169$  we present a new technique that allows us to determine which PGS-class is dominant, via a specific count of density of *local excitations*. In the terminology from [26], it is a specific analysis of *small contours*. See Theorems 4, 5, and 6 in Section 3.4.

#### 1.4 PGSs and EGMs on $\mathbb{H}_2$

On lattice  $\mathbb{H}_2$  we identify the following pair-wise disjoint sets of values of  $D$ : HA1, HA2, HA (the union of HA1 and HA2), HB, HC (all infinite), HD, HE, HS (all finite).

- Class HS: 4 values with *sliding*  $D^2 = 4, 7, 31, 133$ ; see Section 8.
- Class HA1: the values  $D$  from the above Class TA1 such that  $D^2$  is divisible by 3. That is,  $D^2 = 9b^2$  or  $D^2 = 3b^2$  where  $b \in \mathbb{N}$ . The initial list of 30 such values has  $D^2 = 3, 9, 12, 27, 36, 48, 75, 81, 108, 144, 192, 225, 243, 300, 324, 363, 432, 576, 675, 729, 768, 867, 900, 972, 1089, 1137, 1200, 1296, 1389, 1452$ .
- Class HA2: the values  $D$  from the above Class TA2 such that  $D^2$  is divisible by 3. The initial list of 30 such values has  $D^2 = 21, 39, 57, 63, 84, 93, 111, 117, 129, 156, 171, 183, 189, 201, 219, 237, 252, 279, 291, 309, 327, 333, 336, 351, 372, 381, 387, 417, 444, 453$ .
- Class HB: the values  $D$  from the above Class TB such that  $D^2$  is divisible by 3. The initial list of 30 such values has  $D^2 = 147, 273, 399, 441, 507, 588, 651, 741, 777, 819, 903, 1029, 1083, 1092, 1197, 1209, 1281, 1323, 1407, 1443, 1521, 1533, 1596, 1659, 1677, 1764, 1767, 1911, 1953, 2028$ .
- Class HC: the remaining values of  $D$ , except for the values from Classes HD and HE below. Here the initial list of 30 values has  $D^2 = 19, 25, 37, 38, 43, 52, 61, 73, 76, 79, 84, 91, 100, 103, 109, 121, 124, 127, 139, 148, 151, 157, 163, 169, 172, 175, 181, 193, 196, 199$ .
- Class HD: 9 values where  $D^2 = 1, 13, 16, 28, 49, 64, 97, 157, 256$ .
- Class HE: 1 value  $D^2 = 67$ .

In the analysis of the EGMs, the values  $D$  from Class HS are disregarded. As was

said before, the PS theory does not apply for such  $D$ .

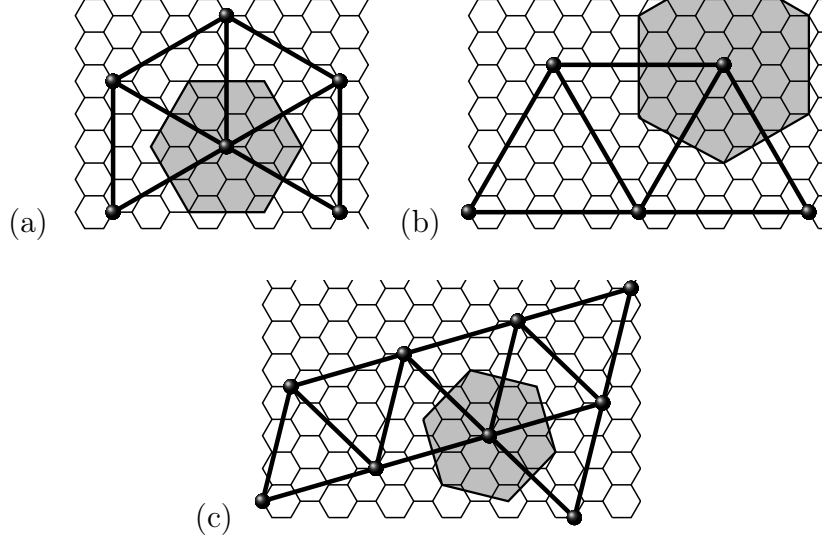


Figure 4:  $\alpha$ -PGSs on  $\mathbb{H}_2$ , for  $D^2 = 48, 81$  (Class HA1, frames (a,b)), and  $D^2 = 39$  (Class HA2, frame (c)), with Voronoi cells (gray hexagons) and choices of  $D$ -rhombuses.

The number of PGSs and EGMs for  $D^2 = 48, 81, 39$  equals 32, 54 and 52, respectively. The PGSs for  $D^2 = 48$  are horizontal, for  $D^2 = 81$  vertical, and for  $D^2 = 39$  inclined.

Now, suppose  $D$  is from Class HA. Then the model on  $\mathbb{H}_2$  with a large fugacity has  $2D^2/3$  EGMs if  $D$  falls in Class TA1 and  $4D^2/3$  if  $D$  falls in Class TA2. See Theorems 7, 8 in Section 3.5. In Class HA, the PGSs stem from  $D$ -sub-lattices in  $\mathbb{A}_2$ . For HA1, the PGSs are all horizontal if  $D^2 = 9b^2$  or all vertical, if  $D^2 = 3b^2$ ; for HA2 the PGSs are all inclined.

We refer to  $D$ -admissible configurations on  $\mathbb{H}_2$  constructed from a  $D$ -sub-lattice as  $\alpha$ -configurations or configurations of type  $\alpha$ , or – when the value  $D$  should be highlighted – as  $(D, \alpha)$ -configurations (in short:  $\alpha$ -ACs or  $(D, \alpha)$ -ACs). We will also use the terms an  $\alpha$ -PGS and a  $(D, \alpha)$ -PGS.

Summarizing, for Class HA we obtain a situation similar to Class TA on  $\mathbb{A}_2$ . Cf. Figure 4.

The picture for Class HB is analogous to that for Class TB. That is, only the dominant  $\alpha$ -PGSs give rise to EGMs, and the issue of dominance is resolved by counting local excitations. Cf. Theorem 9 in Section 3.5. As an example, we analyze the case  $D^2 = 147$  and find out that on  $\mathbb{H}_2$  there are 98 dominant vertical PGSs and 196 non-dominant inclined PGSs. Cf. Figure 5 and Theorem 10. Consequently, the number of  $D$ -EGMs for a large fugacity  $u$  also equals 98, and these EGMs inherit symmetries between the vertical PGSs.

A new situation arises for  $D$  from Class HC. Here the PGSs stem from  $D^*$ -sub-lattices where  $D^* > D$  is the nearest L\"oschian number divisible by 3 (i.e., from Classes HA or HB). The minimal value for the difference  $(D^*)^2 - D^2$  equals 2 and is achieved when  $D^2 = 3b^2 + 3b + 1$  and  $(D^*)^2 = 3b^2 + 3b + 3$ , for integer  $n \geq 2$ . (Here, for  $n = 1$  we obtain  $D^2 = 3b^2 + 3b + 1 = 7$  which yields a value with sliding.) If  $D^*$  has type HA1,

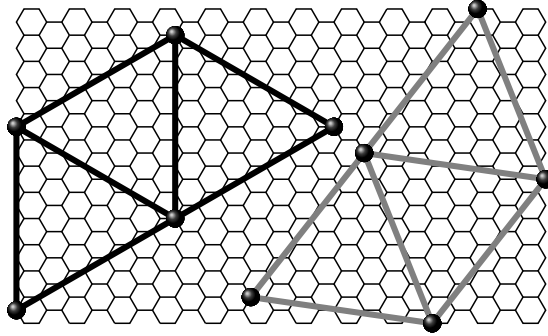


Figure 5:  $\alpha$ -PGSs on  $\mathbb{H}_2$  for  $D^2 = 147$  (Class HB) and  $D^2 = 139$  (Class HC). For  $D^2 = 147$  the vertical PGSs (black rhombuses) are dominant, and the number of EGMs equals 98. However, for  $D^2 = 139$  the inclined PGSs (gray rhombuses) are dominant, and the number of EGMs equals 196.

the number of  $D$ -EGMs in  $\mathbb{H}_2$  equals  $2(D^*)^2/3$  while if  $D^*$  has type HA2, the number of  $D$ -EGMs equals  $4(D^*)^2/3$ . Moreover, the PGSs are  $\alpha$ -configurations and are obtained from each other by  $\mathbb{H}_2$ -shifts for  $D^*$  from Class HA1 and by  $\mathbb{H}_2$ -shifts or reflections for  $D^*$  from Class HA2. Cf. Figure 6.

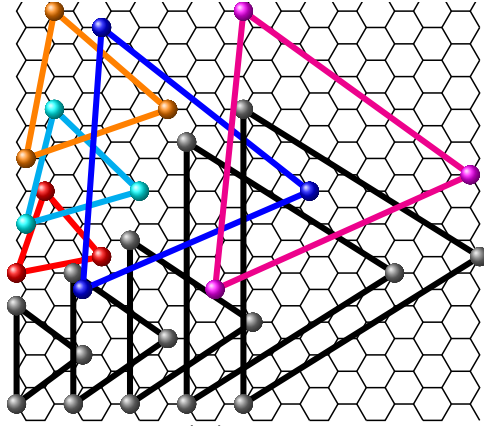


Figure 6:  $\alpha$ -PGSs on  $\mathbb{H}_2$  for a series of values  $D^2$  from Class HC, with  $D^{*2} = D^2 + 2$ , and their associated  $D^*$ -triangles.

(i) For  $D^2 = 19$ ,  $D^{*2} = 21$  (red). (ii) For  $D^2 = 37$ ,  $D^{*2} = 39$  (turquoise). (iii) For  $D^2 = 61$ ,  $D^{*2} = 63$  (orange). (iv) For  $D^2 = 169$ ,  $D^{*2} = 171$  (blue). (v) For  $D^2 = 217$ ,  $D^{*2} = 219$  (purple). The black  $\mathbb{H}_2$ -triangles give the minimal area when the side-lengths are at least  $D$  and the angles at most  $\pi/2$ . However, they do not generate PGSs by extension; they are parts of  $(\beta, D)$ -configurations which are not PGSs; see below. The PGSs are  $(\alpha, D^*)$ -configurations generated from  $D^*$ -triangles of the corresponding color.

For instance, if  $D^2 = 19$  then  $(D^*)^2 = 21$ , and the number of the EGMs for  $D^2 = 19$  equals 28. On the other hand, for  $D^2 = 43$  the value  $(D^*)^2$  is 48. Therefore, for  $D^2 = 43$

the number of EGMs equals 32. Cf. Theorem 11 in Section 3.5.

If  $D^*$  is a value of type HB then again the dominance analysis is needed to determine which PGSs generate EGMs.

Finally, consider  $D^2$  from Classes HD or HE. From now on we refer to the values of  $D^2$  from these classes as *exceptional*. (In fact, these values are exceptions from Class HC.) It is convenient to divide Class HD into two sub-classes: HD1:  $D^2 = 1, 13, 28, 49, 64, 97, 157$ ; HD2:  $D^2 = 16, 256$ . For  $D = D^2 = 1$  we have a single PGS where all sites in  $\mathbb{H}_2$  are occupied. There is just one EGM for all values of  $u$  (not only for  $u$  large), which is a Bernoulli random field over  $\mathbb{H}_2$ , with probability for a site being empty/vacant  $1/(1+u)$  and occupied  $u/(1+u)$ . We will treat the case  $D = 1$  as trivial and omit it from the forthcoming discussions.

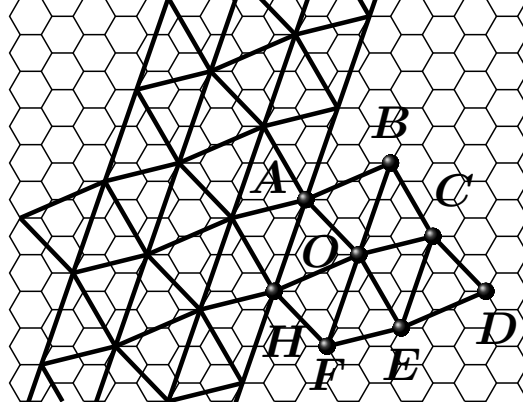


Figure 7: A  $\beta$ -PGS on  $\mathbb{H}_2$  for  $D^2 = 13$ , with  $a = 1$ ,  $b = 3$  (Class HD1). Here  $|AO|^2 = |OC|^2 = |CD|^2 = |HF|^2 = |FE|^2 = 13$ ,  $|BC|^2 = |OE|^2 = 16$ ,  $|AB|^2 = |ED|^2 = |OH|^2 = 19$ ,  $|BO|^2 = |OF|^2 = |CE|^2 = 21$ . Triangles  $OBC$ ,  $FOE$  and  $OCE$  have area  $4\sqrt{3}$ . Triangles  $OAB$ ,  $FHO$  and  $CED$  have area  $17\sqrt{3}/4$ . The number of PGSs equals 66; they are obtained from each other by  $\mathbb{H}_2$ -shifts and rotations by  $\pm 2\pi/3$ . Every PGS generates an EGM, and every EGM is generated by a PGS. Thus, there are 66 EGMs which inherit the symmetries between their generating PGSs.

Take  $D^2 = 13, 28, 49, 64, 97, 157$  (sub-class HD2) and write  $D^2 = a^2 + b^2 + ab$  where  $a, b$  are non-negative integers. Then we have a particular structure of a PGS related to a quadrilateral  $OABC$  in  $\mathbb{H}_2$  where (i) two adjacent sides  $OA$  and  $OC$  have length  $D$  and form an angle  $2\pi/3$ , (ii) two other sides  $AB$  and  $BC$  (also adjacent to each other) have  $|AB|^2 = D^2 + 2a + b + 1$  and  $|BC|^2 = D^2 - a + b + 1$ , and (iii) the shorter diagonal  $OB$  has  $|OB|^2 = D^2 + a + 2b + 1$ . We place particles at the vertices of such a quadrilateral and then extend this pattern to the whole of  $\mathbb{H}_2$ , generating a picture with intermittent stripes parallel to  $OB$ . Such configurations are called  $\beta$ -configurations or configurations of type  $\beta$  (in short:  $\beta$ -ACs); these configurations are not constructed from sub-lattices. These configurations yield PGSs in Class HD1; accordingly, we refer to them as  $\beta$ -PGSs. Cf. Figure 7 where  $D^2 = 13$ . There are 66 PGSs for  $D^2 = 13$ , 132 for  $D^2 = 28$ , 222 for  $D^2 = 49$ , 288 for  $D^2 = 64$ , 426 for  $D^2 = 97$ , and 678 for  $D^2 = 157$ . For a large fugacity  $u$ , each PGS gives rise to a different  $D$ -EGM, and the number of the  $D$ -EGMs matches that of the  $D$ -PGSs. See Theorem 12(i) from Section 3.6.

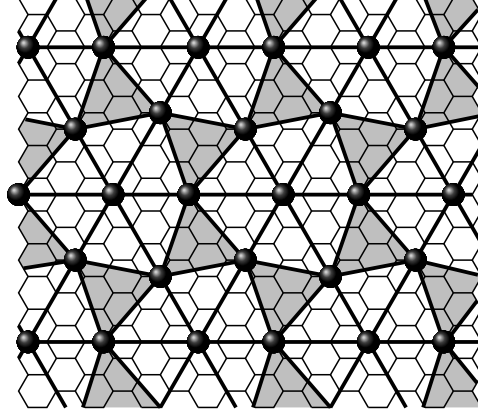


Figure 8: PGSs ( $\gamma$ -configurations) on  $\mathbb{H}_2$  for  $D^2 = 16$ , (Class HD2). Inner equilateral  $(D^2 + D + 1)$ -triangles are colored gray.

Another particular PGS-structure arises for  $D^2 = 16, 256$  (sub-class HD2). For these integers  $D^2 = a^2 + b^2 + ab$  where  $a = 0, b = D$ . Then we take the value  $\overline{D} = 2D + 1$  which is divisible by 3. Hence, an equilateral triangle,  $DEO$ , can be inscribed in  $\mathbb{H}_2$ , with side-length  $\overline{D}$  and a horizontal base  $OE$ . Now, consider an inner equilateral triangle  $ABC$  with side-length  $(D^2 + D + 1)^{1/2}$  inscribed in  $DEO$ : the vertices  $A, B, C$  lie in the sides  $OD, DE$  and  $EO$  and divide them at the ratio  $D : (D + 1)$ . Let us put particles at the vertices of  $A, B, C$  and  $D, E, O$ . The PGSs for  $D^2 = 16, 256$  arise from triangles congruent to  $DEO$ , each carrying the above particles, via the extension to the whole of  $\mathbb{H}_2$ . For this type of configurations we use the terms  $\gamma$ -configurations and  $\gamma$ -PGSs. Cf. Figure 8. There are 54  $D$ -PGSs for  $D^2 = 16$  and 726 for  $D^2 = 256$ . As above, each PGS gives rise to a different EGM, and the number of the EGMs matches that of the PGSs. See Theorem 12(ii) from Section 3.6.

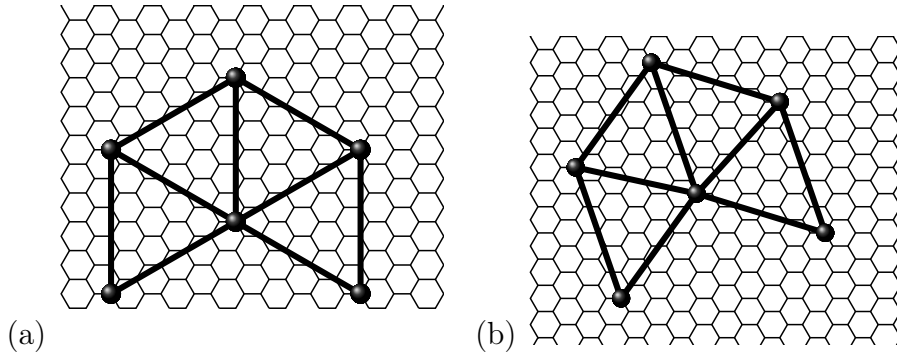


Figure 9: PGSs on  $\mathbb{H}_2$  for  $D^2 = 67$  (Class HE): (a) type  $\alpha$  (vertical), (b) type  $\beta$  (inclined).

The  $\alpha$ -PGSs are conjectured to be dominant.

For  $D^2 = 67$  (Class HE) we have a competition between two types of PGSs: (a) 50 PGSs as in Class HA ( $\alpha$ -configurations) with the squared exclusion diameter 75 and (b) 300 PGSs as in class HD1 ( $\beta$ -configurations). This is formally stated in Theorem 13 in Section 3.7. See Figure 9. We conjecture that the  $\alpha$ -PGSs of type (a) are dominant.

We see that, for values  $D$  from exceptional classes HD and HE on  $\mathbb{H}_2$ , we have PGSs that are not generated from sub-lattices (apart from  $D = 1$ ), yet these cases do not lead to sliding. In contrast, on  $\mathbb{Z}^2$ , if for a given attainable  $D$  there exists a non-lattice PGS then this value of  $D$  exhibits sliding.

## 2 Formal preliminaries and basic facts

### 2.1 The H-C model on $\mathbb{A}_2$

We refer to a two-dimensional unit triangular lattice  $\mathbb{A}_2$  as the set of points  $\mathbf{x} = (x_1; x_2) \in \mathbb{R}^2$  (sites of the lattice) with Euclidean co-ordinates

$$x_1 = m - \frac{1}{2}n \text{ and } x_2 = \frac{\sqrt{3}}{2}n, \text{ where } m, n \in \mathbb{Z}. \quad (2.1)$$

Every site  $\mathbf{x} \in \mathbb{A}_2$  has six neighboring sites  $\mathbf{x}'$  such that the distance  $\rho(\mathbf{x}, \mathbf{x}')$  equals 1. In future we write  $\mathbf{x} \in \mathbb{A}_2$  for brevity. Alternatively to  $\mathbf{x} = (x_1; x_2)$ , we also write  $\mathbf{x} \simeq (m, n) \in \mathbb{A}_2$ . Geometrically, points  $(1; 0) \simeq (1, 0)$  and  $(-1/2; \sqrt{3}/2) \simeq (0, 1)$  lead to a natural basis for  $\mathbb{A}_2$ .

Here and below,  $\rho(= \rho_2)$  stands for the 2D Euclidean metric: for  $\mathbf{x} = (x_1; x_2), \mathbf{y} = (y_1; y_2) \in \mathbb{R}^2$ , the distance  $\rho(\mathbf{x}, \mathbf{y}) = [\rho_1(x_1, y_1)^2 + \rho_1(x_2, y_2)^2]^{1/2}$ , where  $\rho_1(x, y) = |y - x|$ ,  $x, y \in \mathbb{R}$ . Alternatively, for  $\mathbf{x} \simeq (m, n), \mathbf{y} \simeq (u, v) \in \mathbb{A}_2$ ,

$$\rho(\mathbf{x}, \mathbf{y})^2 = (m - u)^2 + (n - v)^2 - (m - u)(n - v).$$

Given  $\mathbf{u} \in \mathbb{A}_2$ , we designate  $\mathbf{T}_{\mathbf{u}} : \mathbb{A}_2 \rightarrow \mathbb{A}_2$  to be an  $\mathbb{A}_2$ -shift by  $\mathbf{u}$ , with  $\mathbf{T}_{\mathbf{u}}\mathbf{x} = \mathbf{x} + \mathbf{u}$ ,  $\mathbf{x} \in \mathbb{A}_2$ . Similarly,  $\mathbf{R} : \mathbb{A}_2 \rightarrow \mathbb{A}_2$  stands for the reflection map about the horizontal axis.

Given a number  $D \geq 1$ , consider  $D$ -admissible configurations ( $D$ -ACs, or, in short, ACs):

$$\phi_{\mathbb{A}_2} : \mathbf{x} \in \mathbb{A}_2 \mapsto \phi_{\mathbb{A}_2}(\mathbf{x}) \in \{0, 1\} \text{ (or shortly } \phi : \mathbb{A}_2 \rightarrow \{0, 1\}^{\mathbb{A}_2})$$

such that for any two *occupied* sites  $\mathbf{x}$  and  $\mathbf{y}$  with  $\phi(\mathbf{x}) = \phi(\mathbf{y}) = 1$  the distance  $\rho(\mathbf{x}, \mathbf{y}) \geq D$ . (We can think that  $\phi(\mathbf{x}) = 1$  means site  $\mathbf{x}$  is occupied in  $\phi$  by a particle, and  $\phi(\mathbf{x}) = 0$  that  $\mathbf{x}$  is vacant in  $\phi$ . Particles are treated as non-overlapped open disks of diameter  $D$  with the centers placed at lattice sites.) We write

$$\mathbf{x} \in \phi \text{ if } \phi(\mathbf{x}) = 1 \text{ and identify } \phi \text{ with the subset in } \mathbb{A}_2 \text{ where } \phi(\mathbf{x}) = 1.$$

The value  $D$  is called as an H-C exclusion diameter. The set of admissible configurations is denoted by  $\mathcal{A} = \mathcal{A}(D, \mathbb{A}_2)$ . As was said in Introduction, we can assume that  $D^2$  is a L\"oschian number:

$$D^2 \in \mathbb{N} \text{ and } D^2 = a^2 + b^2 + ab \text{ where } a, b \in \mathbb{Z}; \quad (2.2)$$

it means that  $D$  is attainable, i.e., there are sites  $\mathbf{x}, \mathbf{y} \in \mathbb{A}_2$  with  $\rho(\mathbf{x}, \mathbf{y}) = D$ . Assumption (2.2) does not restrict generality, as any other  $D' > 1$  can be replaced by the smallest  $D \geq D'$  satisfying (2.2) without changing the set  $\mathcal{A}$ .

Set  $\mathcal{A}$  is a closed subset in the Cartesian product  $\mathcal{X} := \{0, 1\}^{\mathbb{A}_2}$  (the set of all 0, 1-configurations) in the Tykhonov topology. For  $D = 1$ ,  $\mathcal{A} = \mathcal{X}$ .



The notion of an AC can be defined for any  $\mathbb{V} \subset \mathbb{A}_2$ ; accordingly, one can use the notation  $\mathcal{A}(\mathbb{V}) = \mathcal{A}(D, \mathbb{V})$ . The restriction of configuration  $\phi \in \mathcal{A}$  to  $\mathbb{V}$  is denoted by  $\phi \upharpoonright_{\mathbb{V}}$ .

We are interested in some particular probability measures  $\mu$  on  $(\mathcal{X}, \mathfrak{B}(\mathcal{X}))$  sitting on  $\mathcal{A}$  (i.e., such that  $\mu(\mathcal{A}) = \mu(\mathcal{X}) = 1$ ) where  $\mathfrak{B}(\mathcal{X})$  is the Borel  $\sigma$ -algebra in  $\mathcal{X}$ . As we repeatedly stressed, the measures of interest are extreme Gibbs/DLR, probability measures for high densities/large fugacities, which are formally defined below.

Let  $\mathbb{V} \subset \mathbb{A}_2$  be a finite set and  $\phi \in \mathcal{A}$ . We say that a finite configuration  $\psi^{\mathbb{V}} \in \mathcal{A}(\mathbb{V})$  is  $(\phi, \mathbb{V})$ -compatible if the concatenated configuration  $\psi^{\mathbb{V}} \vee (\phi \upharpoonright_{\mathbb{A}_2 \setminus \mathbb{V}}) \in \mathcal{A}$ . The set of  $(\phi, \mathbb{V})$ -compatible configurations is denoted by  $\mathcal{A}(\mathbb{V} \parallel \phi)$ .

Given  $u > 0$ , consider a probability measure  $\mu_{\mathbb{V}}(\cdot \parallel \phi)$  on  $\{0, 1\}^{\mathbb{V}}$  given by

$$\mu_{\mathbb{V}}(\psi^{\mathbb{V}} \parallel \phi) = \begin{cases} \frac{u^{\sharp(\psi^{\mathbb{V}}) - \sharp(\phi^{\mathbb{V}})}}{\mathbf{Z}(\mathbb{V} \parallel \phi)}, & \text{if } \psi^{\mathbb{V}} \in \mathcal{A}(\mathbb{V} \parallel \phi), \\ 0, & \text{if } \psi^{\mathbb{V}} \in \{0, 1\}^{\mathbb{V}} \setminus \mathcal{A}(\mathbb{V} \parallel \phi). \end{cases} \quad (2.3)$$

Here  $\sharp(\psi^{\mathbb{V}})$  and  $\sharp(\phi^{\mathbb{V}})$  stand for the number of particles in  $\psi^{\mathbb{V}}$  and  $\phi^{\mathbb{V}}$ :

$$\sharp(\psi^{\mathbb{V}}) := \#\{x \in \mathbb{V} : \psi(x) = 1\}, \quad \sharp(\phi^{\mathbb{V}}) := \#\{x \in \mathbb{V} : \phi(x) = 1\}.$$

Next,  $\mathbf{Z}(\mathbb{V} \parallel \phi)$  is the *partition function* in  $\mathbb{V}$  with the boundary condition  $\phi$ :

$$\mathbf{Z}(\mathbb{V} \parallel \phi) = \sum_{\psi^{\mathbb{V}} \in \mathcal{A}(\mathbb{V} \parallel \phi)} u^{\sharp(\psi^{\mathbb{V}}) - \sharp(\phi^{\mathbb{V}})}. \quad (2.4)$$

Measure  $\mu_{\mathbb{V}}(\cdot \parallel \phi)$  sits on  $\mathcal{A}(\mathbb{V} \parallel \phi)$ . Parameter  $u > 0$  is called *fugacity* or *activity* (of an occupied site).

A probability measure  $\mu$  on  $(\mathcal{X}, \mathfrak{B}(\mathcal{X}))$  is called a *D-H-C Gibbs/DLR measure* (in short, *D-H-C GM* or *GM* when the reference to  $D$  can be omitted) if (i)  $\mu(\mathcal{A}) = 1$ , (ii)  $\forall$  finite  $\mathbb{V} \subset \mathbb{A}_2$  and a function  $f : \phi \in \mathcal{X} \mapsto f(\phi) \in \mathbb{C}$  depending only on the restriction  $\phi \upharpoonright_{\mathbb{V}}$ , the integral  $\mu(f) = \int_{\mathcal{X}} f(\phi) d\mu(\phi)$  has the form

$$\mu(f) = \int_{\mathcal{X}} \int_{\{0,1\}^{\mathbb{V}}} f(\psi^{\mathbb{V}} \vee \phi \upharpoonright_{\mathbb{A}_2 \setminus \mathbb{V}}) d\mu_{\mathbb{V}}(\psi^{\mathbb{V}} \parallel \phi) d\mu(\phi). \quad (2.5)$$

One can say that under such measure  $\mu$ , the probability of a configuration  $\psi^{\mathbb{V}}$  in a finite volume  $\mathbb{V} \subset \mathbb{A}_2$ , conditional on a configuration  $\phi \upharpoonright_{\mathbb{A}_2 \setminus \mathbb{V}}$ , coincides with  $\mu_{\mathbb{V}}(\psi^{\mathbb{V}} \parallel \phi)$ , for  $\mu$ -a.a.  $\phi \in \{0, 1\}^{\mathbb{H}_2}$ .

In the literature, equality (2.5) is often referred to as the DLR equation for a measure  $\mu$  (in fact, it represents a system of equations labeled by  $\mathbb{V}$  and  $f$ ). For the general theory of Gibbs measures, see the monograph [11], Chapters 3, 4, 5–8.

The *D-H-C GMs* form a *Choquet simplex* (in the weak-convergence topology on the set of probability measures on  $(\mathcal{X}, \mathfrak{B}(\mathcal{X}))$ ), which we denote by  $\mathcal{G} = \mathcal{G}(D, u, \mathbb{A}_2)$ . An *extreme D-H-C GM*  $\mu$  is a *D-H-C GM* which does not admit a non-trivial decomposition  $\mu = a\mu^{(1)} + (1-a)\mu^{(2)}$  in terms of other *D-H-C GMs*  $\mu^{(i)}$ ,  $i = 1, 2$ , with  $a \in (0, 1)$ . As was said, the extreme *D-H-C GMs* (*D-EGMs* or briefly *EGMs*) represent pure phases. The collection of *D-EGMs* is denoted by  $\mathcal{E}(D) = \mathcal{E}(D, u, \mathbb{A}_2)$ . (Argument  $u$  will be systematically omitted.) Any *D-H-C Gibbs measure*  $\mu$  is a barycenter/mixture for some unit mass distribution over  $\mathcal{E}(D)$ .

**Remark 2.1.** The simplest version of the partition function is  $\Xi(\mathbb{V}||\emptyset)$ , with an empty boundary condition:

$$\mathbf{Z}(\mathbb{V}||\emptyset) = \sum_{\psi^{\mathbb{V}} \in \mathcal{A}(\mathbb{V})} u^{\sharp(\psi^{\mathbb{V}})}. \quad (2.6)$$

Despite a straightforward (and appealing) form of  $\Xi(\mathbb{V}||\emptyset)$ , it is not always convenient (or at least not the most convenient) for the rigorous analysis in the *thermodynamic limit*, for a sequence of volumes  $\mathbb{V}_k \nearrow \mathbb{A}_2$  in the Van Hove sense. The corresponding limit Gibbs measure (if it exists) depends on the particular shape of volumes  $\mathbb{V}_k$  which can be in a ‘good’ or ‘bad’ agreement with *symmetries* of the hard-core model on  $\mathbb{A}_2$ . In this paper we concentrate on the partition function  $\Xi(\mathbb{V}||\varphi)$  with a PGS boundary condition  $\varphi$ . We also analyze a periodic version of (2.6).  $\blacktriangle$

A *ground state*  $\varphi \in \mathcal{A}(D)$  in the H-C model with  $u > 1$  is defined by the property that one cannot remove finitely many particles from  $\varphi$  and replace them by a larger number of particles without breaking  $D$ -admissibility. In other words, one cannot find a finite subset  $\mathbb{V} \subset \mathbb{A}_2$  and a configuration  $\psi^{\mathbb{V}} \in \mathcal{A}(\mathbb{V}||\varphi)$  such that  $\sharp\psi^{\mathbb{V}} > \sharp\varphi \upharpoonright_{\mathbb{V}}$ .

A crucial role belongs to *periodic ground states* (PGSs). A  $D$ -AC  $\phi \in \mathcal{A}$  is said to be periodic if there exist two linearly independent vectors  $\mathbf{e}^{(1)}, \mathbf{e}^{(2)} \in \mathbb{A}_2$  such that  $\phi(\mathbf{x}) = \phi(\mathbf{x} + \mathbf{e}^{(i)}) \forall \mathbf{x} \in \mathbb{A}_2, i = 1, 2$ . In terms of  $\mathbb{A}_2$ -shifts  $\mathbf{T}_{\mathbf{u}}$  it means that  $\mathbf{T}_{\mathbf{e}^{(i)}}\phi = \phi$  for  $i = 1, 2$ . The collection of PGSs for a given  $D$  is denoted by  $\mathcal{P}(= \mathcal{P}(D) = \mathcal{P}(D, \mathbb{A}_2))$ .

The PGSs on  $\mathbb{A}_2$  are relatively straightforward and obtained from  $D$ -sub-lattices.

Now we turn to arithmetic properties of a given  $D$ . Any ordered pair of integers  $(a, b)$  which is a solution to equation (2.2) defines a  $D$ -sub-lattice of  $\mathbb{A}_2$  containing the origin and the following 6 sites:

$$(-a, b), (b, a + b), (a + b, a), (a, -b), (-b, a + b), (a + b, -a), \quad (2.7)$$

which all are the solutions to (2.2) as ordered pairs of integers. If  $ab = 0$  or  $a = b$  then the pair  $(a, b)$  defines a single  $D$ -sub-lattice of  $\mathbb{A}_2$  which is mapped into itself under the reflection  $\mathbf{R}$  (Class TA1). If  $ab \neq 0$  and  $a \neq b$  then the pair  $(b, a)$  also defines a  $D$ -sub-lattice of  $\mathbb{A}_2$  which is a reflection by  $\mathbf{R}$  of the sub-lattice defined by  $(a, b)$  (Classes TA2 and TB). For each  $D$ -sub-lattice of  $\mathbb{A}_2$  generated by a solution to (2.2) there are exactly  $D^2$  distinct  $\mathbb{A}_2$ -shifts  $\mathbf{T}_{\mathbf{u}}$  as there are exactly  $D^2$  lattice sites inside the fundamental parallelogram of the  $D$ -sub-lattice. All shifted configurations are PGSs. Moreover, all PGSs corresponding to a given  $D$  are obtained as  $\mathbb{A}_2$  shifts of  $D$ -sub-lattices generated by the solutions to (2.2).

## 2.2 The H-C model on $\mathbb{H}_2$

Formally,  $\mathbb{H}_2$  can be defined as the set-theoretical difference where we remove, from lattice  $\mathbb{A}_2$ , the sub-lattice  $\mathbb{A}_2(\sqrt{3})$  with a fundamental parallelogram  $\{(0, 0), (1, 2), (2, 1), (1, -1)\}$ :

$$\begin{aligned} \mathbb{H}_2 &= \mathbb{A}_2 \setminus \mathbb{A}_2(\sqrt{3}), \\ \text{where } \mathbb{A}_2(\sqrt{3}) &= \left\{ m \cdot (1, 2) + n \cdot (2, 1) : m, n \in \mathbb{Z} \right\}. \end{aligned} \quad (2.8)$$

Equivalently,

$$\mathbb{H}_2 = \mathbb{T}_{(1,0)}\mathbb{A}_2(\sqrt{3}) \cup \mathbb{T}_{(0,1)}\mathbb{A}_2(\sqrt{3}). \quad (2.9)$$

Each site in  $\mathbb{H}_2$  has three neighboring sites, at the Euclidean distance 1. Lattice  $\mathbb{A}_2$  is represented as the union of three disjoint congruent subsets:  $\mathbb{A}_2 = \mathbb{A}_2(\sqrt{3}) \cup \mathbb{T}_{(1,0)}\mathbb{A}_2(\sqrt{3}) \cup \mathbb{T}_{(0,1)}\mathbb{A}_2(\sqrt{3})$ . If  $D^2 \equiv 0 \pmod{3}$  then all 3 vertices of an equilateral  $\mathbb{A}_2$ -triangle  $\triangle$  with the side-length  $D$  lie in the same subset. Otherwise  $D^2 \equiv 1 \pmod{3}$ , and all vertices of  $\triangle$  lie in different subset. Hence, for every L\"oschian number  $D^2$  there are pairs of vertices  $\mathbf{x}, \mathbf{x}' \in \mathbb{H}_2$  for which  $\rho(\mathbf{x}, \mathbf{x}') = D$ .

Lattice  $\mathbb{A}_2$  is represented as a non-disjoint union

$$\mathbb{A}_2 = \mathbb{H}_2 \cup (\mathbb{T}_{(-1,0)}\mathbb{H}_2) = \mathbb{H}_2 \cup (\mathbb{T}_{(1,0)}\mathbb{H}_2). \quad (2.10)$$

As above, we use the notation  $\mathbf{x} = (x; x') \in \mathbb{H}_2$  and  $\mathbf{x} \simeq (m, n) \in \mathbb{H}_2$ .

We use the term an  $\mathbb{H}_2$ -shift for any  $\mathbb{A}_2$ -shift  $\mathbb{T}_{\mathbf{u}}$  where  $\mathbf{u} \simeq (m, n)$  has both  $u_1, u_2$  divisible by 3. Also,  $\mathbf{R}$  stands for the reflection about the horizontal axis:  $\mathbf{R}\mathbf{x} = (n - m, -m)$  for  $\mathbf{x} = (m, n) \in \mathbb{H}_2$ .

The definitions of admissible configurations, compatibility, partition functions, Gibbs measures and extreme Gibbs measures on  $\mathbb{H}_2$  are similar to those on  $\mathbb{A}_2$ , and we do not repeat them. We also continue using a similar notation  $\mathcal{A} = \mathcal{A}(D, \mathbb{H}_2)$ ,  $\mathcal{A}(\mathbb{V}) = \mathcal{A}(D, \mathbb{V})$ ,  $\mathcal{A}(\mathbb{V}|\phi)$ . The definition of a ground state and a periodic ground state on  $\mathbb{H}_2$  are direct repetitions of their counterparts on  $\mathbb{A}_2$ .

As in the case of  $\mathbb{A}_2$ , the crucial notion is a periodic ground state (PGS). However, on  $\mathbb{H}_2$  a PGS is not necessarily obtained from a sub-lattice (although it is the case for Classes HA, HB and HC). The set of PGSs for a given value  $D$  is again denoted by  $\mathcal{P}(D) = \mathcal{P}(D, \mathbb{H}_2)$  and that of EGMs by  $\mathcal{E}(D) = \mathcal{E}(D, u, \mathbb{H}_2)$ , respectively. (As above, argument  $u$  will be systematically omitted.)

## 3 Main theorems

### 3.1 Templates. Contour definitions

First, let us consider the case of  $\mathbb{A}_2$ . For a given  $D$ , *templates*  $F_{k,l} = F_{k,l}^{\mathbb{A}_2}$  are defined by

$$F_{k,l} := \{(m, n) \in \mathbb{A}_2 : kD^2 \leq m < (k+1)D^2, lD^2 \leq n < (l+1)D^2\}, \quad k, l \in \mathbb{Z}. \quad (3.1)$$

Each template contains  $D^4$  points. Note that sites  $(kD^2, lD^2)$  form a sub-lattice  $\mathbb{A}_2(D^2)$ , and all  $D$ -PGSs are periodic relative to it.

The family  $\{F_{k,l}\}$  forms a partition of  $\mathbb{A}_2$ . The template  $F_{0,0}$ , treated as a  $D^2 \times D^2$ -torus, is partitioned into  $D^2$  rhombuses, one partition for each PGS-equivalence class. We frequently omit the indices  $k, l$  in the notation for a template when their values are not important or are evident from the context. Figure 10 shows examples of templates.

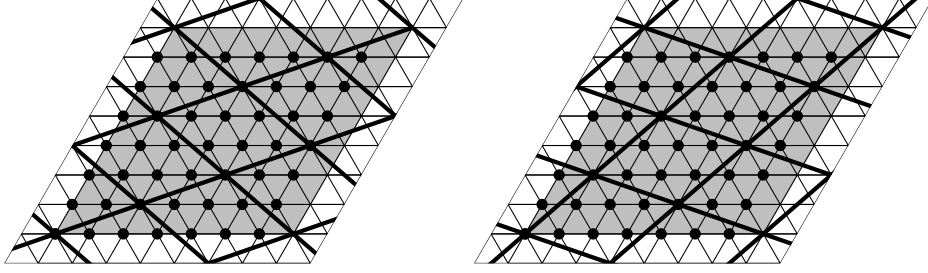


Figure 10: The template (black circles) and  $D$ -rhombuses (thick lines) on  $\mathbb{A}_2$ , for  $D^2 = 7$ .

The gray rhombus represents a fundamental parallelogram for sub-lattice  $\mathbb{A}_2(D^2)$ .

In what follows, we suppose that volume  $\mathbb{V} \subset \mathbb{A}_2$  is a finite union of templates; such a set  $\mathbb{V}$  is called a *basic lattice polygon* (briefly, a basic polygon).

Given a PGS  $\varphi \in \mathcal{P}$  and a basic polygon  $\mathbb{V} \subset \mathbb{A}_2$ , the partition function  $\mathbf{Z}(\mathbb{V} \parallel \varphi)$  in (2.4) gives rise to a Gibbs probability distribution  $\mu_{\mathbb{V}}(\cdot \parallel \varphi)$  on  $\{0, 1\}^{\mathbb{V}}$  concentrated on  $\mathcal{A}(\mathbb{V} \parallel \varphi)$ . We say a PGS  $\varphi \in \mathcal{P}$  *generates* a GM  $\mu_{\varphi}$  if,  $\forall$  sequence of basic polygons  $\mathbb{V}_k \nearrow \mathbb{A}_2$  satisfying the Van Hove condition,

$$\mu_{\varphi} = \lim_{k \rightarrow \infty} \mu_{\mathbb{V}_k}(\cdot \parallel \varphi). \quad (3.2)$$

Equivalently, we say that  $\mu_{\varphi}$  is *generated* by  $\varphi$ .

A specific construction of a GM exploits periodic boundary conditions, in toric volumes  $\mathbb{V}_k = \mathbb{T}(k)$ ,  $k = 1, 2, \dots$ . Here  $\mathbb{T}(k) = \mathbb{T}^{\mathbb{A}_2}(k)$  is given by

$$\mathbb{T}(k) = \{(m, n) \in \mathbb{A}_2 : -kD^2 \leq m < kD^2, -kD^2 \leq n < kD^2; \text{ with identification } (kD^2, n) \equiv (-kD^2, n) \text{ and } (m, kD^2) \equiv (m, -kD^2)\}. \quad (3.3)$$

To determine the admissible configurations in a torus we use the condition that  $\rho^{(k)}(\mathbf{x}, \mathbf{y}) \geq D$ . Here the metric  $\rho^{(k)}$  is the toric metric on  $\mathbb{T}(k)$  defined by

$$\rho^{(k)}(\mathbf{x}, \mathbf{y}) = \left[ \rho_1^{(k)}(x_1, y_1)^2 + \rho_1^{(k)}(x_2, y_2)^2 \right]^{1/2},$$

where  $\mathbf{x} = (x_1, x_2)$ ,  $\mathbf{y} = (y_1, y_2)$ . In turn,  $\rho_1^{(k)}$  is a metric on the interval  $[-kD^2, kD^2]$ , with  $\rho_1^{(k)}(x, y) = \min \{y - x, x + 2kD^2 - y\}$  for  $-kD^2 \leq x \leq y < kD^2$ . The set of admissible configurations in  $\mathbb{T}(k)$  is denoted by  $\mathcal{A}_{\text{per}, k} = \mathcal{A}_{\text{per}, k}(\mathbb{T}(k))$ . In the same spirit as (2.6), the partition function in  $\mathbb{T}(k)$  with periodic boundary condition is determined by

$$\mathbf{Z}_{\text{per}}(\mathbb{T}(k)) = \sum_{\phi_{\mathbb{T}(k)} \in \mathcal{A}_{\text{per}, k}} \prod_{\mathbf{x} \in \mathbb{T}(k)} u^{\phi_{\mathbb{T}(k)}(\mathbf{x})}. \quad (3.4)$$

This in turn defines the Gibbs distribution  $\mu_{\text{per}, k}$ . Next, we set

$$\mu_{\text{per}} = \lim_{k \rightarrow \infty} \mu_{\text{per}, k} \quad (3.5)$$

provided that the limit measure exists.

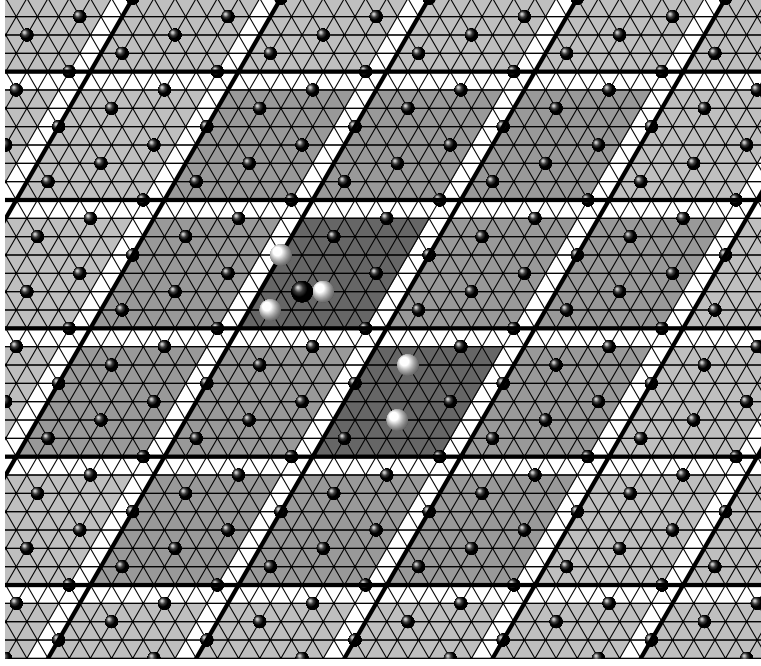


Figure 11: Templates:  $\varphi$ -correct (light-gray) and non- $\varphi$ -correct (medium- and dark-gray), on  $\mathbb{A}_2$ , in a  $D$ -AC for  $D^2 = 7$ .

Figure 11 demonstrates various types of templates. The small black balls indicate occupied sites in a  $D$ -PGS  $\varphi$ . The large black ball together with the small black balls indicate occupied sites  $D$ -AC  $\phi$ . The white balls mark vacant sites in  $\phi$  which would be occupied in  $\varphi$ . The light-gray color indicates  $\varphi$ -correct templates. The dark-gray color indicates non- $\varphi$ -correct templates containing some defects (where  $\phi(\mathbf{x}) \neq \varphi(\mathbf{x})$  for some site  $\mathbf{x}$ ). Over the medium-gray templates, configurations  $\phi$  and  $\varphi$  coincide. However, these templates are still not  $\varphi$ -correct as they have neighboring templates with defects.

The concept of a template can be extended without changes to the case of  $\mathbb{H}_2$  when  $D^2$  is from Classes HA, HB or HC (where the PGSs are  $\alpha$ -configurations). Here templates  $F_{k,l} = F_{k,l}^{\mathbb{H}_2}$  are defined by (3.1) with the requirement  $(m,n) \in \mathbb{H}_2$ ; in other words,  $F_{k,l}^{\mathbb{H}_2} = F_{k,l}^{\mathbb{A}_2} \cap \mathbb{H}_2$ . (Of course, in Class HC the number  $D$  has to be replaced by  $D^*$ .) Then the torus  $\mathbb{T}(k) = \mathbb{T}^{\mathbb{H}_2}(k)$  is introduced, as  $\mathbb{T}^{\mathbb{H}_2}(k) = \mathbb{T}^{\mathbb{A}_2}(k) \cap \mathbb{H}_2$  where  $\mathbb{T}^{\mathbb{A}_2}(k)$  is defined in (3.3). The set  $\mathcal{A}_{\text{per},k}$  and measures  $\mu_{\text{per},k}$  and  $\boldsymbol{\mu}_{\text{per}}$  are defined as above: see (3.4) and (3.5).

For the exceptional values  $D^2$ , the above construction needs the following modifications. For each PGS  $\varphi$  we have a period parallelogram  $\Pi(\varphi)$  with sides  $\mathbf{e}^{(1)}(\varphi) = (e_1^{(1)}(\varphi), e_2^{(1)}(\varphi))$  and  $\mathbf{e}^{(2)}(\varphi) = (e_1^{(2)}(\varphi), e_2^{(2)}(\varphi))$  where  $\mathbf{T}_{\mathbf{e}^{(i)}(\varphi)}\varphi = \varphi$ ,  $i = 1, 2$ :

$$\Pi(\varphi) = \left\{ (m,n) \in \mathbb{H}_2 : (m,n) = \epsilon_1 \mathbf{e}^{(1)}(\varphi) + \epsilon_2 \mathbf{e}^{(2)}(\varphi) \text{ for } 0 \leq \epsilon_i < 1, i = 1, 2 \right\}.$$

Template  $F_{0,0} = F_{0,0}^{\mathbb{H}_2}$  for an exceptional  $D^2$  can be defined as a parallelogram

$$F_{0,0} = \left\{ (m,n) \in \mathbb{H}_2 : (m,n) = \epsilon_1 \bar{\mathbf{e}}^{(1)}(D) + \epsilon_2 \bar{\mathbf{e}}^{(2)}(D) \text{ for } 0 \leq \epsilon_i < 1, i = 1, 2 \right\}. \quad (3.6)$$

Here  $\bar{\mathbf{e}}^{(i)}(D) = (\bar{e}_1^{(i)}(D), \bar{e}_2^{(i)}(D))$ ,  $\bar{e}_j^{(i)}(D) = \text{LCM}\{e_j^{(i)}(\varphi) : \varphi \in \mathcal{P}(D)\}$ ,  $i, j = 1, 2$ . Finally, we set  $F_{k,l} = T_{k\bar{\mathbf{e}}^{(1)}(D) + l\bar{\mathbf{e}}^{(2)}(D)} F_{0,0}$ ,  $k, l \in \mathbb{Z}$ , to form a partition of  $\mathbb{H}_2$ .

Pictorially, each PGS  $\varphi$  is periodic relative to the sub-lattice defined by vectors  $\mathbf{e}^{(i)}(\varphi)$ ,  $i = 1, 2$ . Template  $F_{0,0} = F_{0,0}^{\mathbb{H}_2}$  is the fundamental parallelogram for the lattice, that is, the intersection of the above lattices for all  $\varphi \in \mathcal{P}(D)$ .

Let  $\varphi \in \mathcal{P}(D)$  be a  $D$ -PGS and  $\phi \in \mathcal{A}(D)$  be an admissible configuration, on  $\mathbb{A}_2$  or  $\mathbb{H}_2$ . Following the definition of correctness on P. 561 in [26] we say that a template  $F_{k,l}$  is  $\varphi$ -correct in  $\phi$  if  $\phi(\mathbf{x}) = \varphi(\mathbf{x})$  for every site  $\mathbf{x}$  lying in 9 templates  $F_{k+i,l+j}$ , where  $i, j = -1, 0, 1$ . The 9 templates include the initial template  $F_{k,l}$  and 8 neighboring templates considered as connected to  $F_{k,l}$ . Cf. Figure 11.

A *contour support* in a configuration  $\phi \in \mathcal{A}$  is defined as a connected component of the union of templates which are not  $\varphi$ -correct in  $\phi$  for any  $\varphi \in \mathcal{P}$ . A *contour* in  $\phi$  is defined as a pair

$$\Gamma = (\text{Supp}(\Gamma), \phi \upharpoonright_{\text{Supp}(\Gamma)}) \quad (3.7)$$

consisting of a contour support  $\text{Supp}(\Gamma)$  and the restriction  $\phi \upharpoonright_{\text{Supp}(\Gamma)}$ . These definitions are specifications, for the H-C model, of general definitions on P. 561 in [26]. Accordingly, we define sets  $\text{Int}(\Gamma)$ ,  $\text{Int}_\varphi(\Gamma)$  and  $\text{Ext}(\Gamma)$  by using Eqn (1.5) from [26].

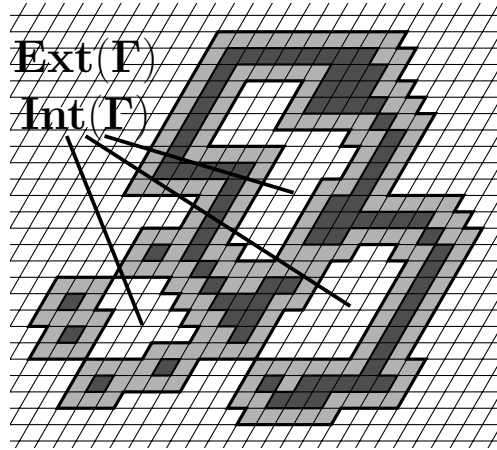


Figure 12: A contour support (the union of gray and dark-gray templates).

Here the internal area  $\text{Int}(\Gamma)$  includes three components  $\text{Int}_{\varphi_i}(\Gamma)$ . The boundary layers are shown as the union of gray templates.

Inside each of  $\text{Ext}(\Gamma)$ ,  $\text{Supp}(\Gamma)$  and  $\text{Int}_\varphi(\Gamma)$  we can specify a *boundary layer*: it is a connected set of templates where each parallelogram has a neighboring template outside the corresponding  $\text{Ext}(\Gamma)$ ,  $\text{Supp}(\Gamma)$ , or  $\text{Int}_\varphi(\Gamma)$ . Each of  $\text{Ext}(\Gamma)$  and  $\text{Int}_\varphi(\Gamma)$  has a single corresponding boundary layer while  $\text{Supp}(\Gamma)$  has several of them. Every boundary layer in  $\text{Supp}(\Gamma)$  has a corresponding (dual) boundary layer inside  $\text{Ext}(\Gamma)$  or  $\text{Int}_\varphi(\Gamma)$ . Moreover, in every boundary layer all occupied sites belong to the same  $\varphi$  (which justifies the notation  $\text{Int}_\varphi(\Gamma)$ ). Finally, following Eqn (1.5) from [26], a contour for which a boundary layer of  $\text{Ext}(\Gamma)$  belongs to the PGS  $\varphi$  is called a  $\varphi$ -contour. See Figure 12.

Physically speaking, a  $\varphi$ -contour emerges when we add to  $\varphi$  an amount of particles at some ‘inserted’ sites and simultaneously remove the particles from  $\varphi$  which are ‘repelled’ by the inserted particles. The latter will be referred to as removed sites/particles. The whole procedure should of course maintain admissibility. In fact, for any attainable  $D^2$  on  $\mathbb{A}_2$  and any attainable  $D^2 \neq 4, 7, 31, 133$  on  $\mathbb{H}_2$  for  $u$  large enough, every EGM  $\mu$  has the property that, with  $\mu$ -probability 1 the AC  $\phi$  has no infinite contours. Cf. Theorem III(iv) in Section 3.2.

Let  $\mathbb{V}$  be a basic polygon and  $\varphi \in \mathcal{P}$  be a PGS. Then the partition function  $\mathbf{Z}(\mathbb{V}||\varphi)$  can be written in the form

$$\mathbf{Z}(\mathbb{V}||\varphi) = \sum_{\{\Gamma_i\} \text{ in } \mathbb{V}} \prod_i w(\Gamma_i) \quad (3.8)$$

Here and below,  $w(\Gamma)$  stands for the statistical *weight* of contour  $\Gamma$ :

$$w(\Gamma) = u^{\#(\psi_\Gamma) - \#(\varphi_\Gamma)}. \quad (3.9)$$

Further, the summation in Eqn (3.8) is extended to collections of contours  $\Gamma_i$  in  $\mathbb{V}$  compatible in the sense of the (general) PS theory; cf. [24], [26]. Here we say that  $\Gamma$  is a contour in  $\mathbb{V}$  if the set  $\text{Supp}(\Gamma) \setminus \mathbb{V}$  is empty or lies in the boundary layer of  $\text{Ext}(\Gamma)$ .

### 3.2 Pirogov–Sinai theory for the H-C model

In Theorems I and II below we summarize our results on PGSs and EGMs on both lattices,  $\mathbb{A}_2$  and  $\mathbb{H}_2$ . These theorems form a prerequisite for the use of the PS theory. Applying the PS theory, we obtain Theorem III which holds true for all Classes of  $D$  except for HS. In Theorems 1–13 we identify the PGSs and the EGMs for the respective Classes of values of  $D$ .

**Theorem I. (i)** *For any attainable  $D > 1$ , the set  $\mathcal{P}(D, \mathbb{A}_2)$  consists of  $D$ -sub-lattices and their shifts and reflections. In particular, set  $\mathcal{P}(D, \mathbb{A}_2)$  is finite.*

**(ii)** *For any attainable non-sliding  $D > 1$ , the set  $\mathcal{P}(D, \mathbb{H}_2)$  is finite. If  $D^2$  is from Classes HA or HB then  $\mathcal{P}(D, \mathbb{H}_2)$  consists of  $(\alpha, D)$ -configurations. If  $D^2$  is from Class HC then  $\mathcal{P}(D, \mathbb{H}_2)$  consists of  $(\alpha, D^*)$ -configurations. If  $D^2$  is from Class HD1 then  $\mathcal{P}(D, \mathbb{H}_2)$  consists of  $(\beta, D)$ -configurations. If  $D^2$  is from Class HD2 then  $\mathcal{P}(D, \mathbb{H}_2)$  consists of  $(\gamma, D)$ -configurations. For  $D^2 = 67$  (Class HE), set  $\mathcal{P}(D, \mathbb{H}_2)$  consists of  $(\beta, D)$ - and  $(\alpha, D^*)$ -configurations where  $(D^*)^2 = 75$ .*

The proof of Theorem I involves the material of Section 4 and completed in Section 4.6.

Let us define

$$S = S(D) = D^2\sqrt{3}/2 = 2 \times \left( \text{the area of a } D\text{-triangle} \right). \quad (3.10)$$

Next, for exceptional non-sliding values  $D^2 = 13, 16, 28, 49, 64, 67, 97, 157, 256$  on  $\mathbb{H}_2$  we set:

$$\begin{aligned} S^{\text{RD}}(\sqrt{13}) &= 16.5\sqrt{3}/2, \quad S^{\text{RD}}(\sqrt{16}) = 20.25\sqrt{3}/2, \quad S^{\text{RD}}(\sqrt{28}) = 33\sqrt{3}/2, \\ S^{\text{RD}}(\sqrt{49}) &= 55.5\sqrt{3}/2, \quad S^{\text{RD}}(\sqrt{64}) = 72\sqrt{3}/2, \quad S^{\text{RD}}(\sqrt{67}) = 75\sqrt{3}/2, \\ S^{\text{RD}}(\sqrt{97}) &= 106.5\sqrt{3}/2, \quad S^{\text{RD}}(\sqrt{157}) = 169.5\sqrt{3}/2, \quad S^{\text{RD}}(\sqrt{256}) = 272.25\sqrt{3}/2. \end{aligned} \quad (3.11)$$

Here the notation  $S^{\text{RD}}(D)$  refers to a minimal re-distributed triangle area for a given value  $D$  from the above list. The general concept of a re-distributed area will be introduced in Section 4.2.

The Peierls bound is established in Theorem II below. It refers to the quantity

$$\|\text{Supp}(\Gamma)\| := \text{the number of (incorrect) templates in } \text{Supp}(\Gamma). \quad (3.12)$$

**Theorem II.** *(The Peierls bound for contours) The weight  $w(\Gamma)$  of contour  $\Gamma = (\text{Supp}(\Gamma), \phi \upharpoonright_{\text{Supp}(\Gamma)})$  obeys the bound*

$$w(\Gamma) \leq u^{-p\|\text{Supp}(\Gamma)\|}. \quad (3.13)$$

Here  $p > 0$  (the Peierls constant) satisfies

- on  $\mathbb{A}_2$ :

$$p = p(D, \mathbb{A}_2) \geq \sqrt{3}/(288S(D)), \quad (3.14)$$

- on  $\mathbb{H}_2$ :

$$p = p(D, \mathbb{H}_2) \geq \sqrt{3}/(288S(D)), \text{ if } D^2 \text{ falls in Class HA or HB,} \quad (3.15)$$

$$p = p(D, \mathbb{H}_2) \geq \sqrt{3}/(288S(D^*)), \text{ if } D^2 \text{ falls in Class HC, where } (D^*)^2 \text{ is the closest L\"{o}schan number with } (D^*)^2 > D^2 \text{ such that } 3 \mid (D^*)^2, \quad (3.16)$$

$$p = p(D, \mathbb{H}_2) \geq \sqrt{3}/(288S^{\text{RD}}(D)) \text{ for } D^2 = 13, 16, 28, 49, 64, 67, 97, 157, 256 \text{ (Classes HD, HE).} \quad (3.17)$$

**Remark 3.1.** The bounds upon  $p$  in Eqns (3.14)–(3.17) are far from optimal and have been selected in a universal form for simplicity. The value  $p$  can be improved at an expense of additional technicalities. ▲

The proof of Theorem II starts in Section 4 and is completed in Section 5.1.

**Theorem III.** *For all  $D$  exists a value  $u_0(D, \mathbb{A}_2) \in (0, \infty)$ , and for all  $D \neq 4, 7, 31, 133$  exists a value  $u_0(D, \mathbb{H}_2) \in (0, \infty)$  such that, for  $u \geq u_0(D, \cdot)$ , on  $\mathbb{A}_2$  or  $\mathbb{H}_2$ , respectively, the following assertions hold true.*

- (i) *Each EGM  $\mu \in \mathcal{E}(D)$  is generated by a PGS. That is, each EGM is of the form  $\mu_\varphi$  for some  $\varphi \in \mathcal{P}(D)$ . If PGSs  $\varphi_i$  generate EGMs  $\mu_{\varphi_i}$ ,  $i = 1, 2$ , and  $\varphi_1 \neq \varphi_2$  then  $\mu_{\varphi_1} \perp \mu_{\varphi_2}$ . The EGMs inherit symmetries between the PGSs: if PGSs  $\varphi_i$  generate EGMs  $\mu_{\varphi_i}$ ,  $i = 1, 2$ , and  $\varphi_1 = T_{\mathbf{u}}\varphi_2$  or  $\varphi_1 = R\varphi_2$  then  $\mu_{\varphi_1} = T_{\mathbf{u}}\mu_{\varphi_2}$  or  $\mu_{\varphi_1} = R\mu_{\varphi_2}$ , respectively.*
- (ii) *EGM-generation is a class property: if a  $\varphi \in \mathcal{P}(D)$  generates an EGM  $\mu_\varphi$  then every PGS  $\tilde{\varphi}$  from the same PGS-equivalence class generates an EGM  $\mu_{\tilde{\varphi}}$ . Such a class is referred to as dominant. If an equivalence class is unique, it is dominant.*
- (iii) *Measure  $\mu_{\text{per}}$  exists and is a uniform mixture of the measures  $\mu_\varphi$  where  $\varphi$  runs through all dominant PGS-equivalence classes. If there is a single equivalence class then  $\mu_{\text{per}}$  is a uniform mixture of all measures  $\mu_\varphi$  where  $\varphi \in \mathcal{P}$ .*



- (iv) Each EGM  $\mu_\varphi$  exhibit the following properties. For  $\mu_\varphi$ -almost all  $\phi \in \mathcal{A}$ :
- (A) All contours  $\Gamma$  in  $\phi$  are finite.
  - (B) For any site  $\mathbf{x}$  there exist only finitely many contours  $\Gamma$  (possibly none) such that  $\mathbf{x} \in \text{Int}(\Gamma) \cup \text{Supp}(\Gamma)$ .
  - (C) There are countably many disjoint connected sets of  $\varphi$ -correct templates one of which is infinite and all remaining ones are finite.
  - (D) For any  $\varphi' \in \mathcal{P} \setminus \{\varphi\}$ , there are countably many disjoint connected sets of  $\varphi'$ -correct templates, and they all are finite.
- (v) Measure  $\mu_\varphi$  admits a polymer expansion and consequently has an exponential decay of correlations.
- (vi) As  $u \rightarrow \infty$ , measure  $\mu_\varphi$  converges weakly to a measure sitting on a single AC  $\varphi$ .

**Proof of Theorem III.** (i, ii) According to Corollary on P. 565 in [26], there exists at least one PGS  $\varphi \in \mathcal{P}(D)$  which generates an EGM  $\mu_\varphi \in \mathcal{E}(D)$ . It is obvious that every PGS  $\tilde{\varphi}$  from the same equivalence class generates an EGM  $\mu_{\tilde{\varphi}}$  and that EGMs  $\mu_\varphi, \mu_{\tilde{\varphi}}$  are related with the same symmetry as PGSs  $\varphi, \tilde{\varphi}$ . The fact that each EGM  $\mu$  is generated by a PGS follows from Corollary on P. 578 in [26], completed with Theorem 1 from [9]. The mutual singularity of measures  $\mu_{\varphi_1}$  and  $\mu_{\varphi_2}$  for  $\varphi_1 \neq \varphi_2$  can be deduced from assertion (iv) which is deduced from [26] below.

Passing to assertion (iii), the main concern is the existence of contours *winding* around the torus  $\mathbb{T}_k$ . However, the  $\mu_{\text{per},k}$ -probability of the event  $\mathcal{W}_k \subset \mathcal{A}_{\text{per},k}$  that such contour is present in an admissible configuration  $\phi_{\mathbb{T}_k^{(1)}}$  becomes negligible as  $k \rightarrow \infty$ , as winding contours are too large. On the remaining event,  $\overline{\mathcal{W}}_k = \mathcal{A}_{\text{per},k} \setminus \mathcal{W}_k$ , the statistics of the random configuration is described in terms of the ensemble of *external contours*. Furthermore, event  $\overline{\mathcal{W}}_k$  can be partitioned into  $\#\mathcal{E}$  parts,  $\overline{\mathcal{W}}_{k,\mu_\varphi}, \mu_\varphi \in \mathcal{E}$ , so that on  $\overline{\mathcal{W}}_{k,\mu_\varphi}$  all external contours are  $\varphi$ -contours, and each  $\overline{\mathcal{W}}_{k,\mu_\varphi}$  will have the same limit probability:

$$\lim_{k \rightarrow \infty} \mu_{\text{per},k}(\overline{\mathcal{W}}_{k,\mu_\varphi}) = \frac{1}{\#\mathcal{E}}. \quad \left( \text{Here we use the property that the ratio } \frac{\mu_{\text{per},k}(\overline{\mathcal{W}}_{k,\mu_\varphi})}{\mu_{\text{per},k}(\overline{\mathcal{W}}_{k,\mu_{\varphi'}})} \right.$$

tends to 1 as  $k \rightarrow \infty$  for any choice of EGMs  $\mu_\varphi, \mu_{\varphi'} \in \mathcal{E}$ . This follows from the contour representation for the sum  $\sum_{\phi_{\mathbb{T}(k)} \in \overline{\mathcal{W}}_{k,\mu_\varphi}} \prod_{\mathbf{x} \in \mathbb{T}_k} u^{\phi_{\mathbb{T}(k)}(\mathbf{x})} = \mathbf{Z}_{\text{per}}(\mathbb{T}(k)) \mu_{\text{per},k}(\overline{\mathcal{W}}_{k,\mu_\varphi}).$  This argument leads to the formula  $\lim_{k \rightarrow \infty} \mu_{\text{per},k} = \frac{1}{\#\mathcal{E}} \sum_{\mu_\varphi \in \mathcal{E}} \mu_\varphi.$

(iv) Statements (A, B) follow from the fact that in an EGM  $\mu_\varphi$ , the probability of a contour  $\Gamma$  is  $\leq u^{\|\text{Supp}(\Gamma)\|p(D)/3}$ . Cf. [26], Theorem on P. 564. In turn, (C, D) follow from (A, B).

Statements (v, vi) follow from [26], Theorem on P. 564. ■

In assertions Theorems 1–13 below we work under the condition  $u > u_0(D, \cdot)$  assumed in Theorem III.

### 3.3 PGSs and EGMs for Class TA

Here and below, we say that a sub-lattice in  $\mathbb{A}_2$  has type  $(a, b)$ , or is an  $(a, b)$ -sub-lattice when it is a  $D$ -sub-lattice generated by the sites  $(0, 0)$  and  $(a+b, -b)$ , where  $a, b \in \mathbb{Z}$ ,  $D^2 = a^2 + b^2 + ab$ . If  $ab = 0$ , the corresponding  $D$ -sub-lattice is horizontal; if  $a = b$ , it is vertical. In cases where  $ab \neq 0$  and  $a \neq b$ , we have inclined  $D$ -sub-lattices. Correspondingly, a PGS-equivalence class is called an  $(a, b)$ -class or class  $(a, b)$  if it contains a sub-lattice of type  $(a, b)$ . We denote this class by  $\mathcal{P}(a, b)$ , and its PGSs are called  $(a, b)$ -PGSs. We also use the term an  $\alpha$ -configuration and its specifications: a  $(D, \alpha)$ -configuration or  $((a, b), \alpha)$ -configuration, or  $\alpha$ -configurations of type  $(a, b)$ , intermittently.

**Theorem 1.** (Class TA1)

- (i) Let  $D$  be an integer not divisible by primes of the form  $3v + 1$ . Then in  $\mathbb{A}_2$  there is a unique  $D$ -sub-lattice which is horizontal and has type  $(D, 0)$ . Thus, on  $\mathbb{A}_2$  there is a single PGS-equivalence class, which contains  $D^2$  different PGSs. The PGSs are horizontal  $((D, 0), \alpha)$ -configurations, hence reflection-invariant. Different PGSs are obtained from each other by  $\mathbb{A}_2$ -shifts. Consequently, for such  $D$  the number of EGMs on  $\mathbb{A}_2$  equals  $D^2$ .
- (ii) Let  $D/\sqrt{3}$  be an integer not divisible by primes of the form  $3v + 1$ . Then in  $\mathbb{A}_2$  there is a unique  $D$ -sub-lattice which is vertical and has type  $(\frac{D}{\sqrt{3}}, \frac{D}{\sqrt{3}})$ . Thus, on  $\mathbb{A}_2$  there is a single PGS-equivalence class, which contains  $D^2$  different PGSs. The PGSs are vertical  $((\frac{D}{\sqrt{3}}, \frac{D}{\sqrt{3}}), \alpha)$ -configurations, hence reflection-invariant. Different PGSs are obtained from each other by  $\mathbb{A}_2$ -shifts. Consequently, for such  $D$  the number of EGMs on  $\mathbb{A}_2$  equals  $D^2$ .

**Theorem 2.** (Class TA2) Let  $D^2$  be an integer whose prime decomposition contains (i) a factor 3 in any power, (ii) primes of the form  $3v + 2$ , in even powers, possibly zero, and (iii) a single prime of the form  $3v + 1$ . Then in  $\mathbb{A}_2$  there are exactly two  $D$ -sub-lattices, which are inclined and taken to each other by reflections. Hence, on  $\mathbb{A}_2$  there is a single PGS-equivalence class, which contains  $2D^2$  PGSs. The PGSs are inclined  $(D, \alpha)$ -configurations, hence not reflection-invariant. Different PGSs are obtained from each other by  $\mathbb{A}_2$ -shifts and reflections. Consequently, for such  $D$  the number of EGMs on  $\mathbb{A}_2$  equals  $2D^2$ .

### 3.4 PGSs and EGMs for Class TB

For a generic  $D$  from Class TB, there are at least three  $D$ -sub-lattices among PGSs on  $\mathbb{A}_2$ .

**Theorem 3.** (Class TB) Suppose that the prime decomposition of  $D^2$  contains (i) a factor 3 in any power, (ii) primes of the form  $3v + 2$ , in even powers, possibly zero, and (iii)  $M \geq 2$  primes of the form  $3v + 1$ , some of which may coincide. Then the following assertions hold true.

- (i) The number of PGS-equivalence classes on  $\mathbb{A}_2$  is  $\geq 2$ , and it increases when  $\lceil M/2 \rceil$  increases.

- (ii) *At most one class contains  $D^2$  PGSs. It consists of horizontal  $(D, 0)$ -PGSs if  $D$  is integer, or of vertical  $(\frac{D}{\sqrt{3}}, \frac{D}{\sqrt{3}})$ -PGSs if  $D/\sqrt{3}$  is integer. All other equivalence classes contain two inclined  $D$ -sub-lattices and  $2D^2$  PGSs each; these sub-lattices are taken to each other by reflections.*
- (iii) *Furthermore, a measure  $\mu_\varphi$  is reflection-invariant iff the PGS  $\varphi$  comes from a dominant equivalence class of cardinality  $D^2$ .*
- (iv) *Let  $J = J(D, \mathbb{A}_2)$  denote the number of dominant equivalence classes labeled by  $1, \dots, J$  in an arbitrary order. Let  $m_j D^2$  stand for the number of PGSs in the dominant class  $j$ , where  $m_j = 1, 2$  and  $1 \leq j \leq J$ . Then the total number of EGMs equals  $D^2 \sum_{j=1}^J m_j$ .*

As we said earlier, we conjecture that the number of dominant classes  $J(D, \mathbb{A}_2) = 1$ . This is confirmed in several examples considered in Theorems 4-6 on  $\mathbb{A}_2$  and Theorem 10 on  $\mathbb{H}_2$ .

The analysis of dominance for selected examples of  $D^2$  from Class TB is given in Theorems 4–6. For these examples, we reach the level of Theorems 1, 2 in the description of the structure of EGMs. The examples have been selected to demonstrate different outcomes of the competition between inclined and horizontal or vertical equivalence classes.

**Theorem 4.** *For  $D^2 = 49$  on  $\mathbb{A}_2$ , there are 147 PGSs divided in two equivalence classes: horizontal  $(7, 0)$  and inclined  $(5, 3)$ . The  $(7, 0)$ -class  $\mathcal{P}(7, 0)$  consists of 49 PGSs and is the only one dominant. The  $(7, 0)$ -PGSs are reflection-invariant and obtained from each other by  $\mathbb{A}_2$ -shifts. Consequently, we have in total 49 EGMs, and they all are of the form  $\mu_\varphi$  where  $\varphi \in \mathcal{P}(7, 0)$ .*

In the next result the choice of the dominant PGS class between the inclined and horizontal ones is inverted.

**Theorem 5.** *For  $D^2 = 169$  on  $\mathbb{A}_2$ , there are 507 PGSs divided in two equivalence classes: inclined  $(8, 7)$  and horizontal  $(13, 0)$ . The  $(8, 7)$ -class  $\mathcal{P}(8, 7)$  consists of 338 PGSs and is the only one dominant. The  $(8, 7)$ -PGSs are not reflection-invariant; they are obtained from each other by  $\mathbb{A}_2$ -shifts and reflections. Consequently, we have in total 338 EGMs  $\mu_\varphi$ , and they all are of the form  $\mu_\varphi$  where  $\varphi \in \mathcal{P}(8, 7)$ .*

Finally, we discuss a case where we have one vertical class,  $(7, 7)$ , and one inclined,  $(11, 2)$ .

**Theorem 6.** *For  $D^2 = 147$  on  $\mathbb{A}_2$ , there are 441 PGSs divided in two equivalence classes, the vertical  $(7, 7)$  and the inclined  $(11, 2)$ . The  $(7, 7)$ -class  $\mathcal{P}(7, 7)$  consists of 147 PGSs and is the only one that is dominant. The  $(7, 7)$ -PGSs are reflection-invariant and obtained from each other by  $\mathbb{A}_2$ -shifts. Consequently, we have in total 147 EGMs, and they all are of the form  $\mu_\varphi$  where  $\varphi \in \mathcal{P}(7, 7)$ .*

### 3.5 PGSs and EGMs for Classes HA, HB and HC

The results for Classes HA and HB go in parallel to those for Classes TA and TB. Recall, for a value  $D^2$  from Classes HA and HB, the PGSs on  $\mathbb{H}_2$  are  $(D, \alpha)$ -PGSs restricted to  $\mathbb{H}_2$ ; see Theorem I(ii). We will use on  $\mathbb{H}_2$  the same terminology as on  $\mathbb{A}_2$ .

**Theorem 7.** (*Class HA1*)

- (i) *Let  $D/3$  be an integer not divisible by primes of the form  $3v + 1$ . Then on  $\mathbb{H}_2$  there is a single PGS-equivalence class, which contains  $2D^2/3$  PGSs. The PGSs are horizontal  $((D, 0), \alpha)$ -configurations, hence reflection-invariant. Different PGSs are obtained from each other by  $\mathbb{H}_2$ -shifts. Consequently, the number of EGMs on  $\mathbb{H}_2$  equals  $2D^2/3$ .*
- (ii) *Let  $D/\sqrt{3}$  be an integer not divisible by primes of the form  $3v + 1$ . Then on  $\mathbb{H}_2$  there is a single PGS-equivalence class, which contains  $2D^2/3$  PGSs. The PGSs are vertical  $((\frac{D}{\sqrt{3}}, \frac{D}{\sqrt{3}}), \alpha)$ -configurations, hence reflection-invariant. Different PGSs are obtained from each other by  $\mathbb{H}_2$ -shifts. Consequently, the number of EGMs on  $\mathbb{H}_2$  equals  $2D^2/3$ .*

**Theorem 8.** (*Class HA2*) *Let  $D^2$  be an integer whose prime decomposition contains (i) at least one factor 3, (ii) primes of the form  $3v + 2$ , in even powers, possibly zero, and (iii) a single prime of the form  $3v + 1$ . Then on  $\mathbb{H}_2$  there is a single PGS-equivalence class, which contains  $4D^2/3$  PGSs. The PGSs are inclined  $(D, \alpha)$ -configurations, hence not reflection-invariant. Different PGSs are obtained from each other by shifts and reflections. Consequently, the number of EGMs on  $\mathbb{H}_2$  equals  $4D^2/3$ .*

In Theorem 9 we use the same terminology of dominant classes as in Theorem 3

**Theorem 9.** (*Class HB*) *Suppose that the prime decomposition of  $D^2$  contains (i) at least one factor 3, (ii) primes of the form  $3v + 2$ , in even powers, possibly zero, and (iii) at least two prime factors of the form  $3v + 1$ , some of which may coincide. Then all PGSs are  $(\mathbb{H}_2, D, \alpha)$ -configurations obtained as the restrictions to  $\mathbb{H}_2$  of their  $(\mathbb{A}_2, D, \alpha)$ -counterparts. Thus, the number of PGS-equivalence classes on  $\mathbb{H}_2$  is the same as on  $\mathbb{A}_2$ . Furthermore, the assertions (ii)–(iv) of Theorem 3 are transferred from  $\mathbb{A}_2$  to  $\mathbb{H}_2$ , with the proviso that the number of PGSs in the equivalence classes is  $2D^2/3$  in place of  $D^2$  and  $4D^2/3$  in place of  $2D^2$ . Hence, in assertion (iv), the total number of  $D$ -PGSs on  $\mathbb{H}_2$  should be equal to  $D^2 \sum_{j=1}^J m_j$  where  $m_j = 2/3, 4/3$ ,  $1 \leq j \leq J$ , and  $J = J(D, \mathbb{H}_2)$ .*

We conjecture that, for any  $D^2$  from Class HB,  $J(D, \mathbb{H}_2) = 1$ .

An analog of Theorem 6 is

**Theorem 10.** *For  $D^2 = 147$  (Class HB), there are 294 PGSs divided in two equivalence classes, the vertical  $(7, 7)$  and the inclined  $(11, 2)$ . The  $(7, 7)$ -class  $\mathcal{P}(7, 7)$  consists of 98 PGSs and is the only one dominant. The PGSs  $\varphi \in \mathcal{P}(7, 7)$  are reflection-invariant and obtained from each other by  $\mathbb{H}_2$ -shifts. Consequently, we have in total 98 EGMs  $\mu_\varphi$ , where  $\varphi \in \mathcal{P}(7, 7)$ .*

Results for Class HC are given in Theorem 11 below.

**Theorem 11.** *Assume  $D^2$  is not divisible by 3 and not from Classes HD, HE or HS. Consider the number  $D^*$  such that  $D^* > D$  and  $(D^*)^2$  is the closest Lösschian number to  $D^2$  divisible by 3. Then the PGSs on  $\mathbb{H}_2$  are the  $(D^*, \alpha)$ -configurations.*

- (A1) *Suppose the value  $D^*$  belongs to Class HA1. Then the assertions of Theorem 7 can be repeated with  $D$  replaced by  $D^*$ . In particular, the number of EGMs on  $\mathbb{H}_2$  equals  $2(D^*)^2/3$ .*
- (A2) *Suppose the value  $D^*$  belongs to Class HA2. Then the assertions of Theorem 8 can be repeated with  $D$  replaced by  $D^*$ . In particular, the number of EGMs on  $\mathbb{H}_2$  equals  $4(D^*)^2/3$ .*
- (B) *Suppose that the above value  $(D^*)^2 > D^2$  belongs to Class HB. Then the assertions of Theorem 9 can be repeated with  $D$  replaced by  $D^*$ . In particular, the total number of EGMs on  $\mathbb{H}_2$  equals  $(D^*)^2 \sum_{j=1}^J m_j$  where  $m_j = 2/3, 4/3$ ,  $1 \leq j \leq J$ , and  $J = J(D^*, \mathbb{H}_2)$ .*

### 3.6 PGSs and EGMs for Class HD

To conclude our results, it remains to consider exceptional non-sliding values  $D^2$ . For Class HD we have the following

**Theorem 12.** *Assume  $D^2 > 1$  is from Class HD.*

- (i) *For  $D^2 = 13, 28, 49, 64, 97, 157$  (sub-class HD1): the number of PGSs on  $\mathbb{H}_2$  equals 66, 132, 222, 288, 426 and 678, respectively, and they are  $(D, \beta)$ -configurations. The PGSs are not reflection-invariant and are obtained from each other by shifts and reflections. The number of the EGMs matches that of the PGSs.*
- (ii) *For  $D^2 = 16, 256$  (sub-class HD2): the number of PGSs on  $\mathbb{H}_2$  equals 54 and 726, respectively, and they are  $(D, \gamma)$ -configurations. The PGSs are not reflection-invariant and are obtained from each other by shifts and reflections. The number of the  $D$ -EGMs matches that of the PGSs.*

### 3.7 PGSs and EGMs for Class HE

Class HE ( $D^2 = 67$ ) is the one where the description of EGMs requires new techniques and is not given in this paper. However, the analysis of the PGSs can be done.

**Theorem 13.** *For the value  $D^2 = 67$  (Class HE): there are 300 PGSs of type  $(D, \beta)$  and 50 PGSs of type  $(D^*, \alpha)$ , with  $(D^*)^2 = 75$ .*

As was said earlier, we conjecture that  $(D^*, \alpha)$ -PGSs form the only dominant equivalence class, and so the number of  $D$ -EGMs equals 50.

## 4 The PGSs on $\mathbb{A}_2$ and $\mathbb{H}_2$ via MRA-triangles

To prove Theorem I, we develop a united approach to the analysis of PGSs covering the whole variety of cases in Theorems 1–13. It is based on the notion of a re-distributed area of a triangle in the Delaunay triangulation (DT) for a  $D$ -AC  $\phi \in \mathcal{A}$  and the concept of a MRA-triangle minimizing a re-distributed area. In our approach, we have been inspired by (i) an idea of a local energy minimizer serving as an indicator of a PGS (see [13]) and (ii) a specific choice of a minimizer as a triangle area in a DT and a related notion of a saturated configuration (see [4]). Elements of such an approach have been used for lattice  $\mathbb{Z}^2$  in [17], Sect. 3.

### 4.1 V-cells, C-triangles and saturated configurations

The key point of our construction is that maximizing the number of particles in an AC  $\phi$  can be done through minimizing triangle areas in the Delaunay triangulation of  $\phi$ ; see below. One caveat here is that minimization should exclude ‘sliver’ obtuse triangles (as their area can be arbitrarily small). The other caveat is that minimization is applied not to the ‘standard’ triangle area but to its modification which we call a re-distributed (RD) area  $s^{\text{RD}}(\triangle)$ . And finally, one has to verify that the triangles minimizing the RD-area (MRA-triangles) form a tessellation of the whole  $\mathbb{A}_2/\mathbb{H}_2$ .

Let us pass to a formal argument. Consider an arbitrary set  $\mathbb{E} \subset \mathbb{R}^2$ , with at least two points, such that  $\rho(\mathbf{x}, \mathbf{y}) \geq D$  for any two distinct  $\mathbf{x}, \mathbf{y} \in \mathbb{E}$ . For each  $\mathbf{x} \in \mathbb{E}$  define the *Voronoi cell*  $\mathcal{V}(\mathbf{x}, \mathbb{E})$  as the set of points  $\mathbf{z} \in \mathbb{R}^2$  satisfying  $\rho(\mathbf{x}, \mathbf{z}) \leq \rho(\mathbf{y}, \mathbf{z})$ ,  $\forall \mathbf{y} \in \mathbb{E} \setminus \{\mathbf{x}\}$ . The Voronoi cells (V-cells, for short) are always convex polygons.

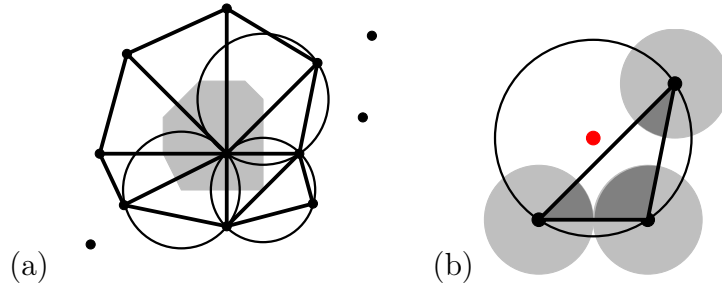


Figure 13: (a) A V-cell (a gray polygon), V-circles and C-triangles. (b) Set  $\mathbb{S}(\triangle)$  for a C-triangle (the union of three dark-gray sectors; see Lemma 4.1).

Frame (a): vertices of a V-cell are centers of V-circles; all points of a  $D$ -AC  $\phi$  lie on V-circles, not inside. Frame (b): The radius of a V-circle around a C-triangle is  $\leq D$ . Consequently, one can't add a particle at the center (a red spot). In a saturated  $D$ -AC  $\phi$ , the radii of V-circles are  $\leq D + 1$ : cf. Lemma 4.2.

We apply the above definition to a given  $D$ -AC  $\phi \in \mathcal{A}(D)$  with at least two particles; this yields a collection of *Voronoi cells*  $\mathcal{V}(\mathbf{x}, \phi)$  constructed for the occupied sites  $\mathbf{x} \in \phi$ . Here  $\mathcal{A}(D)$  may stand for  $\mathcal{A}(D, \mathbb{A}_2/\mathbb{H}_2)$  or  $\mathcal{A}(D, \mathbb{R}^2)$ . If  $\phi$  has no unbounded V-cells then to each cell  $\mathcal{V}(\mathbf{x}, \phi)$  there is assigned a finite set of circles centered at the vertices of  $\mathcal{V}(\mathbf{x}, \phi)$  and passing through  $\mathbf{x}$ . We call them *V-circles* in  $\phi$ . Each  $\mathbf{x} \in \phi$  lies in at least one of V-circles but no  $\mathbf{x} \in \phi$  falls inside a circle. The sites  $\mathbf{y} \in \phi$  lying in a given

V-circle form the vertices of a *constituting polygon*. These polygons form a tessellation of  $\mathbb{R}^2$ : they have disjoint interiors, and the union of their closures gives the entire plane. If a constituting polygon has  $\geq 3$  vertices, it can be divided (non-uniquely) into *constituting triangles* (in short: C-triangles); this produces the *Delaunay triangulation* (DT) of  $\phi$  (and of  $\mathbb{R}^2$ ). See Figure 13 (a).

**Lemma 4.1.** *Let  $\Delta$  be a C-triangle in a  $D$ -AC $\phi$  and consider 3 pair-wise disjoint disks of diameter  $D$  centered at the vertices of  $\Delta$ . Consider 3 sectors in these disks which are intersections of the circles with the angles of  $\Delta$  and let  $\mathbb{S}(\Delta)$  denote the union of these sectors. Then the area of  $\mathbb{S}(\Delta)$ , i.e., the sum of the areas of these 3 sectors, equals  $\pi D^2/8$ .*

**Proof.** Let us stress that  $\mathbb{S}(\Delta)$  not necessarily lies completely inside triangle  $\Delta$ . Nevertheless, the sets  $\mathbb{S}(\Delta)$  where  $\Delta$  runs over C-triangles of  $\phi$  form a partition of the union of the disks  $\bigcup_{\mathbf{x} \in \phi} \mathbb{D}(\mathbf{x}, D/2)$  (modulo a set of measure 0). Here  $\mathbb{D}(u, r)$  stands for the disk of radius  $r > 0$  centered at  $\mathbf{u} \in \mathbb{R}^2$ :  $\mathbb{D}(\mathbf{u}, r) = \{\mathbf{y} \in \mathbb{R}^2 : \rho(\mathbf{u}, \mathbf{y}) \leq r\}$ .

For each angle of size  $\alpha$  in  $\Delta$  the intersection with the corresponding disk is a full sector with the angular measure  $\alpha$  and area  $\alpha D^2/8$ . The sum of the triangle angles equals  $\pi$ . Cf. Figure 13 (b). ■

Lemma 4.1 establishes a principal fact that the number of particles in an AC  $\phi$  equals the doubled number of C-triangles in the DT. Hence, to maximize the number of particles one would like to minimize the area of C-triangles. However, since the triangular areas in a DT can be arbitrarily small (when a C-triangle is obtuse and has a large circumradius, i.e., the radius of the corresponding V-circle), we use the idea of saturation allowing us to discard C-triangles that have the area close to 0; see Lemma 4.2.

A  $D$ -AC  $\phi$  is called *saturated* if no occupied site can be added to it without breaking admissibility. A *saturation* of a given  $D$ -AC  $\phi$  is a completion of  $\phi$  (in some uniquely defined way) with the maximal possible amount of added occupied sites.

Clearly, every PGS configuration is saturated (this is also true for non-periodic GSs). Saturated configurations are convenient as a natural initial step in a procedure of identifying PGSs within the set  $\mathcal{A}(D)$  of admissible configurations. The use of saturated configurations also makes more transparent the derivation of the Peierls bound in Section 5.1.

The idea of a saturated configuration worked well in the study of dense-packed circle configurations in  $\mathbb{R}^2$ ; cf. [4]. We attempt to emulate a similar approach on  $\mathbb{A}_2/\mathbb{H}_2$ . It generates some technical complications that are addressed in Lemmas 4.2 - 4.5.

**Lemma 4.2.** *A saturated configuration on  $\mathbb{A}_2/\mathbb{H}_2$  does not have V-circles of radius  $\geq D + 1$ .*

**Proof.** Suppose there exists a V-circle of radius  $\geq D + 1$ . The center of the V-circle may not lie in  $\mathbb{A}_2/\mathbb{H}_2$  but is at distance  $\leq 1$  from one of the  $\mathbb{A}_2/\mathbb{H}_2$ -sites. Then an additional particle can be added at this site without breaking admissibility. This contradicts the saturation assumption. ■

We would like to note a difference between Lemma 4.2 and Lemma 2 from [4]. We

have a lower bound  $D + 1$  whereas in [4], Lemma 2, one has  $D$ . This creates a particular technical complication arising on  $\mathbb{A}_2/\mathbb{H}_2$  compared with  $\mathbb{R}^2$ .

Lemma 4.2 enables us to discard C-triangles which have a circumradius  $> D + 1$  and focus on those with a circumradius  $\leq D + 1$  in our analysis of PGSs. The remaining obtuse C-triangles are tackled via a routine of the area re-distribution. More precisely, C-triangles with circumradius  $\leq D - 1$  are tackled in Lemmas 4.4, 4.8 and 4.10, depending upon the class of the value  $D^2$ . In Lemmas 4.5.1 - 4.5.3 we treat C-triangles on  $\mathbb{A}_2/\mathbb{H}_2$  with a circumradius between  $D - 1$  and  $D + 1$ . Such a C-triangle, let us denote it by  $\Delta$ , can have area  $< S(D)/2$  (when  $\Delta$  is obtuse). However, it turns out that in this case there will be an adjacent C-triangle  $\Delta'$  (sharing a side with  $\Delta$ ) with a rather large area, so that the area of the union  $\Delta \cup \Delta'$  is  $\geq S(D) + 1$ . It may also happen that two or three C-triangles  $\Delta_j$ , of area  $< S(D)/2$  each, share a common adjacent triangle  $\Delta'$ ; in this case there will again be a lower bound upon the area of their union. Such an observation allows us to circumspect obtuse C-triangles via Lemmas 4.5.1 - 4.5.3. For formal definitions, see Section 4.2.

## 4.2 Redistributed areas for triangles

In this section we introduce re-distributed areas assigned to a C-triangle  $\Delta$ , which can be conveniently lower-bounded. One,  $s^{\text{RD}}(\Delta)$ , characterizes the triangle *per se*, the other,  $\Sigma(\Delta, \phi)$ , considers it in a  $D$ -AC  $\phi$ . The bounds involve the quantities  $S(D)$  and  $S^{\text{RD}}(D)$  determined in (3.10) and (4.2), respectively. This will enable us to analyze the PGSs for the whole array of the situations on  $\mathbb{A}_2/\mathbb{H}_2$ , including the exceptional non-sliding values  $D^2 = 13, 16, 28, 49, 64, 67, 97, 157, 256$  (Classes HD and HE).

An  $\mathbb{A}_2/\mathbb{H}_2$ -triangle  $ABC$  is called a *qualifying triangle* if all its side-lengths are  $\geq D$  while the circumradius is  $\leq D + 1$ . All triangles we consider from now are supposed to be qualifying.

A collection of two triangles  $ABC$  and  $ACE$  with mutually disjoint interiors is called a *2-triangle group* if all sides and diagonals of quadrilateral  $ABCE$  are not shorter than  $D$ , vertex  $E$  does not lie inside the circumcircle of  $ABC$ , and vertex  $B$  does not lie inside the circumcircle of  $ACE$ .

A collection of three triangles  $ABC$ ,  $CDE$  and  $ACE$  with mutually disjoint interiors is called a *3-triangle group* if all sides and diagonals of pentagon  $ABCDE$  are not shorter than  $D$ , vertices  $D, E$  do not lie inside the circumcircle of triangle  $ABC$ , vertices  $A, B$  do not lie inside the circumcircle of  $CDE$ , and vertices  $B, D$  do not lie inside the circumcircle of  $ACE$ .

A collection of four triangles  $ABC$ ,  $CDE$ ,  $EFA$  and  $ACE$  with mutually disjoint interiors is called a *4-triangle group* if all sides and diagonals of hexagon  $ABCDEF$  are not shorter than  $D$ , vertices  $D, E, F$  do not lie inside the circumcircle of  $ABC$ , vertices  $F, A, B$  do not lie inside the circumcircle of  $CDE$ , vertices  $B, C, D$  do not lie inside the circumcircle of  $EFA$ , and vertices  $B, D, F$  do not lie inside the circumcircle of triangle  $ACE$ .

For each triangle group one can calculate the corresponding average triangle area which we call the *re-distributed group area*.

For any triangle  $ABC$  one can consider all triangle groups containing this triangle such that side  $AB$  is shared with another triangle in the group but sides  $BC$  and  $CA$  are



not shared. The minimal redistributed group area among all such groups is called the *AB-re-distributed area* of  $ABC$  and denoted by  $s_{AB}^{\text{RD}}(ABC)$ . The *BC-re-distributed area*  $s_{BC}^{\text{RD}}(ABC)$  and *CA-re-distributed area*  $s_{CA}^{\text{RD}}(ABC)$  are defined in a similar way.

The quantity

$$s^{\text{RD}}(ABC) = \max(s(ABC), s_{AB}^{\text{RD}}(ABC), s_{BC}^{\text{RD}}(ABC), s_{CA}^{\text{RD}}(ABC)) \quad (4.1)$$

is called the *re-distributed area of triangle ABC*. Here and below  $s(ABC)$  stands for the area of  $ABC$ ; a similar meaning will have the notation  $s(\Delta)$ ,  $s(\Delta \cup \Delta')$  and so on. If the maximum in (4.1) is achieved at  $s_{\bullet}^{\text{RD}}(ABC)$  then the corresponding triangle side is called a *re-distributing side* (of  $ABC$ ) and denoted by  $\sigma(ABC)$ .

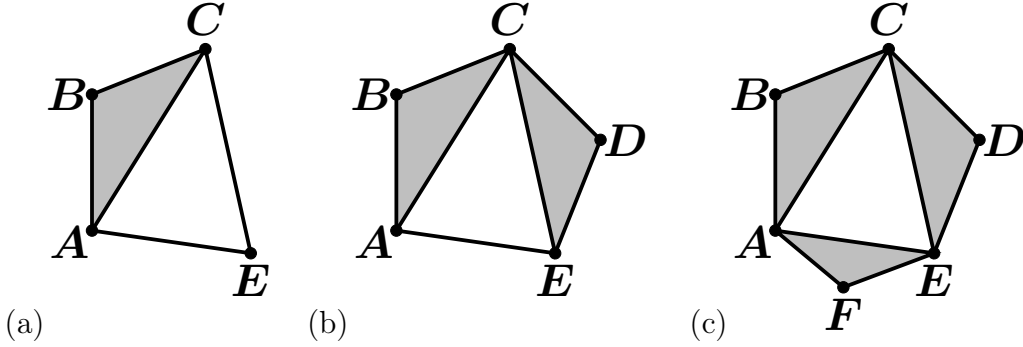


Figure 14: Obtuse C-triangles (gray) with an adjacent acute triangle of a large area.

Frame (a): a 2-triangle group, frame (b): a 3-triangle group, frame (c): a 4-triangle group. A quantitative estimation of the re-distributed area of the involved triangles is provided in Lemmas 4.5.1 - 4.5.3.

The doubled minimal redistributed area is denoted by  $S^{\text{RD}}(D) = S^{\text{RD}}(D, \mathbb{A}_2/\mathbb{H}_2)$ :

$$S^{\text{RD}}(D) = 2 \times \min \left[ s^{\text{RD}}(\Delta) : \Delta \text{ runs over the triangles on } \mathbb{A}_2/\mathbb{H}_2 \right]. \quad (4.2)$$

A triangle  $\Delta$  with minimal re-distributed area, i.e., with  $s^{\text{RD}}(\Delta) = S^{\text{RD}}(D)/2$ , is called an *MRA-triangle*.

Note that if  $\Delta$  has an area  $s(\Delta) < s^{\text{RD}}(\Delta)$  then  $\Delta$  has a re-distributing side.

An important observation is that, by virtue of Lemma 4.1 and the definition of an MRA-triangle, any PGS consists of MRA-triangles. Cf. [13], Criterion on P179. More precisely, we say that a  $D$ -AC is MRA-perfect if its C-triangles are all MRA-triangles.

**Lemma 4.3.** *Given an attainable  $D^2$ , suppose that there exists a perfect  $D$ -AC  $\phi$ . Then any  $D$ -PGS is a perfect configuration.*

**Proof.** Owing to Lemma 4.1, the particle density in  $\phi$  is  $1/S^{\text{RD}}(D)$ . Then any periodic  $D$ -AC has the particle density  $\leq 1/S^{\text{RD}}(D)$ . Next, let  $\psi$  be any periodic  $D$ -AC containing a non-MRA-triangle. Then, in a large basic quadrilateral polygon  $\mathbb{V}$ , one can construct a perturbation of  $\psi$  having more particles in  $\mathbb{V}$  than  $\psi$  has. In fact, such a perturbation will have the same pattern as  $\phi$  in  $\mathbb{V}$ . We will have to remove some particles from  $\psi$  along the boundary  $\partial\mathbb{V}$  but will gain an amount of particle proportional to the number of sites in  $\mathbb{V}$ .

Consequently, any PGS should consist of MRA-triangles. ■

**Remark 4.1.** In the course of this section, we will check that for any attainable  $D^2$  on both  $\mathbb{A}_2$  and  $\mathbb{H}_2$  there exists at least one perfect  $D$ -AC. Moreover, as we show further in this section, for any non-sliding  $D$  the number of perfect configurations (and hence that of the PGSs) is finite. Furthermore, it will be shown that every perfect configuration is periodic, hence a PGS.

Consequently, any non-periodic ground state contains at least one infinite connected component of non-MRA triangles and no finite ones. Moreover, the number of non-MRA triangles in a  $\mathbb{A}_2/\mathbb{H}_2$ -hexagon  $\mathbb{V}(L)$  of side-length  $L$  can only grow linearly with  $L$ ; this means that non-MRA triangles form, effectively, a one-dimensional array. Let us repeat once more that, according to [9], non-periodic ground states do not generate EGMs on  $\mathbb{A}_2/\mathbb{H}_2$ .  $\blacktriangle$

**Lemma 4.4.** *For any  $D^2$  on  $\mathbb{A}_2$  and for any  $D^2$  divisible by 3 on  $\mathbb{H}_2$ :*

- (i) *for a  $D$ -triangle  $\triangle^\circ$ , we have  $s^{\text{RD}}(\triangle^\circ) = \sqrt{3}D^2/4 = S(D)/2$  (cf. Eqn (3.10)),*
- (ii)  *$\forall$   $D$ -admissible  $\mathbb{A}_2/\mathbb{H}_2$ -triangle  $\triangle$  non-congruent to  $\triangle^\circ$  such that the circumradius of  $\triangle$  is  $\leq D - 1$ , we have*

$$s^{\text{RD}}(\triangle) \geq s^{\text{RD}}(\triangle^\circ) + \frac{\sqrt{3}}{8}. \quad (4.3)$$

**Proof.** (i) A  $D$ -triangle  $ABC$  can be complemented by its reflection about a given side, say  $AB$ , to form a 2-triangle group. Hence,  $s_{AB}^{\text{RD}}(ABC) \leq S(D)/2$ . By definition (4.1), it follows that  $s^{\text{RD}}(ABC) = S(D)/2$ .

(ii) The triangles under consideration in assertion (ii) have the maximum angle strictly between  $\pi/3$  and  $2\pi/3$ . The sinus of such an angle is  $> \sqrt{3}/2$ . Hence,  $s(\triangle) > \frac{D^2\sqrt{3}}{4} = \frac{S(D)}{2}$ . This implies (4.3) for the area of an  $\mathbb{A}_2$ -triangle multiplied by  $8/\sqrt{3}$  is integer.  $\blacksquare$

Consider an arbitrary saturated  $D$ -AC  $\phi$  on  $\mathbb{A}_2/\mathbb{H}_2$  and identify all triangles in  $\phi$  with an area  $< S^{\text{RD}}(D)/2$ . For each such triangle  $\triangle$  consider a 2-triangle group  $\triangle \cup \triangle'$  formed by a triangle  $\triangle'$ , called a *donor*, adjacent to  $\triangle$  along the redistributing side  $\sigma(\triangle)$ . If several such 2-triangle groups have a common donor  $\triangle'$  then we unite them into a single 3-triangle group or 4-triangle group. (By construction, a donor  $\triangle'$  has area  $> S^{\text{RD}}(D)/2$ .) In case of a 3-triangle group we have a donor  $\triangle'$  with area  $\geq S^{\text{RD}}(D)/2$  grouped with two adjacent triangles of area  $< S^{\text{RD}}(D)/2$ . In case of a 4-triangle group we have a donor  $\triangle'$  of area  $s(\triangle') \geq S^{\text{RD}}(D)/2$  grouped with three adjacent triangles of area  $< S^{\text{RD}}(D)/2$ . By construction, each triangle  $\triangle$  in  $\phi$  belongs to at most one group. Furthermore, the grouping uniquely assigns the *redistributed group area*  $\Sigma(\triangle, \phi)$  to each triangle  $\triangle$  in the AC  $\phi$ . Namely,  $\Sigma(\triangle, \phi)$  is the total area of the triangles in the group divided by the number of the triangles in the group containing  $\triangle$  in  $\phi$ .

Next, if  $\triangle$  is not a donor then  $\Sigma(\triangle, \phi) \geq s^{\text{RD}}(\triangle) \geq S^{\text{RD}}(D)/2$ . If  $\triangle$  is a donor we have that  $s^{\text{RD}}(\triangle) \geq s(\triangle) > \Sigma(\triangle, \phi) \geq S^{\text{RD}}(D)/2$ ; the last inequality holds since  $\Sigma(\bullet, \phi)$  is the same for all members in the group. Finally, if  $\triangle$  does not belong to any group in  $\phi$  then  $s^{\text{RD}}(\triangle) \geq s(\triangle) = \Sigma(\triangle, \phi) \geq S^{\text{RD}}(D)/2$ ; the equality  $s(\triangle) = \Sigma(\triangle, \phi)$  and inequality  $\Sigma(\triangle, \phi) \geq S^{\text{RD}}(D)/2$  follow directly from the way in which  $\triangle$  is identified in  $\phi$ .

### 4.3 Equality $S^{\text{RD}}(D) = S(D)$ on $\mathbb{A}_2$ and – for $3|D^2$ – on $\mathbb{H}_2$

In this section we give three lemmas, 4.5.1–4.5.3, treating C-triangles on  $\mathbb{A}_2/\mathbb{H}_2$  with a circumradius  $r = D + \delta$ ,  $\delta \in [-1, 1]$ . Then we proceed with Lemma 4.6 which, together with Lemma 4.3, establishes the equality  $S^{\text{RD}}(D) = S(D)$  under some conditions upon  $D^2$ .

**Lemma 4.5.1.** *Suppose that a C-triangle  $\triangle$  has the circumradius  $r = D + \delta$  where  $-1 \leq \delta \leq 1$ . Then*

$$s(\triangle) \geq \frac{D^3}{2r} \sqrt{1 - \frac{D^2}{4r^2}} > \frac{\sqrt{3}D^2}{4} - \frac{D\delta}{2\sqrt{3}}. \quad (4.4)$$

Here  $\frac{D^3}{2r} \sqrt{1 - \frac{D^2}{4r^2}}$  is the area of an isosceles triangle with circumradius  $r$  and two side-lengths  $D$ . The longest side in this triangle has length  $< D\sqrt{3} + \frac{\delta}{\sqrt{3}}$ .

**Proof.** Suppose a C-triangle  $\triangle$  with vertices  $A, B, C$  satisfies the assumptions of the lemma. Let the side-lengths be  $AB = l_0$ ,  $BC = l_1$ ,  $CA = l_2$ , with  $D \leq l_0 \leq l_1 \leq l_2 \leq 2r$ . If two side-lengths are  $> D$ , say  $l_1, l_2 > D$ , then the area of the  $\triangle$  can be made smaller by moving vertex  $C$  along the circumcircle towards  $B$ , until the length of side  $BC$  becomes  $D$ . Indeed, in the process of motion  $l_0$  remains fixed but the height from  $C$  to  $AB$  shortens. Thus, the area of  $\triangle$  is lower-bounded by the area of an isosceles triangle with two side-lengths  $D$  and the remaining side-length  $2D\sqrt{1 - \frac{D^2}{4r^2}}$ . (On  $\mathbb{H}_2$ , it is not necessarily an  $\mathbb{H}_2$ -triangle.) A direct calculation shows that for  $D \geq 1$  and  $\delta \in (-1, 1)$  the bound  $2D\sqrt{1 - \frac{D^2}{4r^2}} < D\sqrt{3} + \frac{\delta}{\sqrt{3}}$  holds true. (The right-hand side is simply the

Taylor expansion in  $\delta$  up to order 1.) The area of such a triangle equals  $\frac{D^3}{2r} \sqrt{1 - \frac{D^2}{4r^2}}$ .

$$\text{Finally, } \frac{D^3}{2r} \sqrt{1 - \frac{D^2}{4r^2}} = \frac{D^3}{2(D + \delta)} \sqrt{1 - \frac{D^2}{4(D + \delta)^2}} > \frac{\sqrt{3}D^2}{4} - \frac{D\delta}{2\sqrt{3}}. \quad \blacksquare$$

**Lemma 4.5.2.** *Suppose that a C-triangle  $\triangle$  with side-lengths  $l_0, l_1, l_2$  has the circumradius  $r = D + \delta$  where  $-1 \leq \delta \leq 1$ . Consider an adjacent C-triangle  $\triangle'$  that shares with  $\triangle$  the longest side (of length  $l_2$ ). Then the area  $s(\triangle \cup \triangle')$  is lower-bounded by the area of a trapeze inscribed in a circle of radius  $r$ , with three sides being of length  $D$ . Furthermore, for  $D^2 \geq 400$  we have  $s(\triangle \cup \triangle') \geq \frac{3\sqrt{3}D^2}{4} - 2\delta^2$ .*

**Proof.** Again, we assume  $D \leq l_0 \leq l_1 \leq l_2 \leq 2r$ . Two vertices of triangle  $\triangle'$  are the end-points of the side of length  $l_2$  and lie in the V-circle of radius  $r$  circumscribing  $\triangle$ . The third vertex of  $\triangle'$  cannot lie inside this V-circle but can be placed on the circle. It also should lie outside the circles of radius  $D$  centered at the end-points of the side of length  $l_2$ . Under these restrictions, the minimal area of  $\triangle'$  is not less than the area of a triangle inscribed in the V-circle which shares the side of length  $l_2$  with  $\triangle$  and has the other side of length  $D$ . (Cf. the proof of Lemma 4.5.1.) If we now minimize the area

of  $\triangle$ , we obtain a pair  $\triangle, \triangle'$  forming a trapeze, as specified in the assertion of Lemma 4.5.2. (Again, on  $\mathbb{H}_2$  the resulting triangle is not necessarily an  $\mathbb{H}_2$ -triangle.)

The area of the trapeze in question equals the sum of the areas of 4 triangles, 3 of which are identical. The area of each of these identical triangles is  $\frac{r^2}{2} \sin(2\alpha)$  where  $\sin(\alpha) = \frac{D}{2r}$ . The area of the fourth triangle is  $\frac{r^2}{2} \sin(2\pi - 6\alpha)$ . All-in-all, the area of the trapeze is  $\frac{r^2}{2} 4 \sin^3(\alpha)$ , which equals

$$\frac{2D^3}{r} \left( \sqrt{1 - \frac{D^2}{4r^2}} \right)^3 = \frac{3\sqrt{3}D^2}{4} - \sqrt{3}\delta^2 + \frac{19\delta^3}{3\sqrt{3}D} - \frac{113\delta^4}{9\sqrt{3}D^2} + \dots$$

A straightforward calculation asserts that for  $D^2 \geq 400$  and  $-1 \leq \delta \leq 1$  this expression is  $\geq \frac{3\sqrt{3}D^2}{4} - 2\delta^2$ , as claimed in the lemma.  $\blacksquare$

**Lemma 4.5.3.** *Suppose that a C-triangle  $\triangle$  has the circumradius  $r = D + \delta$  where  $-1 \leq \delta \leq 1$ . Let  $\triangle'$  be the adjacent C-triangle sharing the longest side with  $\triangle$  (cf. Lemma 4.5.2).*

- (i) *Suppose that  $\triangle'$  is adjacent to another C-triangle,  $\triangle_1$ , with circumradius  $r_1 = D + \delta_1$  where  $-1 \leq \delta_1 \leq 1$ . Then we have  $s(\triangle') \geq 3D^2/4$ .*
- (ii) *Further, suppose  $\triangle'$  is adjacent to other two C-triangles,  $\triangle_1$  and  $\triangle_2$ , with circumradii  $r_1 = D + \delta_1$  and  $r_2 = D + \delta_2$  where  $-1 \leq \delta_1, \delta_2 \leq 1$ . Then  $s(\triangle') \geq D^2$ .*

**Proof.** (i) Here the triangle  $\triangle'$  has one side-length  $\geq D$  and two others  $\geq D\sqrt{3}$  by construction. On the other hand, the side-lengths are  $\leq 2D + 2$  since the circumradius is  $\leq D + 1$ . Therefore, the area of  $\triangle'$  is greater than or equal to the area of a triangle with side-lengths  $D, D\sqrt{3}, D\sqrt{3}$ . The area of such a triangle is, clearly,  $\geq 3D^2/4$ .

(ii) In this case all side-lengths of  $\triangle'$  are  $\geq D\sqrt{3}$ . Hence, the area of  $\triangle'$  is  $\geq D^2$ .  $\blacksquare$

**Lemma 4.6.** *For any  $D^2$  on  $\mathbb{A}_2$  and for any  $D^2$  divisible by 3 on  $\mathbb{H}_2$ , we have that*

$$S^{\text{RD}}(D) = S(D), \tag{4.5}$$

*and the equality  $S^{\text{RD}}(D) = 2s^{\text{RD}}(\triangle)$  is attained only when  $\triangle$  is a  $D$ -triangle. For each of these values of  $D$ , the corresponding MRA-perfect configuration exists and has type  $(D, \alpha)$ .*

**Proof.** In the situation of Lemma 4.4 we have the bound

$$2s^{\text{RD}}(\triangle) \geq S(D) + \frac{\sqrt{3}}{4}. \tag{4.6}$$

Next, in the situation of Lemma 4.5.2 (in particular, for  $D^2 \geq 400$ ) we have:

$$2s^{\text{RD}}(\triangle) \geq \frac{3}{2}S(D) - 2\delta^2 \geq S(D) + \frac{\sqrt{3}}{2}. \tag{4.7}$$

Next, in case (i) of Lemma 4.5.3,

$$3s^{\text{RD}}(\triangle) \geq 2 \left( 2S(D) - \frac{D\delta}{2\sqrt{3}} \right) + \frac{\sqrt{3}}{2}S(D) \geq \frac{3}{2} \left( S(D) + \frac{\sqrt{3}}{2} \right). \quad (4.8)$$

Finally, in case (ii) of Lemma 4.5.3,

$$4s^{\text{RD}}(\triangle) \geq 3 \left( 2S(D) - \frac{D\delta}{2\sqrt{3}} \right) + \frac{2}{\sqrt{3}}S(D) \geq 2 \left( S(D) + \frac{\sqrt{3}}{2} \right). \quad (4.9)$$

Together, (4.6), (4.7), (4.8), (4.9) imply that for  $D^2 \geq 400$  and every C-triangle  $\triangle$  different from a  $D$ -triangle:  $2s^{\text{RD}}(\triangle) > S(D)$ . This implies the assertion of Lemma 4.6 for  $D \geq 400$ .

For  $1 \leq D^2 < 400$  the proof is done by a computer enumeration. ■

#### 4.4 MRA-triangles for Class HC on $\mathbb{H}_2$

Next, we analyze the situation on  $\mathbb{H}_2$ , for values  $D^2$  not divisible by 3.

**Lemma 4.7.** *For any L\"oschian  $D^2 \geq 300$  there exists a L\"oschian number that is  $\geq D^2$ , is divisible by 3 and is at distance at most  $18\sqrt{D}$  from  $D^2$ .*

**Proof.** Consider L\"oschian numbers divisible by 3 of the form

$$(l - 3k)^2 + (l + 3k)^2 + (l - 3k)(l + 3k) = 3l^2 + 9k^2.$$

(It is simply the set of all L\"oschian numbers scaled 3 times.) Now, take an arbitrary L\"oschian number  $D^2$  and find  $l$  such that  $3l^2 \leq D^2 \leq 3(l+1)^2$ . Then find  $k$  such that

$$3l^2 + 9k^2 \leq D^2 \leq \min(3(l+1)^2, 3l^2 + 9(k+1)^2)$$

Then  $9k^2 \leq 6l + 3$ , i.e.  $k \leq \sqrt{(2l+1)/3}$ . The distance from  $D^2$  to  $\min(3(l+1)^2, 3l^2 + 9(k+1)^2)$  is at most

$$\begin{aligned} 9(k+1)^2 - 9k^2 &= 18k + 9 \\ &< 18\sqrt{(2l+1)/3} + 9 < 18\sqrt{l} \leq 18\sqrt{\sqrt{D^2/3}} \leq 18\sqrt{D}, \end{aligned} \quad (4.10)$$

where inequality involving  $l$  in the middle is true for  $l > 9$ . ■

In what follows, we refer to  $D^*(= D^*(D))$  as the nearest L\"oschian number not less than  $D$  such that  $3|(D^*)^2$ .

**Lemma 4.8.** *Any non-equilateral  $D$ -admissible  $\mathbb{H}_2$ -triangle  $\triangle$  with circumradius  $\leq D-1$  and the shortest side-length  $< D^*$  has at least one side with squared length  $\geq D^2 + D + 1$ . Consequently, for the double area  $2s(\triangle)$  we have:*

$$2s(\triangle) \geq h(D) \quad \text{where} \quad h(D) = \min \left[ \frac{D^3}{D-1} \sqrt{1 - \frac{D^2}{4(D-1)^2}}, \frac{1}{2} \sqrt{(3D^2 - D - 1)(D^2 + D + 1)} \right]. \quad (4.11)$$

Furthermore, for  $D^2 \geq 12$ :

$$h(D) > \frac{\sqrt{3}}{2}D^2 + \frac{D}{2\sqrt{3}}. \quad (4.12)$$

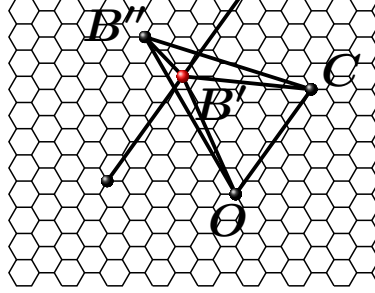


Figure 15

**Proof.** Referring to Figure 15, suppose that triangle  $\triangle$  is  $OCB''$ , and its shortest side is  $OC$ , with  $D \leq |OC| < D^*$ . Hence,  $|OC|^2$  is not divisible by 3.

Let  $B'$  be the vertex of an equilateral triangle, with  $|OB'| = |CB'| = |OC|$ . Then  $B'$  will be at the center of a unit hexagon, as shown in Figure 15. Consequently,  $|B'B''| \geq 1$ , and at least one of the triangles  $OB'B''$  or  $CB'B''$  is obtuse with the corresponding obtuse angle  $\geq 2\pi/3$ . Therefore, by the cosine theorem the squared length of the longest side of the obtuse triangle is at least  $D^2 + D + 1$ . Hence, as long as triangle  $OCB''$  is acute, we have that  $s(OCB'') \geq \frac{1}{2}\sqrt{(3D^2 - D - 1)(D^2 + D + 1)}$ . The latter value is the area of an isosceles triangle with side-lengths  $D$ ,  $D$  and  $\sqrt{D^2 + D + 1}$  (and the circumradius  $D - 1$ ).

On the other hand, if  $OCB''$  is obtuse then, according to Lemma 4.5.1,  $s(OCB'') \geq \frac{D^3}{2(D-1)}\sqrt{1 - \frac{D^2}{4(D-1)^2}}$ .

The last assertion of the lemma is straightforward for  $D^2 \geq 12$ . ■

**Lemma 4.9.** *For any value  $D^2$  of Class HC on  $\mathbb{H}_2$  we have that*

$$S^{\text{RD}}(D) = S(D^*), \quad (4.13)$$

*and the equality  $S^{\text{RD}}(D) = 2s^{\text{RD}}(\triangle)$  is attained only when  $\triangle$  is congruent to a  $D^*$ -triangle  $\triangle^*$ . Moreover, for each value of  $D$  of Class HC, the corresponding MRA-perfect configuration exists and has type  $\alpha(D^*)$ .*

**Proof.** By construction,  $s^{\text{RD}}(\triangle) \geq s(\triangle)$  for any  $D$ -admissible  $\mathbb{A}_2/\mathbb{H}_2$ -triangle. First, we consider triangles satisfying the conditions of Lemma 4.8. For any such  $\triangle$  we have

$$2s^{\text{RD}}(\triangle) \geq 2s(\triangle) \geq h(D). \quad (4.14)$$

If  $D^2 \geq (54)^4$  then, by Lemma 4.7, for any such  $\triangle$ ,

$$h(D) \geq \frac{\sqrt{3}}{2}(D^2 + 18\sqrt{D}) \geq \frac{\sqrt{3}(D^*)^2}{2} = 2s(\triangle^*), \quad (4.15)$$

and therefore  $s^{\text{RD}}(\Delta) > s(\Delta^*)$ . Hence, such a triangle cannot be an MRA-triangle if  $D^2 \geq (54)^4$ . When  $D^2 < (54)^4$  then, instead of utilizing Lemma 4.7 we verify numerically that, apart from 184 values, every  $D^2 < (54)^4$  satisfies the bound  $(D^2 + D/3) > (D^*)^2$ , which again implies that  $s^{\text{RD}}(\Delta) > s(\Delta^*)$ , with the help of (4.11). Cf. Section 9 and Program 1 `NearestLoschianNumber` in the ancillary file. The non-exceptional  $D$  among 184 remaining values are tackled by a separate computer program which calculates  $S^{\text{RD}}(D)$  and verifies (4.13). Cf. Section 9 and Program 2 `SpecialD` in the ancillary file.

Next, we discuss the case where we have a non-equilateral triangle  $\Delta$  with circumradius  $\leq D - 1$  and the shortest side-length  $\geq D^*$ . Here, the inequality  $2s(\Delta) \geq S^{\text{RD}}(D^*)$  is straightforward if  $\Delta$  is acute and follows from Lemma 4.5.1 if  $\Delta$  is obtuse.

Finally, a  $D$ -admissible triangle with circumradius between  $D - 1$  and  $D + 1$  cannot be an MRA-triangle by virtue of an argument similar to the one in the proof of Lemma 4.6. A lower bound  $s^{\text{RD}}(\Delta) > s(\Delta^*)$  for such a triangle  $\Delta$  is obtained by repeating the proof of Lemma 4.6 where we use analogs of inequalities (4.7), (4.8) and (4.9) with the value  $S(D)$  in the RHS replaced by  $S(D^*)$ . Namely, in the situation of Lemma 4.5.2,

$$2s^{\text{RD}}(\Delta) \geq \frac{3}{2}S(D) - 2\delta^2 \geq S(D^*) + \frac{\sqrt{3}}{2}, \quad (4.16)$$

in case (i) of Lemma 4.5.3,

$$3s^{\text{RD}}(\Delta) \geq 2 \left( 2S(D) - \frac{D\delta}{2\sqrt{3}} \right) + \frac{\sqrt{3}}{2}S(D) \geq \frac{3}{2} \left( S(D^*) + \frac{\sqrt{3}}{2} \right), \quad (4.17)$$

and in case (ii) of Lemma 4.5.3,

$$4s^{\text{RD}}(\Delta) \geq 3 \left( 2S(D) - \frac{D\delta}{2\sqrt{3}} \right) + \frac{2}{\sqrt{3}}S(D) \geq 2 \left( S(D^*) + \frac{\sqrt{3}}{2} \right). \quad (4.18)$$

For  $D^2 \geq (54)^4$  bounds (4.16)-(4.18) are a consequence of Lemma 4.7. For non-exceptional  $D^2 < (54)^4$ , (4.16) and (4.17) are verified numerically – cf. Section 9 and Program 1 `NearestLoschianNumber` in the ancillary file – while second bound in (4.18) follows from the second bound in (4.17). This implies the desired estimate  $s^{\text{RD}}(\Delta) > s(\Delta^*)$  for a  $D$ -admissible triangle  $\Delta$  with circumradius between  $D - 1$  and  $D + 1$ .

Thus, it is established that for any  $\Delta$  with circumradius  $\leq D + 1$  not congruent to  $\Delta^*$  we have the bound

$$s^{\text{RD}}(\Delta) > s^{\text{RD}}(\Delta^*). \quad (4.19)$$

This leads to the assertions of Lemma 4.9. ■

## 4.5 MRA-triangles for Classes HD and HE on $\mathbb{H}_2$

In this section we establish the values  $S^{\text{RD}}(D)$  when  $D$  is exceptional and non-sliding. We use the notation  $[l_0^2 | l_1^2 | l_2^2]$ , referred to as a triangle type, to indicate a triangle with side-lengths  $l_0 \leq l_1 \leq l_2$ . For example, in Figure 7, triangles  $AOB$ ,  $AOH$ ,  $HFO$ ,  $CED$  have type  $[13|19|21]$  whereas triangles  $OBC$ ,  $OCE$ ,  $OFE$  have type  $[13|16|21]$ .

**Lemma 4.10.** *The RD-perfect configurations exist for all exceptional  $D^2 = 13, 16, 28, 49, 64, 67, 97, 157, 256$  and are periodic. The corresponding values of  $S^{\text{RD}}(D)$  and triangle groups on  $\mathbb{H}_2$  at which these values are achieved are as follows:*

$$\begin{array}{llll}
S^{\text{RD}}(\sqrt{13}) = 16.5\sqrt{3}/2 & \{[13|16|21], [13|19|21]\} & \beta & \\
S^{\text{RD}}(\sqrt{16}) = 20.25\sqrt{3}/2 & \{[21|21|21], [16|21|25], \\ & [16|21|25], [16|21|25]\} & \gamma & \\
S^{\text{RD}}(\sqrt{28}) = 33\sqrt{3}/2 & \{[28|31|39], [28|37|39]\} & \beta & \\
S^{\text{RD}}(\sqrt{49}) = 55.5\sqrt{3}/2 & \{[49|52|63], [49|61|63]\} & \beta & \\
S^{\text{RD}}(\sqrt{64}) = 72\sqrt{3}/2 & \{[64|73|81]\} & \beta & \\
S^{\text{RD}}(\sqrt{67}) = 75\sqrt{3}/2 & \{[75|75|75]\} & \alpha(\sqrt{75}) & (4.20) \\
S^{\text{RD}}(\sqrt{67}) = 75\sqrt{3}/2 & \{[67|73|84], [67|79|84]\} & \beta & \\
S^{\text{RD}}(\sqrt{97}) = 106.5\sqrt{3}/2 & \{[97|103|117], [97|112|117]\} & \beta & \\
S^{\text{RD}}(\sqrt{157}) = 169.5\sqrt{3}/2 & \{[157|169|183], [157|172|183]\} & \beta & \\
S^{\text{RD}}(\sqrt{256}) = 272.25\sqrt{3}/2 & \{[273|273|273], [256|273|289], \\ & [256|273|289], [256|273|289]\} & \gamma &
\end{array}$$

respectively. For each of these values of  $D$ , the corresponding MRA-perfect configuration exists, and its type is listed in the right column.

**Proof.** The calculation of  $S^{\text{RD}}(D)$  involves a finite number of qualified triangles is performed by Program 2 SpecialD. Cf. Section 9 and ancillary file. ■

**Remark 4.2.** Lemma 4.10 indicates that the exceptional values of  $D$  emerge when the MRA-triangles are non-unique or non-equilateral. As a result, we have PGSs which are not obtained from max-dense sub-lattices. E.g., for  $D^2 = 67$  we have (i) an MRA-triangle that is a  $D$ -triangle with  $D^2 = 75$ , and (ii) a 2-triangle group formed by non-equilateral MRA-triangles.

Another notable case is  $D^2 = 64$  where an MRA-triangle is unique but not equilateral (and forms a group on its own). Here all occupied sites in the  $\beta$ -PGSs have V-cells of area  $72\sqrt{3}/2$ ; these V-cells are congruent hexagons. However, there exist ACs where some V-cells (still hexagons) have area  $71.5\sqrt{3}/2$ . ▲

## 4.6 Proof of Theorem I

**Proof of Theorem I.** Owing to Lemma 4.3, Theorem I follows from Lemma 4.6 and 4.9 and 4.10 establishing the existence of RD-perfect configurations for all non-sliding values of  $D$ . ■

**Remark 4.3.** A corollary of Theorem I is that the particle density in a PGS (per a unit Euclidean area) equals  $1/S^{\text{RD}}(D)$ . ▲

## 5 The Peierls bound

### 5.1 The Peierls bound via MRA-triangles

As was said, an application of the PS theory needs a Peierls bound. Here we establish the Peierls bound by using the machinery of MRA-triangles. We again begin with some



auxiliary notions and statements. Throughout Section 5.1 we assume that on  $\mathbb{A}_2$ ,  $D$  takes any attainable value while on  $\mathbb{H}_2$  the value  $D$  is non-sliding (i.e., not from Class HS).

Let  $\phi^*$  be a saturation of a given  $D$ -AC  $\phi$ . If an added occupied site  $x \in \phi^* \setminus \phi$  lies in a template then, clearly, this template is incorrect (more precisely, non- $\varphi$ -correct in  $\varphi$  for each  $\varphi \in \mathcal{P}$ ). We say that such a template is an *s-defect* (in  $\phi$ ). Another possibility for a defect is where, in the saturation  $\phi^*$ , a template has a non-empty intersection with one of C-triangles that is not an MRA-triangle. We call it a *t-defect* (again in  $\phi$ ). Finally, an incorrect template can be simply a neighbor of an s- or a t-defect. We call it an *n-defect* (still in  $\phi$ ). Observe that any triangle intersecting the support of the n-defect template is an MRA-triangle.

We would like to note that C-triangles considered in Lemmas 4.5.1–4.5.3 lead to t-defects by definition.

**Lemma 5.1.** (A Peierls bound in terms of defects) *Let  $D$  be not from Class HS. Consider a  $\varphi$ -contour  $\Gamma = (\text{Supp}(\Gamma), \phi \upharpoonright_{\text{Supp}(\Gamma)})$  containing  $m = \|(\text{Supp}(\Gamma))\|$  incorrect templates. Additionally, assume that  $m = i + j + k$  where  $i, j, k$  give the amount of s-, t- and n-defects in  $\phi$ , respectively. Then for the weight  $w(\Gamma)$  we have that*

$$w(\Gamma) \leq u^{-i-j\sqrt{3}/(32S^{\text{RD}}(D))}. \quad (5.1)$$

**Proof.** The integer value  $i$  contributed by s-defects is straightforward, so we consider the saturation  $\phi^*$  and its t-defects only.

Observe that, according to Lemmas 4.4, 4.6, 4.9, 4.10, the re-distributed area of any C-triangle that is not an MRA-triangle is at least  $\frac{1}{2} \left( S^{\text{RD}}(D) + \frac{\sqrt{3}}{2} \delta(D) \right)$ , where  $\delta(D) \geq 1/2$ . (The overall minimal value  $1/2$  for  $\delta(D)$  is attained, e.g., for  $D^2 = 16$  in Lemma 4.10.)

Further, a C-triangle that is not an MRA-triangle can be shared by at most 4 templates. Therefore,  $j$  templates with t-defects contain (in the  $\mathbb{R}^2$ -sense) at least  $j/4$  C-triangles that are not MRA-triangles. Consider a torus  $\mathbb{T}$  formed by an integer number of templates and containing  $\text{Supp}(\Gamma)$ . Then  $\mathbb{T}$  contains at most  $s(\mathbb{T})/S^{\text{RD}}(D)$  C-triangles where  $s(\mathbb{T})$  is the area of  $\mathbb{T}$ .

On the other hand, the maximal possible amount of C-triangles in  $\phi^* \upharpoonright_{\mathbb{T}}$  is  $\leq (s(\mathbb{T}) - j\sqrt{3}/16)/S^{\text{RD}}(D)$ . Next, owing to Lemma 4.1, the number of particles in  $\phi^* \upharpoonright_{\mathbb{T}}$  and  $\varphi \upharpoonright_{\mathbb{T}}$  is obtained by dividing the amount of C-triangles by a factor 2. Finally, we can pass from  $\mathbb{T}$  to  $\text{Supp}(\Gamma)$  as the number of particles in  $\phi^* \upharpoonright_{\mathbb{T} \setminus \text{Supp}(\Gamma)}$  and  $\varphi \upharpoonright_{\mathbb{T} \setminus \text{Supp}(\Gamma)}$  is the same by construction. ■

Informally, Lemma 5.1 states that the increment of ‘energy’ (i.e., decrease in the number of particles) caused by a deviation from a PGS is lower-bounded proportionally to the ‘size’ of the deviation. This is the gist of Peierls bounds used in the Pirogov–Sinai theory and its applications.

**Lemma 5.2.** *Let  $\varphi', \varphi'' \in \mathcal{P}(D)$  be two distinct PGSs. Consider a  $D$ -AC  $\phi$  containing a connected component  $\Lambda$  of  $\varphi'$ -correct templates enclosed by a connected component of  $\varphi''$ -correct templates. Then  $\phi$  contains a closed chain of adjacent non-MRA C-triangles enclosing  $\Lambda$ .*

**Proof.** On  $\mathbb{A}_2$  and on  $\mathbb{H}_2$  for  $D$  from Classes HA, HB, HC, the MRA-triangles are equilateral. Such triangles from two distinct PGSs cannot share a side in a  $D$ -AC. For  $D$  from Classes HD and HE on  $\mathbb{H}_2$  the assertion is verified case-by-case. ■

**Proof of Theorem II.** The theorem is a direct consequence of Lemmas 5.1 and 5.2 with an additional factor  $1/9$  accounting for the possibility for each s- or t-defect to be surrounded by 8 n-defects. ■

## 5.2 A Peierls bound via Voronoi cells

An alternative method of establishing the Peierls bound is to use V-cells: it works on  $\mathbb{A}_2$  and – when  $3|D^2$  – on  $\mathbb{H}_2$  (Classes HA and HB). Thus, from now on until the end of Section 5.2 we assume that the attainable value  $D^2$  is arbitrary on  $\mathbb{A}_2$  and is divisible by 3 on  $\mathbb{H}_2$ . Consequently, the PGSs are configurations of type  $(D, \alpha)$  (obtained from  $D$ -sub-lattices). The V-cell method is considerably shorter than the MRD-triangle method but it has a drawback that the obtained Peierls constant  $\bar{p} = \bar{p}(D)$  is not explicit.

It is known [10, 14] that for any given  $D$ , a V-cell with the minimal possible area among  $D$ -ACs  $\phi \in \mathcal{A}(D, \mathbb{R}^2)$  is a perfect hexagon with the side length  $D/\sqrt{3}$  and area  $S = S(D)$  defined in Eqn (3.10). We call it a *perfect* V-cell. A  $D$ -AC  $\phi \in \mathcal{A}(D, \mathbb{R}^2)$  is called *V-perfect* if it contains only perfect V-cells. The only V-perfect  $D$ -AC  $\phi \in \mathcal{A}(D, \mathbb{R}^2)$  are triangular lattices in  $\mathbb{R}^2$  with the distance  $D$  between neighboring lattice sites (see again [14]).

**Lemma 5.3.** *For each  $D$  there exists a number  $\bar{\delta} = \bar{\delta}(D, \mathbb{A}_2/\mathbb{H}_2) > 0$  such that the area of a non-perfect V-cell in any AC  $\phi \in \mathcal{A}$  is  $> S + \bar{\delta}(D)$ .*

**Proof.** As follows from [14], to analyze optimal and next-to-optimal V-cells for  $\mathbf{x}$  in  $\phi \in \mathcal{A}$ , it suffices to consider sites at distance at most  $4D$  from  $\mathbf{x}$  which yields finitely many possibilities of drawing V-cells on  $\mathbb{A}_2$  or  $\mathbb{H}_2$ . There are always an optimal and a next-to-optimal cells as not all possibilities are the same. ■

**Remark 5.1.** It is precisely the fact that  $\bar{\delta}$  is not determined explicitly that leads to a non-explicit Peierls constant  $\bar{p}$  in Lemma 5.4. ▲

Given a basic polygon  $\mathbb{V}$ , a PGS  $\varphi \in \mathcal{P}$  and an AC  $\phi_{\mathbb{V}} \in \mathcal{A}(\mathbb{V}||\varphi)$ , we have the set-theoretical identity

$$\bigcup_{\mathbf{x} \in \phi_{\mathbb{V}}} \mathcal{V}(\mathbf{x}, \phi_{\mathbb{V}}) = \bigcup_{\mathbf{x} \in \varphi|_{\mathbb{V}}} \mathcal{V}(\mathbf{x}, \varphi|_{\mathbb{V}}). \quad (5.2)$$

Therefore, since PGS  $\varphi$  is an  $(D, \alpha)$ -configuration, for the partition function (2.4) we have that

$$\mathbf{Z}(\mathbb{V}||\varphi) = \sum_{\phi_{\mathbb{V}} \in \mathcal{A}(\mathbb{V}||\varphi)} \prod_{\mathbf{x} \in \phi_{\mathbb{V}}} u^{-S^{-1}(|\mathcal{V}(\mathbf{x}, \phi_{\mathbb{V}})| - S)}. \quad (5.3)$$

Here, and in Lemma 5.4 below, we use the notation  $|\mathcal{V}(\mathbf{x}, \phi_{\mathbb{V}})|$  and  $|\mathcal{V}(\mathbf{x}, \phi|_{\Gamma})|$  for the area of  $\mathcal{V}(\mathbf{x}, \phi_{\mathbb{V}})$  and  $\mathcal{V}(\mathbf{x}, \phi|_{\Gamma})$  where, in turn,  $\phi|_{\Gamma} := \phi|_{\text{Supp}(\Gamma)}$ . We also write  $|\text{Supp}(\Gamma)|$  for the area of  $\text{Supp}(\Gamma)$ .

Recall, the quantities  $\|\text{Supp}(\Gamma)\|$  and  $w(\Gamma)$  are defined in Eqns (3.12) and (3.9), respectively.

**Lemma 5.4.** (A Peierls bound via V-cells) *There exists a constant  $\bar{p} = \bar{p}(D) > 0$  such that for any contour  $\Gamma = (\text{Supp}(\Gamma), \phi \upharpoonright_\Gamma)$  we have*

$$w(\Gamma) = \prod_{\mathbf{x} \in \phi \upharpoonright_\Gamma} u^{-S^{-1}(|\mathcal{V}(\mathbf{x}, \phi \upharpoonright_\Gamma)| - S)} \leq u^{-\bar{p}(D)\|\text{Supp}(\Gamma)\|}. \quad (5.4)$$

**Proof.** The equality in Eqn (5.4) is simply a re-writing of (3.9). Further, we need to consider sites  $\mathbf{x}$  where  $|\mathcal{V}(\mathbf{x}, \phi \upharpoonright_\Gamma)| > S$ ; otherwise (i.e., when  $|\mathcal{V}(\mathbf{x}, \phi \upharpoonright_\Gamma)| = S$ ) site  $\mathbf{x}$  does not contribute into (5.4). Observe that

$$\text{if } |\mathcal{V}(\mathbf{x}, \phi \upharpoonright_\Gamma)| - S \geq S \text{ then } |\mathcal{V}(\mathbf{x}, \phi \upharpoonright_\Gamma)| - S \geq \frac{1}{2} |\mathcal{V}(\mathbf{x}, \phi \upharpoonright_\Gamma)|.$$

On the other hand, by Lemma 5.3,

$$\text{if } |\mathcal{V}(\mathbf{x}, \phi \upharpoonright_\Gamma)| - S < S \text{ then } |\mathcal{V}(\mathbf{x}, \phi \upharpoonright_\Gamma)| - S \geq \bar{\delta} \geq \frac{\bar{\delta}}{2S} |\mathcal{V}(\mathbf{x}, \phi \upharpoonright_\Gamma)|.$$

According to the definition of a  $\varphi$ -correct template, we have an inequality

$$\sum_{\mathbf{x} \in \phi \upharpoonright_\Gamma} |\mathcal{V}(\mathbf{x}, \phi \upharpoonright_\Gamma)| \mathbf{1}\left(|\mathcal{V}(\mathbf{x}, \phi \upharpoonright_\Gamma)| > S\right) \geq \frac{1}{9D^2} |\text{Supp}(\Gamma)|.$$

Also,  $\|\text{Supp}(\Gamma)\| = \kappa |\text{Supp}(\Gamma)|$  where  $\kappa = 1/S^2 = 4/(3D^4)$ . Thus, we can take

$$\bar{p}(D) = \frac{\kappa}{9D^2} \min\left(\frac{1}{2}, \frac{\bar{\delta}}{\sqrt{3}} D^{-2}\right). \quad (5.5)$$

■

### 5.3 Proof of Theorems 1–3 (Classes TA1, TA2, TB), Theorems 7–9 (Classes HA1, HA2, HB), Theorem 11 (Class HC), Theorems 12 (Classes HD1 and HD2) and 13 (Class HE)

Owing to Theorems I and II, the proof of the listed theorems is reduced to an explicit description of the PGS-equivalence classes. The structure of these classes follows from the arithmetic properties of the value  $D^2$  to which the conditions of each theorem explicitly refer. Once again, in Theorem 13 we restrict ourselves to the analysis of PGSs only.

## 6 Proof of Theorems 4–6 and 10

### 6.1 Dominance for the H-C model

Our study of dominance follows an approach developed in [25], [26] and [3]. In particular, we use an appropriate family of *small* contours (see Definition 1 on page 566 in [26]) and

then compare the *free energies* of the corresponding *truncated models* to decide which PGS-equivalence class is dominant.

In the examples of dominance presented in Theorems 4–6 (Class TB), and 10 (Class HB) we have that all PGSs are  $\alpha$ -configurations; this fact generates a number of similarities in the analysis of these examples. Let us first give a common summary of our construction.

The ‘smallest’ contour in a PGS is generated by the removal of a single particle. The statistical weight of such a contour is  $u^{-1}$ ; we can say that it represents a  $u^{-1}$ -excitation. The *density* of such  $u^{-1}$ -contours is the same in each of the PGSs  $\varphi \in \mathcal{P}$ . Similarly, the removal of two particles at distance  $D$  from each other generates a contour of statistical weight  $u^{-2}$ . Again, the density of such  $u^{-2}$ -contours is the same in every PGS  $\varphi \in \mathcal{P}$ .

The next category of a small contour is generated when three particles are removed at the vertices of a  $D$ -triangle  $\Delta$ , and one particle is inserted at a site inside  $\Delta$ . Here the new occupied site should lie at a distance  $\geq D$  from any other sub-lattice site. As before, the corresponding contour has statistical weight  $u^{-2}$ . We can speak of a *single insertion* repelling 3 particles from a PGS. Next, we will have to deal with double, triple, and quadruple admissible insertions maintaining the weight  $u^{-2}$  for the emerging contour. To stress the latter property, we will often speak of  $u^{-2}$ -insertions.

Figures 16–22 show the structure of  $u^{-2}$ -insertions for the cases considered in Theorems 4–6 and 10. Double admissible insertions occur when 4 particles are removed from the vertices of a  $D$ -rhombus formed by two adjacent  $D$ -triangles  $\Delta_1, \Delta_2$ , and 2 particles are inserted inside  $\Delta_1 \cup \Delta_2$ . (For  $D^2 = 49$  on lattice  $\mathbb{A}_2$  (Theorem 4), the single and double  $u^{-2}$  suffice.) Next, triple admissible insertions occur when 5 particles are removed from the boundary of a trapeze formed by three pair-wise adjacent  $D$ -triangles  $\Delta_1, \Delta_2, \Delta_3$ , and 3 particles are inserted inside  $\Delta_1 \cup \Delta_2 \cup \Delta_3$ . Finally, quadruple admissible insertions occur when 6 particles are removed from the boundary of an  $2D$ -triangle by four pair-wise adjacent  $D$ -triangles  $\Delta_1, \Delta_2, \Delta_3, \Delta_4$ , and 4 particles are inserted inside  $\Delta_1 \cup \Delta_2 \cup \Delta_3 \cup \Delta_4$ .

Any other contour in the truncated model for the considered examples has statistical weight at most  $u^{-3}$ . This statement requires a certain effort to verify (including a substantial computer assistance); it is done in Section 7 in the form of Lemmas 7.1–7.4. With Lemmas 7.1–7.4 at hand, we can use in a standard way the polymer expansions for the free energies of the truncated models (see, e.g., Sections 1.7, 2.1 in [26] or Section 3.a in [23]). This allows us to upper-bound the contribution to these free energies from contours with weight  $\leq u^{-3}$  by  $cu^{-3}$  where  $c > 0$  is an absolute constant. Thus, for  $u$  large enough the determination of a dominant class is reduced to the count of densities of single, double, triple and quadruple insertions.

## 6.2 Proof of Theorem 4

For  $D^2 = 49$  on  $\mathbb{A}_2$ , we have two PGS-equivalence classes (inclined and horizontal); they are determined by inclined  $D$ -sub-lattices containing sites  $(3, 5)$  or  $(5, 3)$  and a horizontal one containing site  $(7, 0)$ . We will use pairs  $(5, 3)$  and  $(7, 0)$  for referring to these sub-lattices and their associated PGSs. We want to check that the horizontal  $(7, 0)$ -PGSs are dominant and the inclined  $(5, 3)$ -PGSs are not.

Any inclined  $D$ -triangle for  $D^2 = 49$  covers 12 sites where we have a single  $u^{-2}$ -

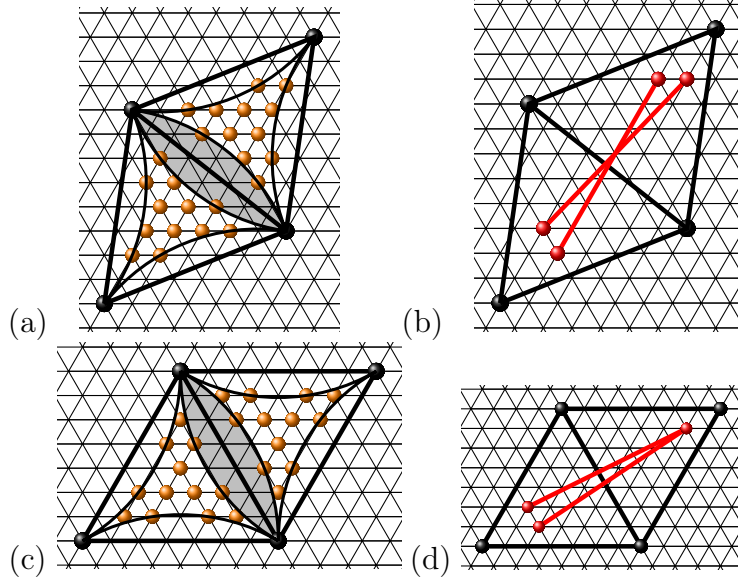


Figure 16: Single and double  $u^{-2}$ -insertions for  $D^2 = 49$  on  $\mathbb{A}_2$ .

For each PGS there are 12 sites inside a  $D$ -triangle (orange balls) where a single insertion repels 3 particles at the vertices of the triangle (black balls). Examples of double insertions repelling 4 particles at the vertices of  $D$ -rhombus are shown in red. There are 6 double insertions in a  $(5, 3)$ -rhombus and 7 in a  $(7, 0)$ -one. As there is no other  $u^{-2}$ -insertions, the  $(7, 0)$ -class is dominant.

insertion repelling precisely 3 particles at the vertices of this triangle. In Figure 16 (a) these sites are marked by orange balls, while the repelled sites from a PGS are marked by black balls. The orange balls are placed at sites covered by closed concave circular triangles. On the other hand, open bi-convex lenses indicate positions where an inserted particle repels 4 black balls at the vertices of a  $D$ -rhombus which yields a  $u^{-3}$ -insertion.

Similarly, any horizontal triangle also covers 12 sites where a single insertion repels 3 particles at the vertices of a  $D$ -triangle. We use the same legend to mark these possibilities in Figure 16 (c): closed concave circular triangles cover single  $u^{-2}$ -insertions, open bi-convex lenses indicate positions where an inserted particle repels 4 black balls at the vertices of a  $D$ -rhombus, yielding an  $u^{-3}$ -insertion.

Thus, both inclined and horizontal PGSs have the same density of single  $u^{-2}$ -insertions.

The small contour which detects a difference is constructed when 4 particles at the vertices of a  $D$ -rhombus are removed and 2 particles inside the rhombus are inserted, maintaining admissibility. The statistical weight of this contour also equals  $u^{-2}$ . Figures 16 (b) and 16 (d) show examples of double  $u^{-2}$ -insertions marked by red. For any inclined  $(5, 3)$ -rhombus there are 6 such pairs of sites. For any  $(7, 0)$ -rhombus there are 7 such pairs.

Any other contour in the truncated model for  $D^2 = 49$  has statistical weight at most  $u^{-3}$ ; this is proven in Lemma 7.1 in Section 7. Therefore, only the horizontal PGS-equivalence class contains the dominant PGSs. ■

### 6.3 Proof of Theorem 5

The argument in the proof of Theorem 5 is similar to that of Theorem 4, except for specific numbers of small contours. Here we distinguish between inclined  $(8, 7)$ - and horizontal  $(13, 0)$ -PGSs. The first difference with Theorem 4 is in the categories of contours having the statistical weight  $u^{-2}$ . As before, we have single and double admissible  $u^{-2}$ -insertions; see Figure 17.

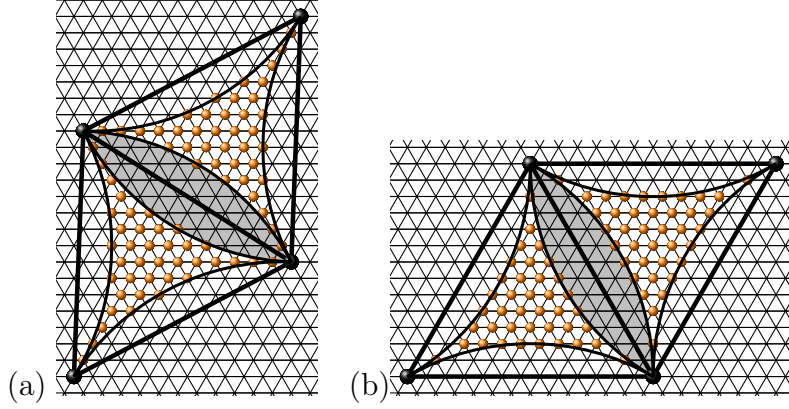


Figure 17: Single  $u^{-2}$ -insertions for  $D^2 = 169$  on  $\mathbb{A}_2$ .

We again use orange balls and circular triangles for marking the positions where an inserted particle repels 3 vertices of a  $D$ -triangle in a PGS. In both PGS types the number of single  $u^{-2}$ -insertions equals 39 per triangle or 78 per a  $D$ -rhombus.

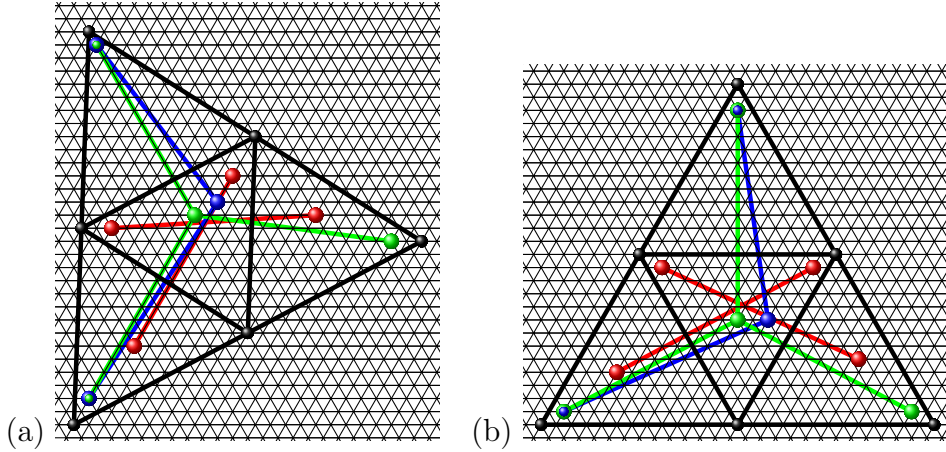


Figure 18: Double, triple and quadruple  $u^{-2}$ -insertions for  $D^2 = 169$  on  $\mathbb{A}_2$ .

Examples of double  $u^{-2}$ -insertions repelling 4 vertices of a  $D$ -rhombus are shown in red. There are 113 double insertions in an  $(8, 7)$ -rhombus and 86 in a  $(13, 0)$ -rhombus. Examples of triple  $u^{-2}$ -insertions are shown in blue: they repel 5 sites on the boundary of a trapeze. Quadruple  $u^{-2}$ -insertions (green) repel 6 sites on the boundary of a  $2D$ -triangle. The number of triple insertions is 61 in an  $(8, 7)$ - and 20 in a  $(13, 0)$ -triangle, while the number of quadruple insertions is 39 in an  $(8, 7)$ -PGS and 3 in an  $(13, 0)$ -PGS.

In addition, we can place 3 particles in a trapeze and also 4 particles in a  $2D$ -triangle: see Figure 18. The number of single insertions equals 39 per a triangle or 78 per a  $D$ -rhombus in both PGS types. However, in the remaining three categories of  $u^{-2}$ -insertions, the  $(8, 7)$ -PGSs dominate distinctively, with 113 vs 78 doubles in a  $D$ -rhombus, 61 vs 20 triples in a trapeze and 39 vs 3 quadruples in a  $2D$ -triangle. The enumeration of cases above can be performed manually but we also present a Java routine which automates this task. Cf. Program 3 `CountExcitations` in the ancillary file and Section 9.

The verification that no other contour with statistical weight smaller than  $u^{-3}$  exists for the horizontal  $D$ -sub-lattice is done in Lemma 7.2 in Section 7; it requires a more massive enumeration than in Lemma 7.1 and therefore relies on a computer-assisted argument. ■

## 6.4 Proof of Theorem 6

The argument for  $D^2 = 147$  on  $\mathbb{A}_2$  repeats that for  $D^2 = 49, 169$  and is again based on an exact count of  $u^{-2}$ -insertions. Here we distinguish between two PGS types referred to as vertical and  $(7, 7)$ - and inclined  $(11, 2)$ -PGSs.

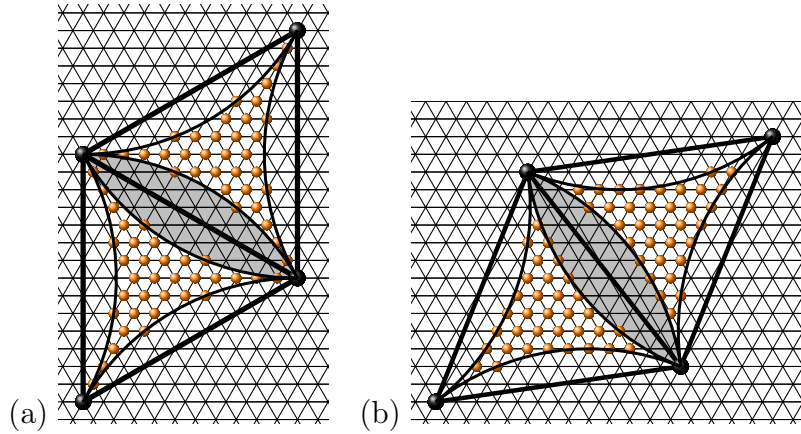


Figure 19: Single  $u^{-2}$ -insertions for  $D^2 = 147$  on  $\mathbb{A}_2$ : (a) in a  $(7, 7)$ -PGS and (b) in an  $(11, 2)$ -PGS.

As before, circular triangles and orange balls mark the positions where an inserted particle repels 3 vertices of a  $D$ -triangle in a PGS. In both PGS types the number of single  $u^{-2}$ -insertions equals 34 per a  $D$ -triangle or 68 per a  $D$ -rhombus.

Single  $u^{-2}$ -insertions do not favor any specific PGS: their number equals 34 per triangle or 68 per rhombus in all PGSs. However, the double, triple and quadruple  $u^{-2}$ -insertions favor the  $(7, 7)$ -PGSs. Viz., the number of double insertions is 86 in a  $(7, 7)$ - and 51 in an  $(11, 2)$ -rhombus, the number of triple insertions is 39 in a  $(7, 7)$ - and 1 in an  $(11, 2)$ -triangle, and the number of quadruple insertions is 1 in a  $(7, 7)$ - and 0 in an  $(11, 2)$ -triangle. Again, this enumeration can be performed manually or by executing the Java routine from Program 3 `CountExcitations`. Cf. Figures 19 and 20. The proof is completed by applying Lemma 7.3 guaranteeing that the  $u^{-2}$ -insertions are the only ones listed above. ■

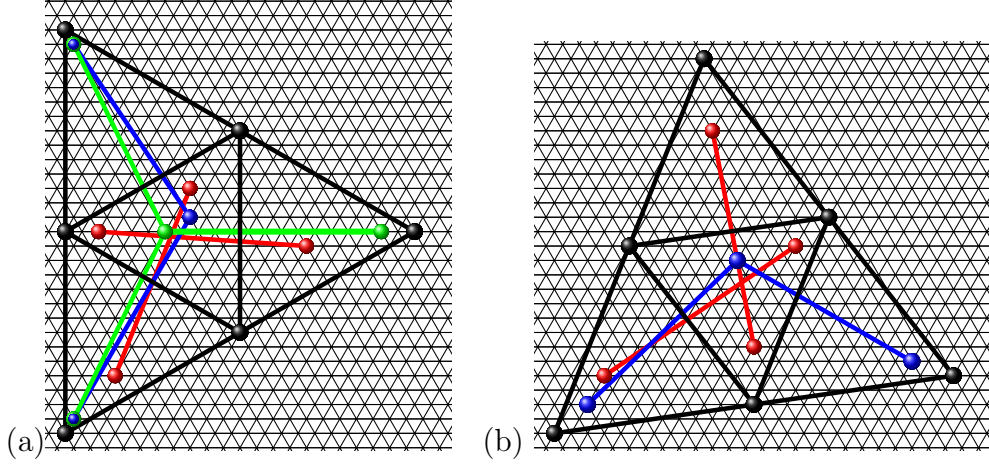


Figure 20: Double, triple and quadruple  $u^{-2}$ -insertions for  $D^2 = 147$  on  $\mathbb{A}_2$ , in a  $(7, 7)$ -PGS (a) and an  $(11, 2)$ -PGS (b).

Double  $u^{-2}$ -insertions (red) again repel 4 vertices of a rhombus; triple insertions (blue) repel 5 sites on the boundary of a trapeze; quadruple insertions (green) repel 6 sites on the boundary of a  $2D$ -triangle. There are 86 double insertions in  $(7, 7)$ - and 51 in an  $(11, 2)$ -rhombus. Next, we have 39 triple insertions in a  $(7, 7)$ - and 1 in an  $(11, 2)$ -triangle. Finally, the number of quadruple insertions is 1 in a  $(7, 7)$ -PGS and 0 in an  $(11, 2)$ -PGS.

We do not know if the contours of weight  $u^{-2}$  always suffice to determine dominant PGSs and if a dominant PGS class is always unique. A numerical calculation covering  $D^2 \leq 100000$  confirms that there is only one  $D$ -sub-lattice which dominates in the amount of  $u^{-2}$ -contours. We conjecture that it is the sub-lattice which has an orange ball in a site at the shortest distance from the triangle vertex among all  $D$ -sub-lattices.

## 6.5 Proof of Theorem 10

Once more, we follow the established scheme of counting the  $u^{-2}$ -insertions. As in Theorem 6, we distinguish between the inclined  $(11, 2)$ - and vertical  $(7, 7)$ -PGSs types, now on  $\mathbb{H}_2$ . The number of vertical PGSs equals 98 while the number of inclined PGSs is 196.

As before, the  $u^{-1}$ -contours do not make a distinction. The analysis of dominance focuses on admissible  $u^{-2}$ -insertions.

A vertical  $(7, 7)$ -PGS is shown in Figure 21. As earlier, single  $u^{-2}$ -insertions remove 3 particles at the vertices of a  $D$ -triangle and add one inside the same triangle. They are again marked by orange balls in frame (a). The number of such insertions is 21 in triangles  $OAB$ ,  $OCD$  (and also  $BFC$  in frame (b)), and 25 in triangles  $OBC$ ,  $ODE$  (and also  $CDG$  in frame (b)). In total, we have 46 single insertions in each of five rhombuses  $OABC$ ,  $OBFC$ ,  $OBDC$ ,  $OCGD$ ,  $OCDE$  featured in frame (b).

Double  $u^{-2}$ -insertions remove 4 particles at the vertices of a  $D$ -rhombus and add 2 particles inside the same rhombus. In Figure 21 (b), a double  $u^{-2}$ -insertion is marked by a red bar. The number of admissible double insertions inside every  $D$ -rhombus equals 108.

Triple and quadruple admissible  $u^{-2}$ -insertions for vertical PGSs are also shown in Figure 21 (b). In a triple insertion 5 particles are removed and 3 added (blue balls joined



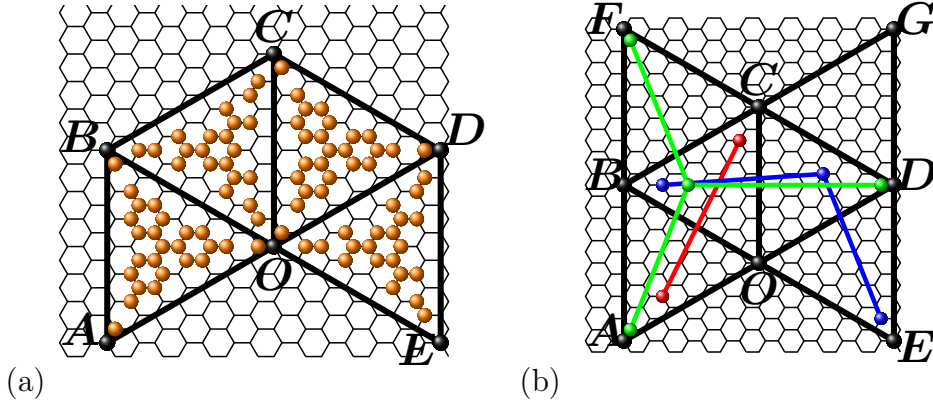


Figure 21: Admissible  $u^{-2}$ -insertions in a vertical PGS for  $D^2 = 147$  on  $\mathbb{H}_2$ .

(a) Single insertions are again marked by orange balls: they repel 3 vertices of the covering  $D$ -triangle. (b) A double insertion is marked by a red bar; here we remove 4 vertices of the covering  $D$ -rhombus. Triple insertions are represented by a pair of blue bars and a triple of green bars. Such insertions remove 5 vertices in a PGS, on the boundary of the covering trapeze. Quadruple insertions repel 6 vertices of a  $2D$ -triangle (triangles  $AFD$  and  $GBE$ ), with a single insertion in each of 4 involved  $D$ -triangles. Such an insertion is represented by a triple of green bars. As in the previous examples, there is no other admissible  $u^{-2}$ -insertion.

by blue bars), whereas in a quadruple insertion 6 particles are removed and 4 added (green balls joined by tripods of green bars), following the same geometric pattern as before (a trapeze or a  $2D$ -triangle). In total, we have 63 triple  $u^{-2}$ -insertions per a  $D$ -rhombus.

Quadruple admissible  $u^{-2}$ -insertions cannot occur inside the  $2D$ -triangle  $EBG$ . However, for triangle  $AFD$  they can occur, and their number equals 9. Hence, the number of quadruple insertions with the middle point of a tripod inside triangle  $OBC$  equals 9. Thus, the total number of admissible quadruple  $u^{-2}$ -insertions in a  $D$ -rhombus is 9. According to Lemma 7.4, the list of all admissible  $u^{-2}$ -insertions is exhausted by the aforementioned possibilities. All-in-all, the above count yields 226 admissible  $u^{-2}$ -insertions per a  $D$ -rhombus in a vertical PGS.

The situation with an inclined  $(11, 2)$ -PGSs for  $D^2 = 147$  on  $\mathbb{H}_2$  is shown in Figure 22. In frame (a) we again put orange balls in positions where a single insertion repels three occupied sites at the vertices of the covering  $D$ -triangle. The number of such insertions is 24 in triangles  $OAB$  and  $OCD$  and 22 in triangles  $OBC$  and  $ODE$ , with 46 insertion per a  $D$ -rhombus. Next, in frame (b) we mark by a red bar an admissible double insertion removing 4 vertices of the covering  $D$ -rhombus. The number of double  $u^{-2}$ -insertions is 23 in all rhombuses in the inclined PGS. Thus, the total amount of double insertions equals 69 per a  $D$ -rhombus.

As before, triple insertions repelling 5 vertices in an inclined PGS occur when 3 particles are put in a trapeze, one insertion for each involved triangle. The total number of admissible triple  $u^{-2}$ -insertions per a  $D$ -rhombus is 3.

Lastly, quadruple insertions repelling 6 vertices could have occurred when 4 particles

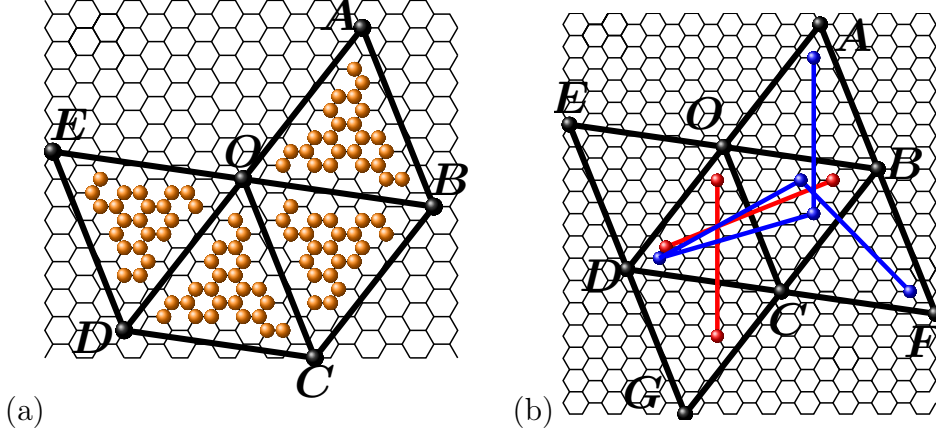


Figure 22: Admissible  $u^{-2}$ -insertions in an inclined PGS for  $D^2 = 147$  on  $\mathbb{H}_2$ .

The marking here is as in the previous figure. (a) As in Figure 21 (a), single insertions with a triple repulsion are marked by orange balls: they repel 3 vertices of the covering  $D$ -triangle. (b) Again, double insertions repel 4 vertices only when the latter ones are the vertices of the covering  $D$ -rhombus. Such insertions are marked by red bars. Triple insertions are marked by pairs of blue bars joining triples of occupied sites.

are put in a  $2D$ -triangle. However, in an inclined PGS such insertions do not exist. According to Lemma 7.4, the list of admissible  $u^{-2}$ -insertions in an inclined PGS is exhausted by the above types. All-in-all, the number of admissible  $u^{-2}$ -insertions per a  $D$ -rhombus in an inclined PGS equals 118. Hence, for  $D^2 = 147$  on  $\mathbb{H}_2$ , the vertical PGS class is dominant, and for  $u$  large enough we have 98 EGMs generated by the (7, 7)-PGSs. ■

## 7 Proof of technical assertions from Theorems 4–6, 10

In this section we verify that the small contours with a weight  $\geq u^{-2}$  which were determined in Section 6 are the only ones possible for the selected values of  $D^2$ , and any other contour has the statistical weight  $\leq u^{-3}$ . The corresponding statements are Lemmas 7.1–7.3 on  $\mathbb{A}_2$  and Lemma 7.4 on  $\mathbb{H}_2$ ; the latter, essentially, implied by Lemma 7.3.

The argument is based on the following construction. Without loss of generality we can assume that the underlying PGS  $\varphi \in \mathcal{P}(D)$  has  $\varphi(\mathbf{0}) = 1$  (i.e.,  $\varphi$  is a  $D$ -sub-lattice in  $\mathbb{A}_2$ ). Recall, a  $\varphi$ -contour  $\Gamma$  can be obtained by adding finitely many particles at some inserted sites, and then removing the particles from  $\varphi$  which are repelled by the inserted ones (removed sites/particles). The resulting admissible configuration is denoted by  $\phi$ . One can also remove from  $\phi$  any additional particles but such an unforced removal can only decrease the weight  $w(\Gamma)$  and therefore will be disregarded.

As we saw earlier, every inserted site repels from  $\varphi$  either 3 or 4 removed sites. The inserted sites which repel 3 removed sites are located inside closed concave circular triangles identified in the proof of Theorems 4–6 (orange balls in Figures 16, 17, 19). The complement (in  $\mathbb{R}^2$ ) to these triangles consists of mutually disjoint open circular

bi-convex lenses (gray areas in Figures 16, 17, 19). A particle inserted in a lattice site belonging to a lens repels 4 removed sites.

Consider a  $D$ -connected component  $\Delta$  of the set of removed sites (together with the corresponding inserted sites). Let  $\sharp(\Delta)$  denote the difference between the numbers of removed and inserted sites in  $\Delta$ . Our goal is to verify that the weight  $u^{-\sharp(\Delta)}$  of any such component is at most  $u^{-3}$ , i.e.,  $\sharp(\Delta) \geq 3$ . Note that a contour support has been defined in Section 3.1 by using the notion of a template; hence it can include more than one  $\Delta$ . In that case the statistical weight of the contour is the product of the statistical weights of constituting  $D$ -connected components, and for our purposes it is enough to estimate the weight of a single component  $\Delta$ .

To evaluate  $\sharp(\Delta)$ , it is convenient to introduce a *total repelling force*  $F(\mathbf{x}) = F(\mathbf{x}, \phi)$  acting (in the resulting AC  $\phi \in \mathcal{A}(D)$ ) upon a removed site  $\mathbf{x} \in \varphi$ . Such a force is accumulated from all inserted sites  $\mathbf{y}_i \in \phi$  that repel site  $\mathbf{x}$ :  $F(\mathbf{x}) = \sum_i F(\mathbf{x}, \mathbf{y}_i, \phi)$ .

We require that every summand  $F(\mathbf{x}, \mathbf{y}_i, \phi)$  is non-negative and depends only on the Euclidean distance  $\rho(\mathbf{x}, \mathbf{y}_i)$  between  $\mathbf{x}$  and  $\mathbf{y}_i$ . The square of this distance  $\rho(\mathbf{x}, \mathbf{y}_i)^2$  is always a positive integer, and we use a shorthand notation  $f_r$  for  $F(\mathbf{x}, \mathbf{y}, \phi)$ , with  $r = \rho(\mathbf{x}, \mathbf{y})^2 \in \mathbb{N}$ ,  $\mathbf{x} \in \varphi$ ,  $\mathbf{y} \in \phi$ . With this notation at hand,  $\forall \mathbf{x} \in \varphi$ ,

$$F(\mathbf{x}) := \sum_{r < D^2, \mathbf{y} \in \phi} f_r \mathbf{1}(\mathbf{y} \text{ removes } \mathbf{x}, \text{ and } r = \rho(\mathbf{y}, \mathbf{x})^2), \quad \text{where } f_r \geq 0. \quad (7.1.A)$$

The coefficient  $f_r$  is referred to as a *local repelling force* at distance  $\sqrt{r}$ . A dual quantity  $G(\mathbf{y}) = G(\mathbf{y}, \phi)$  represents the *total repelling force* generated by an inserted site  $\mathbf{y}$ :

$$G(\mathbf{y}) := \sum_{r < D^2, \mathbf{x} \in \varphi} f_r \mathbf{1}(\rho(\mathbf{x}, \mathbf{y})^2 = r, \mathbf{x} \text{ is removed by } \mathbf{y}), \quad \mathbf{y} \in \phi. \quad (7.1.B)$$

Our aim is to find  $f_r$  such that, for any site  $\mathbf{x} \in \varphi$  and any site  $\mathbf{y} \in \phi$  removing 3 or 4 sites from  $\varphi$ ,

$$(a) \quad F(\mathbf{x}, \phi) \leq 1, \quad (b) \quad G(\mathbf{y}, \phi) = 1. \quad (7.2)$$

Owing to (7.2), if the *deficit*  $\delta(\mathbf{x}) = \delta(\mathbf{x}, \phi)$  of the removed site  $\mathbf{x}$  is calculated as  $1 - F(\mathbf{x})$  then  $\delta(\mathbf{x}) \geq 0$ , and

$$\sharp(\Delta) = \sum_{\mathbf{x} \in \varphi} \delta(\mathbf{x}, \phi) \mathbf{1}(\text{site } \mathbf{x} \text{ is removed when passing from } \varphi \text{ to } \phi). \quad (7.3)$$

From now on we assume that the configuration  $\phi$  has a single  $D$ -connected component  $\Delta$ , and the rest of the argument deals with this  $\Delta$ . Figure 23 shows a fragment of a set  $\Delta$  with a collection of inserted and removed sites.

The next observation is that set  $\Delta$  consists of *internal* sites for which all 6 sub-lattice neighbors also belong to  $\Delta$  and *boundary* sites which have at least one occupied  $D$ -sub-lattice neighbor (obviously, not belonging to  $\Delta$ ). Each  $D$ -connected component of the boundary sites in  $\Delta$  defines a closed broken line in  $\mathbb{R}^2$ , and the set  $\Delta$  can be understood as  $\mathbb{R}^2$ -polygon with the boundary  $\partial\Delta$  formed by these broken lines.

In general, the boundary  $\partial\Delta$  can have several connected components: one external and zero or more internal ones. An ambiguous situation arises when 4  $D$ -segments from

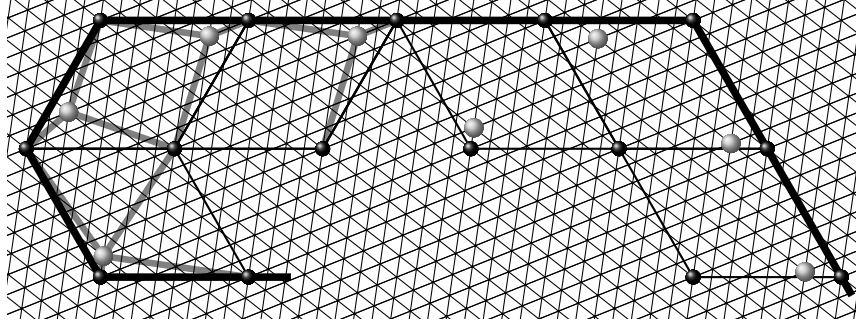


Figure 23: A fragment of set  $\Delta$ , for an inclined PGS  $\varphi$ , for  $D^2 = 169$ . Black balls in Figures 23–25 mark removed sites  $\mathbf{x} \in \varphi$  while gray balls mark inserted sites  $\mathbf{y} \in \phi$ . Gray lines indicate which sites are removed by a given inserted site. Thick black lines indicate the boundary  $\partial\Delta$ .

$\partial\Delta$  meet at the same boundary site (i.e., this site has 2 opposite  $D$ -neighbors that are occupied). In that case we fictitiously cut this site along the short line segment (of length less than 1) which passes through this site and has both ends inside  $\Delta$  (viewed as an open polygon in  $\mathbb{R}^2$ ). This removes the ambiguity, and the exterior and the interior of  $\Delta$  become uniquely defined.

It is clear that, as an  $\mathbb{R}^2$ -polygon,  $\Delta$  can only have vertices with angles  $\pi/3$ ,  $2\pi/3$  and  $4\pi/3$ . We say that the corresponding removed sites from  $\partial\Delta$  are of type  $\pi/3$ ,  $2\pi/3$  and  $4\pi/3$  respectively. The remaining sub-lattice sites from  $\partial\Delta$  correspond to the angle  $\pi$ ; we say that such a site has type  $\pi$ .

If a vertex  $\mathbf{x} \in \partial\Delta$  is repelled only by a single inserted site  $\mathbf{y}$  then imagine the particle at  $\mathbf{y}$  being deleted. Then vertex  $\mathbf{x}$  also disappears from  $\Delta$  (as nothing repels it anymore), and the value  $\sharp(\Delta)$  does not increase. (Actually,  $\sharp(\Delta)$  remains intact if  $\mathbf{y}$  repels a single vertex  $\mathbf{x}$  in  $\Delta$ .) In Figures 24, 25 we refer to such a site  $\mathbf{x}$  as *deletable*.

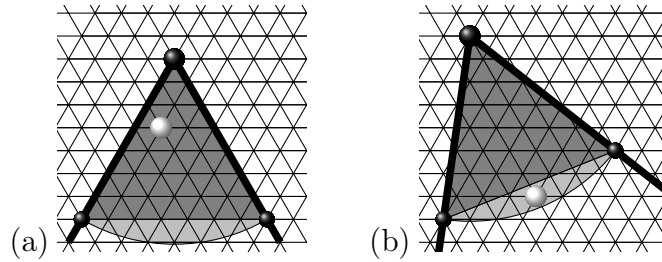


Figure 24: A deletable vertex of type  $\pi/3$  (a large black ball), in a horizontal PGS (a) and in an inclined PGS (b), for  $D^2 = 49$ . The white balls show sites of insertion. The same meaning is assigned in Figure 25.

Medium-size black balls in Figures 23, 24 mark the positions of removed sites of type  $\pi$  in  $\partial\Delta$ .

In view of the above definition, every polygon  $\Delta$  that can be reduced, by the process of deletion, to an irreducible polygon  $\Delta^0$ , for which  $\sharp(\Delta^0) \leq \sharp(\Delta)$ . By definition, a polygon  $\Delta$  with a single inserted site is irreducible. The simplest form of  $\Delta^0$  is a  $D$ -triangle with a single inserted site, where  $\sharp(\Delta^0) = 2$ . We would like to: (i) list all  $\Delta$ s that are reduced

to a  $D$ -triangle (possibly, with the help of a computer), and (ii) demonstrate that for all other irreducible polygons  $\Delta^0$ , we have  $\sharp(\Delta^0) \geq 3$ .

In fact, the next irreducible case is where  $\Delta^0$  is a  $D$ -rhombus with a single inserted site: it has  $\sharp(\Delta^0) \geq 3$ , in agreement with property (ii).

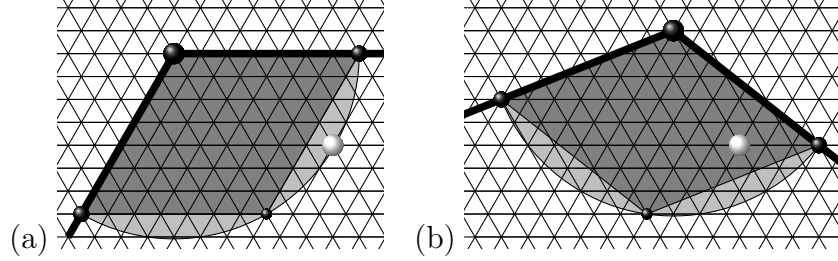


Figure 25: A deletable vertex of type  $2\pi/3$  (a large black ball), in a horizontal PGS (a) and in an inclined PGS (b), for  $D^2 = 49$ .

For any other (larger) irreducible polygon  $\Delta^0$ , the boundary  $\partial\Delta^0$  must have (i) no vertex of type  $\pi/3$  and (ii) at least 6 vertices of type  $2\pi/3$ . Each of the latter 6 vertices is repelled by exactly two inserted sites. Our goal in the lemmas below is to find, for the corresponding value of  $D^2$ , a collection of repelling forces  $\{f_r\}$  such that

$$\delta(\mathbf{x}) > 1/3 \text{ for any } \mathbf{x} \in \partial\Delta^0 \text{ of type } 2\pi/3. \quad (7.4)$$

This would imply the desired assertions, as  $6\delta(\mathbf{x}) > 2$ .

Let us now pass to specific cases. The proofs of Lemmas 7.1–7.4 require a finite enumeration which was done by computer. Cf. Programs 4 `VerifyRepellingForces` and 5 `CountMinDelta` in Section 9 and in the ancillary file.

The first case is  $D^2 = 49$  on  $\mathbb{A}_2$ . Define the following family  $\{f_r\}$ :

$$\begin{aligned} f_1 &= 44/56, & f_3 &= 40/56, & f_4 &= 40/56, & f_7 &= 31/56, & f_9 &= 31/56, \\ f_{12} &= 22/56, & f_{13} &= 22/56, & f_{16} &= 17/56, & f_{19} &= 17/56, & f_{21} &= 17/56, \\ f_{25} &= 8/56, & f_{27} &= 8/56, & f_{28} &= 8/56, & f_{31} &= 8/56, & f_{36} &= 4/56, \\ f_{37} &= 4/56, & f_{39} &= 4/56, & f_{43} &= 4/56, & f_{48} &= 4/56. \end{aligned} \quad (7.5)$$

The values  $r = 1, 3, 4, 7, 9, 12, 13, 16, 19, 21, 25, 27, 28, 31, 36, 37, 39, 43, 48$  in (7.5) represent all squared Euclidean distances from  $\mathbf{0}$  to the  $\mathbb{A}_2$ -sites within an open  $\mathbb{R}^2$ -disk of radius 7.

**Lemma 7.1.** *The family (7.5) gives a collection of local repelling forces for  $D^2 = 49$  on  $\mathbb{A}_2$  satisfying (7.2) and (7.4), for both horizontal and inclined PGSs. More precisely, for this collection,  $\forall$  irreducible polygon  $\Delta^0$  and vertex  $\mathbf{x} \in \partial\Delta^0$  of type  $2\pi/3$ ,*

$$\delta(\mathbf{x}) \geq 1 - f_{19} - f_{31} = 1 - f_{21} - f_{27} = 31/56. \quad (7.6)$$

**Remark 7.1.** For the proof of Theorem 4, it suffices to find a collection  $\{f_r\}$  only for inclined PGSs. Cf. Lemma 7.2. However, it turns out that the family  $\{f_r\}$  in (7.5) serves both types of PGSs. ▲

Next, we deal with  $D^2=169$ . Here we consider the values  $r$  representing the squared Euclidean distances from  $\mathbf{0}$  to all  $\mathbb{A}_2$ -sites within an open  $\mathbb{R}^2$ -disk of radius 13. For such values  $r$  we set:

$$\begin{aligned}
f_1 &= 131/135, & f_3 &= 127/135, & f_4 &= 251/270, & f_7 &= 241/270, & f_9 &= 116/135, \\
f_{12} &= 37/45, & f_{13} &= 221/270, & f_{16} &= 7/9, & f_{19} &= 133/180, & f_{21} &= 383/540, \\
f_{25} &= 179/270, & f_{27} &= 19/30, & f_{28} &= 169/270, & f_{31} &= 317/540, & f_{36} &= 281/540, \\
f_{37} &= 14/27, & f_{39} &= 131/270, & f_{43} &= 41/90, & f_{48} &= 37/90, & f_{49} &= 43/108, \\
f_{52} &= 103/270, & f_{57} &= 35/108, & f_{61} &= 53/180, & f_{63} &= 151/540, & f_{64} &= 5/18, \\
f_{67} &= 7/27, & f_{73} &= 119/540, & f_{75} &= 11/54, & f_{76} &= 109/540, & f_{79} &= 11/60, \\
f_{81} &= 22/135, & f_{84} &= 83/540, & f_{91} &= 2/15, & f_{93} &= 31/270, & f_{97} &= 29/270, \\
f_{100} &= 1/9, & f_{103} &= 4/45, & f_{108} &= 2/27, & f_{109} &= 2/27, & f_{111} &= 7/108, \\
f_{112} &= 1/15, & f_{117} &= 2/45, & f_{121} &= 11/270, & f_{124} &= 23/540, & f_{127} &= 11/270, \\
f_{129} &= 4/135, & f_{133} &= 4/135, & f_{139} &= 2/135, & f_{144} &= 1/54, & f_{147} &= 2/135, \\
f_{148} &= 2/135, & f_{151} &= 1/270, & f_{156} &= 1/270, & f_{157} &= 1/180 & f_{163} &= 0.
\end{aligned} \tag{7.7}$$

**Lemma 7.2.** *The family (7.7) gives a collection of local repelling forces for  $D^2 = 169$  on  $\mathbb{A}_2$  satisfying (7.2) and (7.4), for horizontal  $(13, 0)$ -PGSs. More precisely, for this collection,  $\forall$  irreducible polygon  $\Delta^0$  in a horizontal  $(13, 0)$ -PGS and vertex  $\mathbf{x} \in \partial\Delta^0$  of type  $2\pi/3$ ,*

$$\delta(\mathbf{x}) \geq 1 - f_{28} - f_{133} = 93/270. \tag{7.8}$$

Finally, we consider the example of  $D^2=147$  on  $\mathbb{A}_2$ . Set:

$$\begin{aligned}
f_1 &= 24/24, & f_3 &= 24/24, & f_4 &= 24/24, & f_7 &= 23/24, & f_9 &= 22/24, \\
f_{12} &= 21/24, & f_{13} &= 21/24, & f_{16} &= 20/24, & f_{19} &= 19/24, & f_{21} &= 18/24, \\
f_{25} &= 16/24, & f_{27} &= 15/24, & f_{28} &= 15/24, & f_{31} &= 14/24, & f_{36} &= 12/24, \\
f_{37} &= 12/24, & f_{39} &= 11/24, & f_{43} &= 10/24, & f_{48} &= 9/24, & f_{49} &= 8/24, \\
f_{52} &= 7/24, & f_{57} &= 6/24, & f_{61} &= 5/24, & f_{63} &= 4/24, & f_{64} &= 4/24, \\
f_{67} &= 4/24, & f_{73} &= 3/24, & f_{75} &= 3/24, & f_{76} &= 2/24, & f_{79} &= 2/24, \\
f_{81} &= 2/24, & f_{84} &= 2/24, & f_{91} &= 1/24, & f_{93} &= 1/24, & f_{97} &= 1/24,
\end{aligned} \tag{7.9A}$$

with

$$f_r = 0 \text{ for } r > 97. \tag{7.9B}$$

This yields a family of values  $f_r$  where  $r$  represents the squared Euclidean distance from  $\mathbf{0}$  to all  $\mathbb{A}_2$ -sites within an open  $\mathbb{R}^2$ -disk of radius  $\sqrt{147}$ .

**Lemma 7.3.** *The family (7.9A,B) gives a collection of local repelling forces  $\{f_r\}$  for  $D^2 = 147$  on  $\mathbb{A}_2$  satisfying (7.2) and (7.4), for inclined  $(11, 2)$ -PGSs. More precisely, for this collection,  $\forall$  irreducible polygon  $\Delta^0$  in an inclined  $(11, 2)$ -PGS and vertex  $\mathbf{x} \in \partial\Delta^0$  of type  $2\pi/3$ ,*

$$\delta(\mathbf{x}) \geq 1 - f_{37} - f_{100} = 1/2. \tag{7.10}$$

Next, we extend our analysis to  $\mathbb{H}_2$ . Consider the values  $f_r$  given by Eqns (7.9A,B) for  $r$  representing the squared Euclidean distance  $\leq 147$  between two  $\mathbb{H}_2$ -sites. We call it the  $\mathbb{H}_2$ -projected family (7.9A,B).

**Lemma 7.4.** *The  $\mathbb{H}_2$ -projected family (7.9A, B) gives a collection of local repelling forces  $\{f_r\}$  for  $D^2 = 147$  on  $\mathbb{H}_2$  satisfying (7.2) and (7.4), for inclined (11, 2)-PGSs. More precisely, for this collection,  $\forall$  irreducible polygon  $\Delta^0$  in an inclined (11, 2)-PGS and vertex  $\mathbf{x} \in \partial\Delta^0$  of type  $2\pi/3$ , the bound (7.10) holds true.*

**Remark 7.2.** In essence, the local repelling forces  $f_r$  are related to an attempt to improve a Peierls constant for the listed values  $D^2 = 49, 147, 169$ . In our opinion, this method in its present form can work only for moderate values of  $D^2$ .  $\blacktriangle$

## 8 A brief note on sliding on $\mathbb{H}_2$

As was noted, the values  $D^2 = 4, 7, 31, 133$  from Class HS exhibit sliding on  $\mathbb{H}_2$ . This is characterized by a cost-free passage from one type of PGSs to another. For  $D^2 = 4$

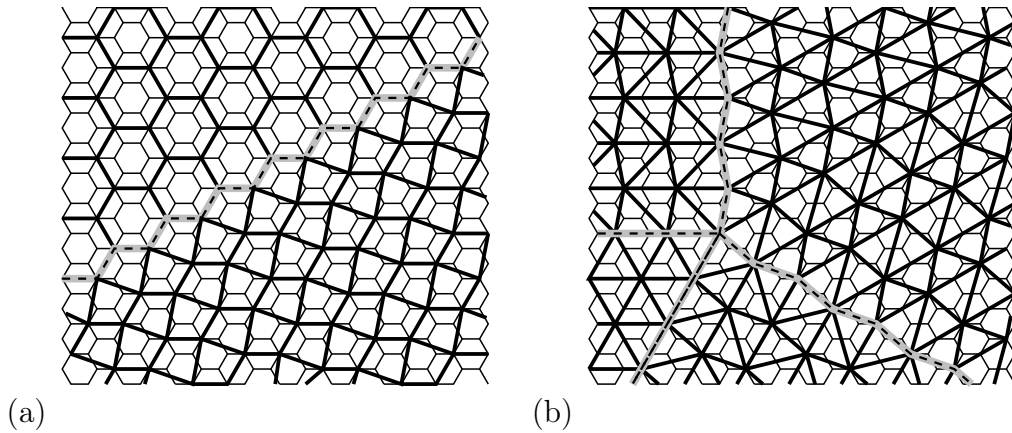


Figure 26: PGSs for  $D^2 = 4$  (frame (a)) and  $D^2 = 7$  (frame (b)).

Dotted gray lines mark the ‘cost-free’ boundaries between PGSs.

we have two types of PGSs: (a) one formed by hexagons with side-length 2, and (b) the other formed by  $\beta$ -configurations. These patterns can be intermittent in a stripe-like fashion, which generates countably many PGSs with no loss in the weight in the course of transition. See Figure 26 (a).

Similarly, for  $D^2 = 7$  we have the following types of PGSs: (a) an  $(\alpha, D)$ -configuration for  $D^2 = 9$ , (b) an assortment of  $\beta$ -configurations of various shapes and orientations. Again, it is possible to combine these patterns and generate countably many PGSs with no loss in the weight in the course of transition. See Figure 26 (b).

For  $D^2 = 31$ , we have a competition between strips formed by  $\tilde{D}$ -triangles with  $\tilde{D}^2 = 36$  and triangles with squared side-lengths 31, 36, 43. Such triangles share common sides and have equal areas. Again, the separation line does not incur a loss in weight.

Similarly, for  $D^2 = 133$ , we have a competition between strips formed by  $\tilde{D}$ -triangles with  $\tilde{D}^2 = 144$  and triangles with squared side-lengths 133, 144, 157. Such triangles again share a common side and have equal areas. As earlier, the separation line does not incur any loss in weight.

A pattern resembling that for  $D^2 = 31, 133$  is typical for sliding on  $\mathbb{Z}^2$ ; cf. [17].

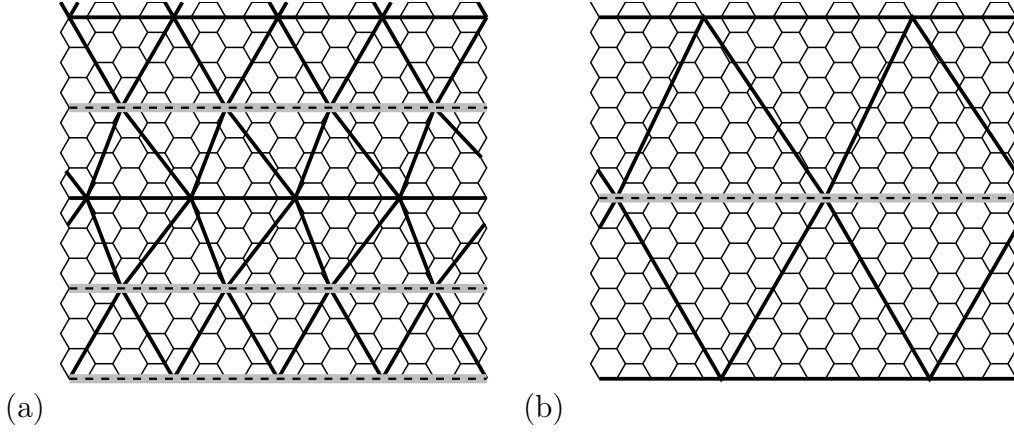


Figure 27: PGSs for  $D^2 = 31$  (frame (a)) and  $D^2 = 133$  (frame (b)).  
As before, dotted gray lines mark the ‘cost-free’ boundaries between PGSs.

## 9 Comments on computer programs used in the proofs

The ancillary file to this paper contains five Java programs and their outputs. These programs are used to (a) assist the proof of Lemmas 4.9, 4.10, (b) identify distinguishing small contours (admissible  $u^{-2}$ -insertions) for the values  $D^2 = 49$ ,  $D = 169$  and  $D^2 = 147$  and (c) assist the proof of Lemmas 7.1–7.4. Lemmas 4.9 and 4.10 are parts of the proof of Theorem I(ii) (in the part concerning Classes HD and HE) and Theorems 12 and 13. Lemmas 7.1–7.4 are parts of the proof of Theorems 4–6 and 10, for  $D^2 = 49$ ,  $D = 169$  and  $D^2 = 147$ . The routines can be executed on any computer hosting Java Development Kit version 1.4 and later. The routine from Program 5 requires 3GB of RAM while other routines are not resource hungry. Executions of all routines take from few seconds to 60 minutes.

Program 1 **NearestLoschianNumber** is a routine working on  $\mathbb{H}_2$ . It checks that, apart from 184 values, for each  $D^2 < (54)^4$  such that  $D^2$  is not divisible by 3, (i) the inequality involving the RHS of Eqn (4.11) holds true:  $\frac{\sqrt{3}}{2}D^2 + \frac{D}{2\sqrt{3}} > \frac{\sqrt{3}(D^*)^2}{2} = 2s(\Delta^*)$ , (ii) inequalities (4.16), (4.17) are satisfied. It leads to the conclusion that for each  $D^2 < (54)^4$ , apart from the above 184 values, if  $D^2$  is not divisible by 3 then this value  $D^2$  belongs to Class HC: the PGSs are  $(\alpha, D^*)$ -configurations, where  $D^* > D$  is the nearest Löschian number such that  $3|(D^*)^2$ . This assists the proof of Lemmas 4.9 and 4.10.

Program 2 **SpecialD** is a routine analyzing the 184 values  $D^2$  detected by Program 1. It specifies the values forming Classes HD, HE and HS on  $\mathbb{H}_2$ . This routine (i) extracts the exceptional values  $D^2 = 4, 7, 13, 16, 28, 31, 49, 64, 67, 97, 133, 157, 256$  (Classes HD, HE, HS) and identifies the PGSs for the exceptional non-sliding  $D^2 \neq 4, 7, 31, 133$ , (ii) checks that each  $D^2$  among the above 184 values which is not from Classes HD, HE, HS belongs to Class HC. Again, this assists the proof of Lemmas 4.9 and 4.10.

Program 3 **CountExcitations** is a routine calculating, for a given sub-lattice in  $\mathbb{A}_2$  or  $\mathbb{H}_2$ , the amount of distinguishing small contours (admissible  $u^{-2}$ -insertions) of the types used in the proofs of Theorems 4–6, 10. The execution results are presented only for  $D^2 = 49$ ,  $D = 169$  and  $D^2 = 147$  and the sub-lattices used in the proof of Lemmas 7.1–7.4.



Program 4 `VerifyRepellingForces` is a routine that verifies, for  $D^2 = 49, 169, 147$ , and a family of local repelling forces  $\{f_r\}$ , if Eqn (7.2) is satisfied.

Program 5 `CountMinDelta` is a routine that checks inequality (7.4), for a given sublattice and a family of local repelling forces, for  $D^2 = 49$ ,  $D = 169$  and  $D^2 = 147$ .

Programs 4, 5 assist the proof of Lemmas 7.1–7.4.

**Acknowledgement** IS and YS thank the Math Department, Penn State University, for hospitality and support. YS thanks St John’s College, Cambridge, for long-term support.

## References

- [1] Barbier, J., Krzakala, F., Zdeborova, L., Zhang, P. The hard-core model on random graphs revisited. *J. Phys.: Conf. Ser.* **473**, 012021 (2013).
- [2] Baxter, R. Hard hexagons: exact solutions. *J. Phys. A: Math. Gen.*, **13** (1980), L61-L70.
- [3] Brémont, J., Slawny, J. Phase transitions in systems with a finite number of dominant ground states. *J. Stat. Physics*, **54**, (1989), 89-161.
- [4] Chang, H.-C., Wang, L.-C. A simple proof of Thue’s theorem on circle packing. arXiv:1407.2199, 2010.
- [5] Charbonneau, P., Kurchan, J., Parisi, G., Urbani, P., Zamponi, F. Glass and jamming transitions: from exact results to finite-dimensional descriptions. *Annual Rev. Cond. Mat. Phys.*, **8** (2016), 1-26.
- [6] Connelly, R., W. Dickinson. Periodic planar disc packings. *Phil. Trans. Roy. Soc.*, **A372**, 20120039. <http://dx.doi.org/10.1098/rsta.2012.0039>
- [7] Conway, J., Sloane, N. *Sphere packings, lattices and groups*, 3rd Ed (With contributions by E. Bannai, R.E. Borcherds, J. Leech, S.P. Norton, A.M. Odlyzko, R.A. Parker, L. Queen and B.B. Venkov.) New York: Springer, 1999.
- [8] Dobrushin R.L. The problem of uniqueness of a Gibbsian random field and the problem of phase transitions. *Funct. Anal. Appl.* **4:4** (1968), 302–312.
- [9] Dobrushin R., Shlosman S., The problem of translation invariance of Gibbs states at low temperatures. *Mathematical Physics Reviews* **5**, 53-195. Soviet Sci. Rev. Sect. C Math. Phys. Rev., 5, Harwood Academic Publ., Chur, 1985.
- [10] Fejes Tóth, L. Some packing and covering theorems. *Acta Sci. Math.*, **12A** (1950), 62-67.
- [11] Georgii, H.O. *Gibbs measures and phase transitions*. De Gruyter, 2011.
- [12] Heilmann, O.J., Praestgaard, E. Phase transition of hard hexagons on a triangular lattice. *J. Stat. Physics*, **9** (1973), 1-22.

- [13] Holsztynski, W., Slawny, J. Peierls condition and number of ground states. *Comm. Math Phys.* **61** (1978), 177-190.
- [14] Hsiang, W-Y. Simple proof of a theorem of Thue on the maximal density of circle packings in  $E^2$ , *L'Enseignement Mathématique*, **38** (1992), 125-131.
- [15] Jauslin, I., Lebowitz, J.L. High-fugacity expansion, Lee-Yang zeros and order-disorder transitions in hard-core lattice systems. *Comm. in Math. Phys.*, **364**:2 (2018), 655-682.
- [16] Krzakala, F., Montanari, F., Ricci-Tersenghi, F., Semerjian, G., Zdeborova, L. Gibbs states and the set of solutions of random constraint satisfaction problems. *Proc. Nat. Acad. Sci. USA*, **104**:25 (2007), 10318-10323.
- [17] Mazel, A., Stuhl, I., Suhov, Y. High-density hard-core model on  $\mathbb{Z}^2$  and norm equations in ring  $\mathbb{Z}[\sqrt[6]{-1}]$ . arXiv:1909.11648v2, 2019.
- [18] Misaghian, M. Factor rings and their decompositions in the Eisenstein integers ring  $\mathbb{Z}[\omega]$ . *Armenian J. of Mathematics*, **5**:1 (2013), 58-68.
- [19] Nair, U.P. Elementary results on the binary quadratic form  $a^2 + ab + b^2$ . arXiv: math.0408107v1, 2004
- [20] Parisi, G., Zamponi, F. Mean-field theory of hard-sphere glasses and jamming. *Rev. Mod. Phys.*, **82** (2010), 789-845.
- [21] Peled, R., Samotij, W. Odd cutsets and the hard-core model on  $\mathbb{Z}^2$ . *Annales de l'IHP, Probabilités et Statistiques*, **50** (2014), 975-998.
- [22] Pirogov, S.A., Sinai, Ya.G. Phase diagrams of classical lattice systems. *Teor. Mat. Fiz.* **25** (1975), 1185-1192; **26** (1976), 61-76.
- [23] Seiler, E. *Gauge theories as a problem of Constructive Quantum field theory and Statistical mechanics*. Lecture Notes in Physics, **159**. Berlin: Springer, 1982.
- [24] Sinai, Ya. G. *Theory of phase transitions: rigorous results*. Oxford et al.: Pergamon Press, 1982.
- [25] Slawny, J. Low-temperature expansion for lattice systems with many ground states. *J. of Stat. Physics*, **20** (1979), 711-717.
- [26] Zahradnik, M. An alternate version of Pirogov-Sinai theory. *Comm. Math Phys.* **93** (1984), 559-581.